Metabolic Abnormalities and Adipose Tissue Leukocyte Dynamics in a Murine

Model of Obesity, Weight Loss, and Weight Regain

By

Brian Francis Zamarron

A dissertation submitted in partial fulfillment
of the requirements for the degree of
Doctor of Philosophy
(Immunology)
in the University of Michigan
2017

Doctoral Committee:

      Associate Professor Carey N. Lumeng, Chair
      Professor Cheong-Hee Chang
      Professor Philip King
      Associate Professor John Osterholzer
      Assistant Professor Darleen Sandoval

Brian Francis Zamarron

zamarrbf@umich.edu

ORCID ID: 0000-0001-6549-4230

DEDICATION

To my mother, who wasn't able to pursue the opportunities I've enjoyed

To my partner in mischief Alyson

ACKNOWLEDGEMENTS

I would like to thank my advisor, Dr. Carey Lumeng, for his support when I approached him in 2012 about starting a series of weight loss experiments which would requiring a series of 6-11 month long experimental setups. The results from those initial experiments ended up being completely different from what we were expecting to find and formed the basis of my entire doctoral research. I would like to also acknowledge the members of my committee for their collective input towards my research design which helped guide my projects at each stage.

I would also like to thank the members of the Lumeng laboratory for their help over the years as well. Discussions about research, problems and, more often than not, pie made my time here at Michigan quite unique. I'd be remiss to not specifically mention the various undergraduate students which I have mentored over the years and became capable and important members of the Lumeng laboratory. My time spent training and mentoring these students was certainly rewarded back again with the help they've been able to provide and I wish them the best of luck going forward.

Finally, I need to acknowledge the other members of the University of Michigan Immunology Program. First the students – The discussions I've had with students has covered a range of topics from simple research to existential life crises about life after graduation. I'll miss those I've grown close to, and I lament not having the time to become better acquainted with others. I wish us all the best of luck regardless of our future paths. Second is Bethany Moore and Zarinah Aquil – Beth has become a fantastic strength for the Immunology program and I know the students appreciate her ridiculous efforts made to help support the community. The same could be easily said of Zarinah, whose job I'm sure feels about as easy as squeezing blood from a turnip more often than not. Thank you both.

TABLE OF CONTENTS

LIST OF FIGURES

LIST OF TABLES

ABSTRACT

Obesity is associated with pro-inflammatory changes within adipose tissue which are mechanistically linked to the development of cardiometabolic disease. Currently, little is known regarding whether weight loss resolves obesity-induced changes including adipose tissue inflammation. We sought to clarify unresolved mechanisms that control adipose tissue leukocyte dynamics and metabolic dysfunction during obesity, weight loss, and weight regain. We first identified CD64 as a better marker than what has been previously used for identifying adipose tissue macrophages in mice. Use of this marker allows the definitive identification of macrophages from dendritic cells within adipose tissue and resolves controversies in the field regarding this population. Obesity was induced using a high-fat diet (60% kcal derived from fat) for 12 weeks and weight loss was achieved by switching animals back to normal diet (13.5% kcal derived from fat) for an additional 8-24 weeks. We show that even a prolonged six-month weight loss cycle in mice fails to completely resolve obesity-induced adipose tissue macrophage activation which may contribute to the persistent adipose tissue damage and reduced insulin sensitivity observed in formerly obese mice. Finally, we investigated if unique metabolic abnormalities develop in formerly obese mice upon HFD re-challenge for an additional 6 weeks. Weight regain was associated with impaired adipose tissue expansion, hyperinsulinemia, hepatic steatosis and elevated serum transaminase concentrations. We conclude that obesity imparts a lasting impact on adipose tissue immune and metabolic function that persists despite weight loss and may have long-term negative effects on health. As a result, weight regain in formerly obese mice is accompanied by hastened development of potentially severe metabolic abnormalities.

Chapter 1 – Introduction

This dissertation describes three projects undertaken in an attempt to resolve several unanswered questions regarding adipose tissue leukocyte dynamics and metabolic perturbations during obesity, weight loss, and weight regain. The following introduction will briefly outline relevant background material and highlight aspects of what is known and unknown regarding insulin resistance development with obesity. I will provide working definitions for obesity and hyperglycemia, detail the importance of adipose distribution, and highlight comorbidities associated with obesity which are most pertinent for this dissertation. I will then introduce our mouse model of obesity and describe what is known regarding the involvement of obesity-associated inflammation in establishing insulin resistance in both rodents and humans. Finally, I will provide specific background information helpful for understanding the context, motivations, and objectives for chapters 2-4 and highlight the unresolved issues in the field that my work has tried to address.

Defining Obesity

Obesity is increasingly recognized as a worldwide public health issue over the last few decades. Obesity is known as a major risk factor for the development of severe metabolic disorders including type 2 diabetes and cardiovascular disease. Before delving into the complexities of obesity-induced physiological changes, it's critical to provide clear definitions. Obesity is a condition of excessive fat accumulation, typically in adipose tissue. There are a number of techniques capable of accurately measuring body fat accumulation *in vivo* including densitometry, magnetic resonance imaging and dual-energy X-ray absorptiometry (1). These methods calculate body fat as a percent of total body weight. Obesity is typically defined as $\geq 25\%$ fat mass in men and $\geq 30\%$ fat mass in women (2-4). While these methods are useful for precise measurement of fat mass,

they are often only used for research purposes and not widely-used in clinical practice. Instead, body weight and body mass index (BMI), weight in kilograms divided by height in meters squared, are the most commonly used assessments for determining overweight and obesity in humans due to simplicity and cost efficiency (1). The World Health Organization has determined various BMI cutoff values to determine weight classifications based on comorbidities risk associated with a given BMI range (Table 1) (5; 6). Unfortunately, the diagnostic accuracy of BMI as an assessment of adiposity is known to be limited and unreliable in certain subjects making BMI a useful screening tool for obesity but a poor measure of percent body fat. A systematic review of the literature comparing BMI with body fat percent revealed the commonly used BMI cutoff value of 30 tends to have high specificity but low sensitivity for identifying obesity (3). So while more than 95% of subjects with BMI values ≥ 30 kg/m^2 can also be defined as obese by body fat percent, more than half of people with excess adiposity may be missed using a BMI cutoff value of ≥ 30 kg/m^2 (7; 8).

Table 1 – Classification of obesity and comorbidity risk in adults. Recreated from Ruth Chan and Jean Woo 2010 (6).

Classification	BMI	Co-morbidity Risk
Underweight	<18.5	Low
Normal Weight	18.5-24.9	Low
Overweight	25.0-29.9	Increased
Obese Class I	30.0-24.9	Moderate
Obese Class II	35.0-39.9	Severe
Obese Class III	>40.0	Very Severe

Distribution of adiposity

Fat distribution is just as critical of a determinant for overall cardiometabolic risk as adiposity and BMI. Excess visceral intra-abdominal, or central fat, is associated with increased metabolic disease risk (9). Waist circumference is often used as a surrogate marker of central adiposity due to the higher costs associated with more precise body

composition measurement techniques. Waist circumference and BMI are highly correlated; waist measures in men and women > 102 cm and > 89 cm, respectively, are associated with an overall BMI of $\geq$ 30 kg/m^2 and increased cardiometabolic disease risk (9-11). Waist circumference measures both subcutaneous and visceral adipose tissue mass and therefore cannot distinguish which fat depot is associated with increased cardiometabolic risk. The general consensus is that visceral adipose tissue expansion, rather than subcutaneous, is associated with increased risk for development of metabolic disorders. Visceral adipose tissue expansion is associated with ectopic fat deposition in liver and muscle tissue while subcutaneous adipose expansion is not (12; 13). Several hypotheses have been proposed to explain this phenomena; one model suggests that obesity-associated dysfunction in adipose tissue may eventually limit its lipid storage capacity. The result is that excess lipid begins to "spill over" into other metabolically relevant organs thus increasing fat deposition in liver, muscle tissue and kidneys (14). Ectopic lipid accumulation and lipotoxicity is correlated with increased insulin resistance and cardiometabolic disease development (15-18). Obesity and metabolic dysfunction is also associated with increased circulating markers of inflammation. Visceral, but not subcutaneous, adipose tissue is a major source of circulating inflammatory cytokines during obesity in both humans and mice (19-22). Rodent visceral gonadal white adipose tissue depot is therefore used as a murine equivalent of human visceral omental tissue due to similarities in gene expression and obesity-associated inflammation (23). In male mice this depot is termed the epididymal white adipose tissue depot (eWAT). The use of rodent models of obesity will be discussed in more detail below.

Epidemiology of Obesity

The prevalence of obesity increased dramatically worldwide within the last few decades. The National Health and Nutrition Examination Survey (NHANES) is a cross-sectional study of the health and nutritional status of both children and adults in the United States conducted by the Center for Disease Control and Prevention. According to NHANES data, the overall prevalence of obesity, defined by BMI, in the U.S. during 2011-2014 was 36.5% in adults and 17.0% in youths between 2-19 years of age (24).

Obesity prevalence was highest among adults age 40-59 years at 40.2% and dropped to 37.0% in adults age 60 years and over. Obesity rates were slightly higher among women (38.3%) than men (34.3%). Prevalence rates change depending on ethnicity and were lowest among Asian adults (11.7%) and highest among non-Hispanic black (48.1%) and Hispanic populations (42.5%). Obesity prevalence among Non-Hispanic white populations was 34.5%. More alarmingly, the overall trend for both adult and youth populations suggest obesity rates continually increased between 1999 and 2014. A systematic review estimated the number of overweight or obese individuals worldwide was over 2.1 billion in 2013 and found that prevalence has increased substantially over the past three decades (25). Increases were seen in both developed and developing countries with no country showing declines within this timeframe.

There is a substantial cost, both economic and health, associated with obesity. A systematic review estimated that the direct medical cost of overweight and obesity in the U.S. equated to between 5% and 10% of total healthcare spending (26). The primary concerns with rising obesity rates are the substantially elevated risks for development of life-threatening comorbidities.

Comorbidities Associated with Obesity

Obesity substantially increases morbidity and mortality among older adults in large part due to the increased risk for development of chronic diseases including, but not limited to, type 2 diabetes mellitus, cardiovascular disease, cancer, hypertension, and sleep apnea (27-30). The risk of death is increased by as much as 3-fold in obese subjects compared to normal-weight individuals (28). For the purposes of this dissertation, I will focus on discussing the mechanisms by which obesity contributes to the development of insulin resistance, type 2 diabetes, and non-alcoholic fatty liver disease (NAFLD) development.

Insulin Resistance and Type 2 Diabetes

4

Insulin resistance refers to the inability of cells to properly respond to insulin resulting in dysregulated glucose metabolism. One of the more prominent consequences of insulin resistance is reduced glucose uptake by cells in muscle, liver, and fat to a given amount of insulin leading to chronically elevated plasma glucose levels. Pancreatic beta cells increase insulin production in an attempt to maintain blood glucose within a normal range. Failure to produce sufficient quantities of insulin leads to hyperglycemia and the development of type 2 diabetes. There are a few measures of measuring glycemic control and insulin resistance which are all related but have subtle diagnostic differences. One of the most common is fasting blood glucose where blood or plasma glucose levels are measured after a period of fasting for 6-8 hours which is the time needed to reach a natural lower plateau for blood insulin and glucose. Humans can be considered to have impaired fasting blood glucose levels between 100 mg/dl and 125 mg/dl and diabetes as ≥126 mg/dl (31; 32). Glucose tolerance tests are also commonly used diagnostic tools whereby a glucose load is provided to fasted patients and blood glucose is then measured up to two hours later. Using a glucose tolerance test, type 2 diabetes can be defined as a 2-hour blood glucose level in excess of 200 mg/dl following oral glucose administration (32). Hemoglobin A1c levels, also known as glycated hemoglobin, are also a commonly used diagnostic tool which provides a marker for average blood glucose levels over the past 2-3 months. High blood glucose increases the percent of glycated hemoglobin throughout the 2-3 month life span of red blood cells. As a result, variables that affect blood cell survival can also affect glycated hemoglobin levels irrespective of actual blood glucose levels (33). Nevertheless, it can be useful for tracking long-term glycemic control in patients with diabetes being defined as ≥6.5% and normal glycated hemoglobin ranges falling below 6.0% (32). While I will primarily focus on insulin's role in glycemic control, it's important to note that insulin is a multi-purpose hormone. As a result, insulin resistance also results in disruption to a number of metabolic pathways including carbohydrate metabolism, lipid metabolism, and protein production (34).

Individuals with higher BMI have increasingly higher risk for the development of type 2 diabetes. A recent study using the electronic health records system found that a BMI of 30-35 kg/m^2 increased a subject's relative risk ratio for diabetes development by 2.5 and a BMI of ≥40 kg/m^2 increased relative risk to 5.1 compared to normal weight

subjects (35). The World Health Organization has criteria to define normoglycemia ($\leq$ 106 mg/dl), prediabetes (between 106 mg/dl and 126 mg/dl) and diabetes ($\geq$126 mg/dl). Using these criteria, Ligthart *et al.* found that the lifetime risk for diabetes development in patients aged 45 years with prediabetes to be 74%, suggesting substantial risk for eventual type 2 diabetes development once insulin resistance has started (36).

Non-alcoholic Fatty Liver Disease Development

Non-alcoholic fatty liver disease is also strongly correlated with obesity and insulin resistance. Between 84% and 96% of patients undergoing bariatric surgery present with NAFLD (37). Between 25% and 55% of these patients have progressed to the more severe nonalcoholic steatohepatitis state, characterized by hepatic inflammation, and between 34% and 47% have developed hepatic fibrosis. Advanced stages of NAFLD are associated with liver damage, cirrhosis, liver failure, and hepatocellular carcinoma (37; 38). NAFLD is also intimately connected with insulin resistance and metabolic syndrome. Hepatic insulin resistance is observed in many cases of NAFLD and is associated with obesity and type 2 diabetes (39-41). Several publications suggest that NAFLD causes systemic insulin resistance (42), but this remains an open question in the field as others assert that hepatic steatosis is not sufficient to cause insulin resistance (43). Regardless, the literature clearly shows NAFLD is a common and pertinent disease feature in patients presenting with obesity and metabolic syndrome. The association of NAFLD with obesity and insulin resistance highlights the range of physiological consequences incurred with excess adiposity.

Murine Models of Obesity

A number of rodent models for obesity exist and are widely used by researchers to investigate obesity-induced insulin resistance and cardiometabolic disease development. Spontaneous mutations in the C57BL/6 strain led to the discovery of the well-known leptin-deficient ($Lep^{ob/ob}$) and leptin receptor-deficient ($LepR^{db/db}$) mice which represent genetic models of obesity development as leptin deficiency causes hyperphagia which

leads to excessive weight gain starting between 3-4 weeks of age in mice. These mice can grow in excess of 100g total body weight and develop insulin resistance. Despite widespread use, the leptin deficient model also introduces experimental artifacts which can confound results. Leptin is a highly conserved hormone that is both structurally and functionally similar to the cytokine interleukin 6 (IL-6). As a result, leptin influences systemic innate and adaptive immune responses (44). For example, leptin deficient mice are resistant to both actively and passively induced experimental autoimmune encephalomyelitis with reduced proliferative responses to introduced antigens (45). This limits the potential utility of the leptin deficient mouse model when investigating the association of inflammation with obesity and insulin resistance. In addition, while the heritability of obesity appears to be high in humans, monogenic mutations leading to human obesity are rare (46; 47).

Our laboratory has instead adopted the use of a diet-induced obesity (DIO) model in mice using a hypercaloric 60% high-fat diet (HFD) which is fed *ad libitum* for 10-20 weeks (48-51). This model was designed to better represent conditions leading to obesity development in humans due to caloric excess. The pharmacologic predictive validity of this model is good; DIO rats and mice are responsive to anti-obesity drugs found effective in humans including glucagon-like peptide-1 receptor agonists, sibutramine, and contrave (52-55). Several higher-fat diet variants are available and have been used by researchers worldwide for decades. One of the common HFD formulations was developed by Research Diets Inc. in 1996 at the request of an investigator who required a defined diet product. This HFD formula contained a caloric energy contribution of 20% from protein, 35% from carbohydrate, and 45% from fat. For the studies presented in this dissertation, we used a higher fat diet with the caloric energy composition being 20% from protein, 20% from carbohydrate and 60% from fat. While the original 45% HFD was designed to more closely mimic Westernized diets in humans, both diets continue to be used today and there is no consensus on which is the better diet for use in mouse models of obesity and cardiometabolic disease. Through internal comparisons of the commonly available high-fat diets, we have found that the 60% HFD induces more consistent weight gain and insulin resistance. Guo *et al.* tracked body weight gain and weekly NMR spectroscopy measurements of body composition in mice fed a 60% HFD

(56). Mice fed HFD started at 26g total body weight and 7% body fat and, after 19 weeks HFD, increased up to ~47.5g and 41% body fat (Table 2) (56). Our data largely matches these observations. In our laboratory, after 20 weeks of 60% HFD an average mouse weighs 52.9g ($\pm$ 1.69 SD) with 42.08% body fat ($\pm$ 0.50 SD). An average age-matched normal diet fed mouse weighs 29.73g ($\pm$ 0.11 SD) with 17.31% body fat ($\pm$ 1.46 SD). A body fat composition of 40% matches what might be expected in an individual with a BMI of approximately 40 kg/m^2 (57). Based on these predictable body composition changes with HFD, we typically provide HFD for at least 12 weeks and I set a lower threshold of obesity as $\geq$40g total body weight (Table 2).

Table 2 – Body fat percent in C57BL/6 male mice increases with body weight. Table created from body weight and body composition curves in Guo *et al.* 2009 (56).

Body Weight (grams)	Body Fat (%)	Weeks on 60% HFD
26	7	0
30	16	~1
35	25	~4
40	33	~8
45	40	~12

The DIO model in rodents induces metabolic disorder changes consistent with what's been observed in human subjects. Rodents with DIO experience hyperleptinemia, hyperinsulinemia and hyperglycemia similar to humans with obesity (58). Comparative functional genomics revealed the visceral eWAT depots of rats and mice with DIO have similar expression profiles as obese human adipocytes and the authors concluded the DIO rodent model appropriately models human obesity (23). In particular, both rodents and humans with obesity showed upregulation of immune response-related and angiogenesis genes in adipose tissue when compared to lean controls. As a result, the eWAT depot is generally viewed as a murine equivalent to human visceral adipose tissue (omental adipose depot) given the similarities in expansion, leukocyte accumulation and inflammation changes observed in the literature.

As a final note, it should be mentioned that obesity and insulin resistance development is not equivalent among different mouse strains. Leptin deficiency in BALB/cJ mice showed a 35%-40% reduction in total body weight gain and a 60% decrease in adipose mass. Despite reduced adiposity, BALB/cJ mice have worse insulin resistance and hyperlipidemia compared to C57BL/6 mice (59). Leptin deficiency in FVB/N mice also worsens insulin resistance and increases blood glucose (60). This strain effect variation is observed in DIO rodent models as well (61; 62). There are also sex differences in response to HFD. Female DIO mice are resistant to weight gain and insulin resistance development (63). Our studies exclusively used male C57BL/6 mice, but it's important to note the potential variation that exists in HFD response between strains and sex, and is a subject of continued investigation by the Lumeng laboratory and others.

Molecular Drivers of Obesity-Associated Insulin Resistance and Inflammation

An interesting phenomenon exists, termed metabolically healthy obesity, defined as the presence of obesity despite the absence of metabolic and cardiovascular disease (64-67). Precise definitions for this phenomenon are variable, making exact prevalence calculations difficult, but it's suggested that as many as one in three subjects with obesity are metabolically healthy (65; 68). This is a highly contentious and hotly debated topic with some suggesting it's simply a matter of time before metabolically healthy obese patients develop metabolic syndrome. Regardless, the data clearly indicate that while BMI and excess adiposity correlate strongly with cardiometabolic disease risk, there are additional mechanisms at play that modify actual disease development. Over the past decade numerous laboratories have begun to focus on inflammation as the potential mechanistic link between obesity and cardiometabolic disease development.

Obesity-Associated Adipose Tissue Inflammation

Over one hundred years ago, extremely high doses of sodium salicylate (upwards of 7.5 g/d) were found to alleviate the symptoms of diabetes mellitus, providing the first published evidence for the potential role of inflammation in insulin resistance (69-71). It wasn't until the early 2000s that the link was established showing inhibition of nuclear

factor kappa-B kinase subunit beta (NF-κB), a major transcription factor important for regulating immune responses, was the mechanism responsible for improved metabolic health (72; 73). Publications from the early 1990s reinvigorated a modern day interest in inflammation as a potential mechanistic link between obesity and metabolic dysfunction. In 1993 two landmark publications identified the cytokine tumor necrosis factor (TNFα) as being overproduced in the adipose tissue of obese mice and, through neutralization studies, showed TNFα played a direct role in obesity-associated insulin resistance (74; 75). Interest in obesity-associated inflammation has grown tremendously in recent years; a PubMed search for ["adipose tissue" AND inflammation] over the last twenty years returns approximately 7,500 publications with over 900 published per year since 2013. Obesity is now known to elevate production of several pro-inflammatory cytokines and chemokines within adipose tissue including TNF-α, IL-1β, IL-6, leptin, IL-8, CCL2, and MCP-1 and is associated with elevated acute-phase response proteins in serum (76-78). The NF-κB, c-Jun N-terminal kinase (JNK), and inflammasome pathways are all activated within adipose tissue of obese subjects and have been implicated in the development of insulin resistance (73; 79-81).

Molecular Links between Inflammation and Insulin Resistance

Inflammation-induced downstream defects of the insulin receptor signaling response system is hypothesized as one of the primary mechanistic links between inflammation and insulin resistance (Figure 1-1). Insulin binding to the insulin receptor, a tyrosine kinase receptor, initiates an autophosphorylation cascade on the receptor's tyrosine residues. The activated insulin receptor can then further phosphorylate tyrosine residues on downstream signaling proteins including the insulin receptor substrate (IRS) family (82). Tyrosine phosphorylation of IRS proteins allows further downstream activation of the phosphatidylinositol 3-kinase (PI3K)/protein kinase B (AKT) and mitogen-activated protein kinase pathways (82). Glucose transporter type 4 (GLUT4) expression on the plasma membrane of cells permits circulating glucose uptake in response to insulin signaling. PI3K pathway activation is known to be essential, but not sufficient, for rapid translocation of GLUT4 to the plasma membrane. Inflammation

signaling pathways, however, are capable of directly inhibiting the insulin signaling cascade. JNK activation can cause insulin resistance through the direct phosphorylation of serine residues on IRS-1 which disrupts binding and inhibits tyrosine kinase cascade activity (83; 84). IKKβ activity inhibits insulin signaling through activation of NF-κB and the production of proinflammatory cytokines such as TNFα, IL-6 and IL-1β. These cytokines feed back onto insulin-responsive cells thereby increasing JNK activation. In addition, these cytokines promote suppressor of cytokine signaling (SOCS) production which can also promote insulin resistance through inhibition of tyrosine phosphorylation on the insulin receptor and IRS proteins (85; 86).
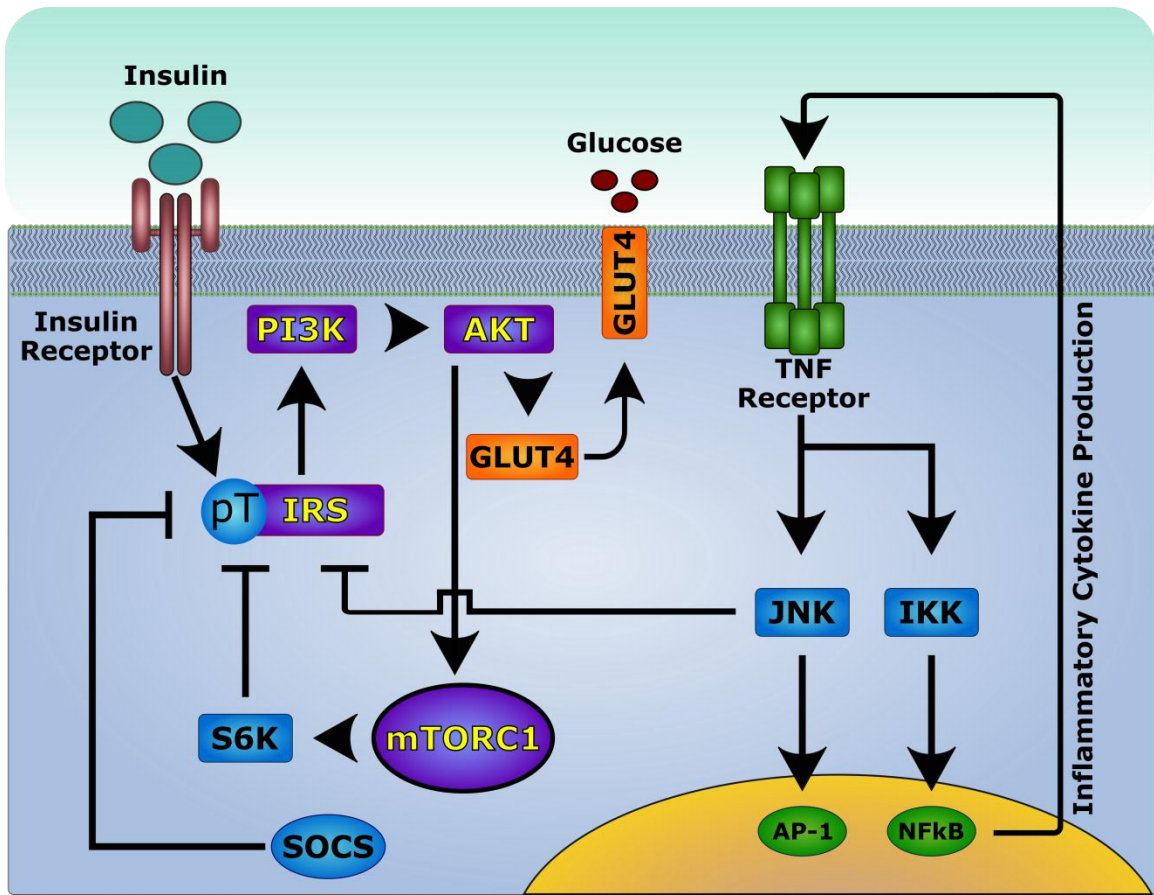
Figure 1-1 – Inhibitory effects of inflammation on insulin signaling. Under homeostatic conditions, insulin activates an IRS/PI3K/AKT dependent pathway to promote GLUT4 translocation to the surface membrane. In contrast, under inflammatory conditions, TNFa-mediated activation of JNK promotes direct inhibition of IRS through phosphorylation of serine residues which reduces binding efficiency and reduces tyrosine phosphorylation on IRS. Thereafter, activation of NFκB enhances inflammatory cytokine production which can feed back onto the cell to further perpetuate inhibition of downstream insulin signaling. Insulin signaling is

also self-regulatory, in both homeostatic and inflammatory conditions, through activation of mTORC1 and S6 kinase which inhibits IRS activity through serine phosphorylation.

However, there is also evidence suggesting that low levels of inflammatory signaling, for instance TNFα, is actually necessary for optimal adipogenesis and adipocyte function (87). In addition, genetic models that enhance NF-κB activity can prevent DIO and insulin resistance due to increased energy expenditure despite increased systemic TNFα and IL-6 (88). Human clinical trials using TNFα antagonists have shown little improvement in insulin sensitivity and hyperglycemia (89-91), though it's been argued the few existing studies are underpowered and that TNFα-antagonism merits more carefully designed investigation (92). IL-1β antagonism or neutralization in clinical trials has shown improvements in insulin sensitivity while reducing markers of metabolic syndrome, but with unknown long-term efficacy and unknown mechanism (93-95). So while inflammatory pathway activation can directly inhibit insulin signaling, our understanding of inflammation's full involvement in insulin resistance and adipose tissue function is far from complete. Overall, I believe this highlights the complex and multifactorial nature of cardiometabolic disease development with obesity.

Adipose Tissue as the Center of Obesity-Associated Inflammation

Obesity is associated with dramatic inflammatory changes within adipose tissue including dramatic shifts in both innate and adaptive leukocyte populations (96; 97). A critical question in the field is what mechanism(s) are responsible for initiating inflammatory responses within adipose tissue and adipocytes during obesity. Potential activating pathways leading to adipose tissue inflammation during obesity include toll-like receptor signaling, inflammasome activation, ER stress, cellular stress, adipocyte death, adipocyte hypoxia and increased microbial contamination just to name a few (97). These changes eventually encourage the recruitment and activation of pro-inflammatory leukocytes (97; 98). The prevailing hypothesis is that continual accumulation and activation of pro-inflammatory leukocytes contributes to a state of chronic low-grade inflammation which promotes localized and systemic insulin resistance (99-102).

Leukocyte Mediators of Obesity-Associated Inflammation

Adipose tissue can be broadly separated into two main fractions including mature adipocytes and an inter-adipocyte stromal-vascular fraction (SVF) containing a variety of cells including preadipocytes, endothelial cells, and leukocytes. Both lean and obese adipose tissue contains a resident leukocyte population comprised of nearly the full range of immune cell types. Obesity causes dramatic changes in relative leukocyte population frequencies and activation profiles within adipose tissue. These changes are further complicated and compounded by the extended chronic stimulus period which can last for decades. The relative obesity-associated change of various leukocyte populations in adipose tissue is provided (Table 3). Certain leukocyte populations are associated with lean adipose tissue, maintenance of homeostatic function, insulin sensitivity, and low inflammation. These include regulatory $CD4^+$ T cells (Tregs), $CD4^+$ type 2 helper T cells (Th2), M2-like resident macrophages, eosinophils, and group 2 innate lymphoid cells (97; 103-105). Their insulin sensitizing effects are thought to be largely due to secretion of type 2 cytokines including IL-4, IL-10, IL-13 and IL-33 (106). Other leukocyte populations are associated with obese adipose tissue and are thought to contribute to adipose tissue dysfunction, inflammation, and insulin resistance both locally and systemically. These include Th1 cells, Th17 cells, $CD8^+$ cytotoxic T cells, M1-like pro-inflammatory macrophages, dendritic cells (DC), natural killer cells (NK), B cells, and neutrophils (Figure 1-2) (104; 107-109). Accumulation of these leukocytes enhances production of pro-inflammatory cytokines including IFNγ, TNFα, IL-1β and IL-6. Some populations are known to be present in adipose tissue, but have unknown function in regulating metabolism due to few published findings or contradictory results. These include, but are not limited to, natural killer T cells (NKT), mast cells and γδ T cells.

The prevailing model suggests that the cytokine environment of lean adipose tissue helps to promote M2-like macrophages and preserves insulin sensitivity. The inflammatory cytokine environment associated with obese adipose tissue initiates a cycle of chronic inflammation and leukocyte accumulation which promotes insulin resistance both locally and systemically. For the purposes of this introduction, I will provide more

detail on what's known regarding T cell and macrophage population dynamics within adipose tissue. These are the best studied adipose tissue leukocyte populations and an extensive background literature exists regarding these cells in the context of obesity.

Table 3 – Relative leukocyte population changes in murine epididymal adipose tissue with obesity. Data derived from our own data, Mraz and Haluzik 2014, and Sun *et al.*2012 (97; 103).

Leukocyte Population	Relative Change (% of SVF)
Macrophage	Increased
Dendritic Cell	Unknown/Possibly Increased
CD4$^+$ T cell (non-Treg)	Increased
CD4$^+$ Regulatory T cell	Reduced
CD8$^+$ T cell	Increased
B cell	Increased
Eosinophil	Reduced
Natural Killer T cell	Reduced
Natural Killer cell	Increased
Mast Cell	Increased
Neutrophil	Increased
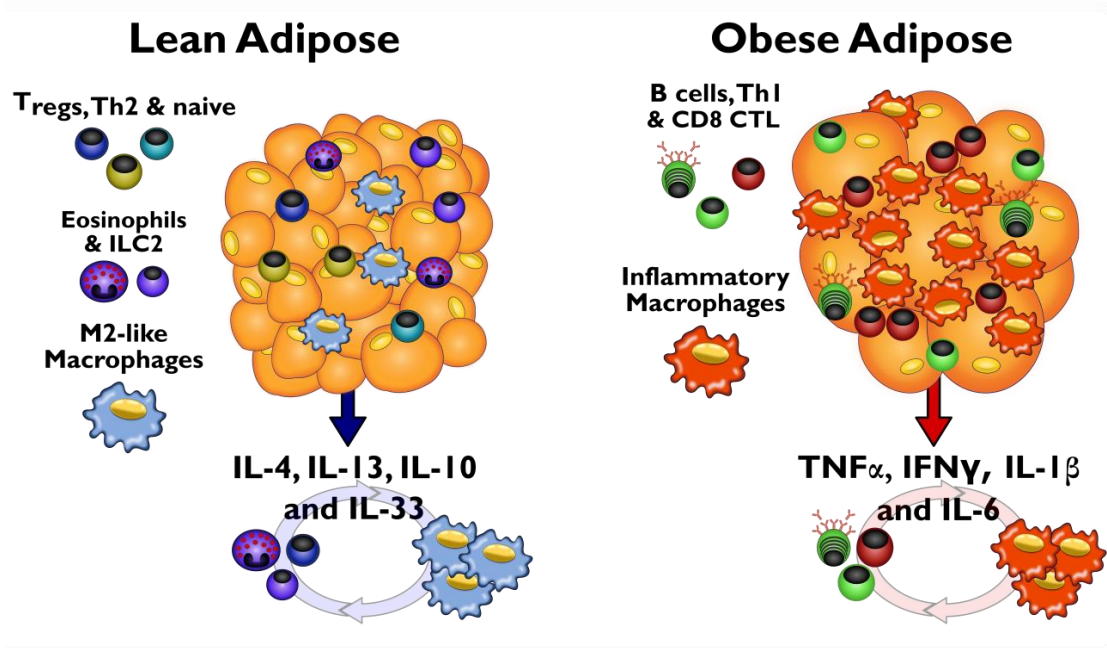
Figure 1-2 – Cartoon depiction of leukocyte population changes that occur with obesity and the resulting inflammatory signaling cascade that promotes insulin resistance. The cytokine environment and leukocyte populations found in lean adipose tissue are thought to promote the continued maintenance of low inflammation, insulin tolerance, and proper adipose tissue function. Obesity induces dramatic changes in the cytokine expression profile of adipose tissue which perpetuates a cycle of inflammatory leukocyte activation and recruitment. These inflammatory changes are thought to be central to the development of adipose dysfunction, insulin resistance, and, ultimately, cardiometabolic diseases. ILC2 = Innate lymphoid group 2 cells; CTL = Cytotoxic T lymphocyte; Treg = Foxp3$^+$ regulatory T lymphocyte.

T Lymphocytes

Obesity is associated with increases in the quantity of both CD4$^+$ and CD8$^+$ T lymphocytes in adipose tissue. Obesity is also associated with qualitative shifts in the polarization state of adipose-resident T cell populations. Adipose tissue of lean mice has a higher frequency of naïve T cells and Foxp3$^+$ Tregs (110). With obesity there's a reduction in the relative frequency of Tregs and naïve T cells in visceral adipose tissue. Instead, T cells from visceral adipose tissue of obese mice tend to polarize towards a type 1 cytokine signature with increased production of IFNγ and granzyme B (111). We've observed T cell accumulation and activation in eWAT as early as 2-3 weeks after starting HFD with elevated IFNγ and IL-2 production observed after *ex vivo* stimulation (Figure 1-3). IFNγ deficient mice have reduced adipose tissue macrophage (ATM) accumulation and reduced pro-inflammatory cytokine expression including TNFα and MCP-1 (111).

15

Depletion of T cells in WT DIO mice with a CD3-specific antibody increases adipose tissue Tregs and ameliorated insulin resistance for months despite continued HFD exposure (112). CD8-deficient mice also have reduced ATM accumulation, adipose tissue inflammation, and improved systemic insulin resistance (109).

Interestingly, despite lacking all T and B cells, obese $Rag1^{-/-}$ mice still develop hyperglycemia and insulin resistance (112), and we have observed that obese $Rag1^{-/-}$ mice still accumulate ATM. These data show that T cells are not necessary for obesity-associated insulin resistance development. However, $Rag1^{-/-}$ mice also lack cells thought to help regulate inflammation within adipose tissue including CD4$^+$ Th2-polarized cells and Tregs. In support of this theory, adoptive transfer of CD4$^+$Foxp3$^-$ T cells into DIO $Rag1^{-/-}$ mice increased Th2-polarized adipose tissue T cells and improves insulin resistance (112). Depletion of Tregs in Foxp3-DTR transgenic mice increased adipose tissue inflammation and increased serum insulin levels (110). Overall, the literature suggests that the balance of adipose-resident pro-inflammatory T cells (Th1, Th17, and CD8$^+$ cytotoxic T cells) versus regulatory T cells (Th2 and Tregs) is critical for determining the development of obesity-associated inflammation and insulin resistance.

There are several outstanding questions in the field regarding the mechanisms mediating T cell activation and polarization during obesity. The antigens responsible, which antigen presenting cells (APC) are involved, where T cell activation and expansion occurs, and how leukocyte activation is regulated all remain relative unknowns.
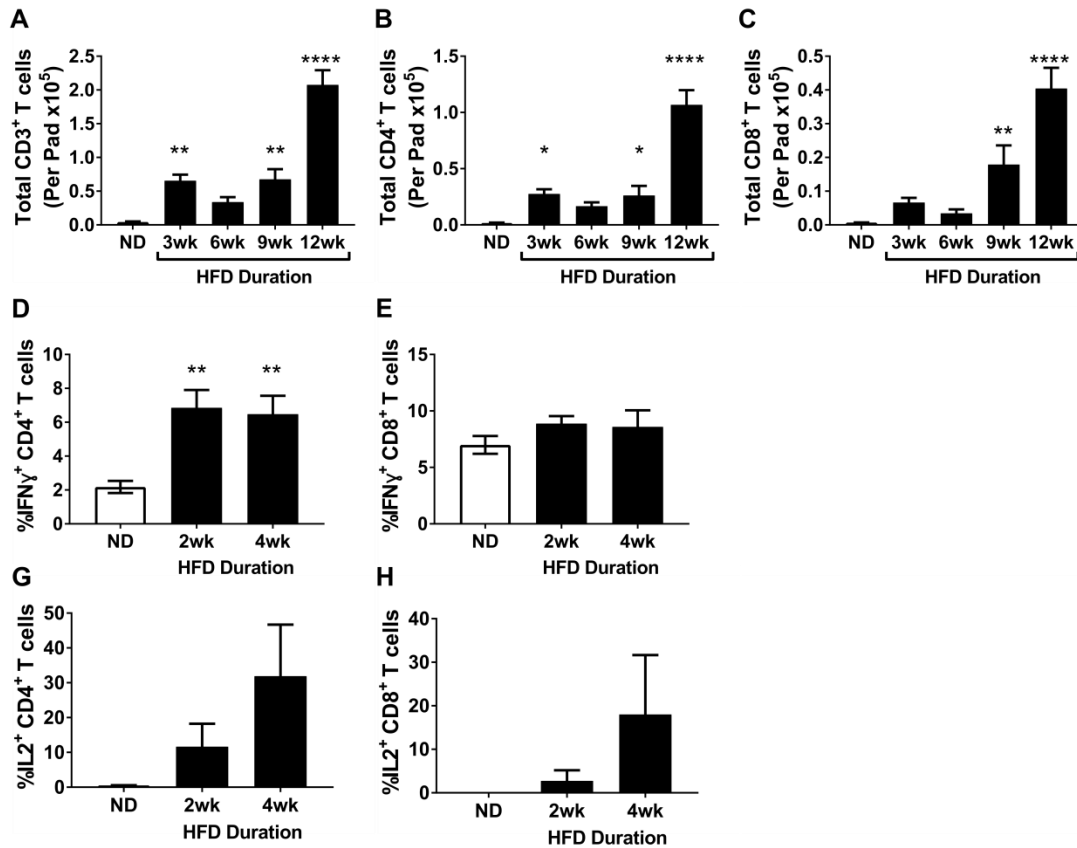
Figure 1-3 – Early progressive accumulation and activation of epididymal adipose tissue T cells in diet-induced obese C57BL/6J mice. (A-C) Obesity promotes the accumulation of CD3$^+$ T cells in eWAT which increases with more time spent on HFD. As early as 2 weeks on HFD (D and G) CD4+ T cells polarize towards expression of IFNγ and IL-2 after ex vivo stimulation with phorbol 12-myristate 13-acetate and ionomycin while (E and H) CD8+ T cells show no change in IFNγ but increased IL-2 expression. For A-H, cells were analyzed by flow cytometry after isolation from whole epididymal adipose tissue using collagenase digestion.

Macrophages

In 2003, two publications by Xu *et al.* and Weisberg *et al.* demonstrated that macrophages accumulated in obese adipose tissue but did not increase in other organs such as liver, lung or spleen (113; 114). More importantly, these two groups concluded the accumulated ATMs were primarily responsible for the elevated TNFα, iNOS and IL-6 expression observed in obese adipose tissue. ATM accumulation in obese human subjects is primarily observed in the visceral omental fat depot but, to a lesser degree, ATMs also accumulate in the subcutaneous adipose tissue (115; 116). In mice, ATM

accumulation during obesity is also primarily observed in the visceral eWAT depot, but also occurs in subcutaneous depots.

ATMs are also found in the adipose tissue of lean mice and humans. ATMs from adipose tissue of lean mice express a gene profile similar to M2 alternatively activated macrophages including *Il10*, *Ym1*, *Arg1*, and *Mgl1*. In 2007, it was found that obesity promotes the CCR2-dependent accumulation of a pro-inflammatory CD11c$^+$ ATM population which did not express these M2-like genes and, instead, produced inflammatory mediators including TNFα and iNOS (117). These recruited CD11c$^+$ ATMs become the dominant ATM population and make up as much as 60-75% of all eWAT ATMs during obesity. More than 90% of macrophages in the adipose tissue of obese mice and humans localize to dead, or dying, adipocytes forming clusters which are now referred to as crown-like structures (CLS) (118). Lumeng *et al.* found that the CLS-associated macrophages in obese eWAT expressed M1-like proinflammatory markers and were primarily derived from newly recruited macrophages (119). These publications provided evidence for a new way to identify and separate murine ATMs based on surface marker expression which correlated with functional polarization differences. Resident M2-like macrophages found in lean adipose tissue were identified as F4/80$^+$CD11b$^+$CD11c$^-$ leukocytes. The recruited pro-inflammatory ATMs that accumulate in obese adipose tissue were identified as F4/80$^+$CD11b$^+$CD11c$^+$ leukocytes (Figure 1-4).

Recruited CD11c$^+$ ATMs are believed to be critical for the development of metabolic dysfunction in obese mice. In support of this, depletion of ATMs during obesity with liposome-encapsulated clodronate improves insulin resistance and reduces hyperglycemia in DIO and leptin-deficient mice (120; 121). Ablation of CD11c$^+$ cells, through use of CD11c-driven expression of diphtheria toxin receptor improved insulin sensitivity and reduced inflammatory markers within adipose tissue (122). Use of CCR2 antagonists in DIO mice reduced ATM content, reduced adipose tissue inflammation and improved insulin resistance without lowering body weight or reducing hepatic steatosis (123). Overexpression of the CCR2 ligand, CCL2, specifically in adipose tissue increases macrophage accumulation, insulin resistance, and hepatic steatosis. Alternatively, CCL2-

deficient DIO mice have reduced ATMs, reduced insulin resistance, and reduced hepatic steatosis (124). However, there's no way to verify that the metabolic improvements observed in these studies were specifically due to the ATM population changes observed. There's the potential for off-target effects on other adipose resident leukocyte populations (for example DCs) or even macrophage changes in other metabolic tissues which could be partly responsible for metabolic improvements. Methods of specifically targeting and/or differentiating ATMs are necessary to fully resolve the role that pro-inflammatory ATMs play in the development of insulin resistance and adipose tissue dysfunction during obesity.

Figure 1-4 – Polarization of pro-inflammatory CD11c^{+} macrophages in adipose tissue during obesity. Obesity encourages the CCR2-dependent recruitment of blood monocytes which are activated towards an M1-like profile while in adipose tissue to produce pro-inflammatory cytokines. Historically, adipose tissue macrophages have been identified as CD11b^{+}F4/80^{+} leukocytes which were then separated by surface expression of markers like CD206 for anti-inflammatory M2-like ATMs or CD11c for M1-like inflammatory ATMs.

Scope of the Dissertation

Excellent progress has been made in the last decade towards understanding the molecular and cellular drivers of inflammation during the onset of obesity. Unfortunately, much less is known about how inflammation and adipose-resident leukocytes are altered after weight loss in formerly obese subjects. Recent publications have begun to suggest certain obesity-associated features, such as adipose tissue inflammation, persist through weight loss despite improvements in systemic insulin resistance and glycemic control in both mice and humans (125; 126). Maintenance of inflammation after weight loss has

been largely evaluated by whole tissue gene expression and little is known regarding what changes occur in adipose-resident leukocyte populations or their activation profiles. We also don't know how these persistent obesity-associated features may impact local and systemic metabolic health in formerly obese mice.

My research has focused on trying to better understand the dynamics of adipose tissue leukocytes during weight loss and to identify potential residual metabolic abnormalities that persist in formerly obese mice. Presented below are specific backgrounds, motivations, and objectives for three major projects completed in pursuit of this research.

Context for Chapter 2 – Definitive delineation of adipose tissue macrophages and adipose tissue dendritic cells in mouse and humans

Historically, F4/80 has been used as a macrophage-specific marker in adipose tissue. However, it is well known that F4/80 is a poor marker for separating certain myeloid populations, such as DCs and eosinophils, in other tissues (127). Similarly, CD11c is often used as a classic marker for the identification of DCs, but CD11c is also upregulated on activated macrophages and ATMs during obesity. As a result, the separation of these two adipose tissue myeloid populations using historic markers has been difficult and imprecise. Upon starting this project, the exact discrimination of macrophages and dendritic cells in adipose tissue was poorly defined. Part of this was due to the need for better markers to define their respective functions in adipose tissue. Delineation of ATMs and ATDCs is important for understanding if they play synergistic, redundant, or even antagonistic functions in establishing and maintaining adipose tissue inflammation during obesity.

Our objective was to test a new macrophage-specific marker (CD64) for discrimination of ATMs from adipose tissue DCs (ATDC). We show that F4/80 is expressed on other adipose-resident leukocyte populations, including eosinophils and DCs, in addition to labeling ATMs. Using this marker, we were able to distinguish CD11c$^+$ ATMs and CD11c$^+$ ATDCs and we verify our findings by showing distinct gene

expression profiles for these two populations. Through this work, we hope to improve our understanding of the relative functions of ATM versus ATDC during obesity and weight loss. Other markers, such as F4/80 or CD11b, can be used in conjunction with CD64 but we have found add little additional discriminatory value beyond what CD64 provides. Based on findings from this project, ATMs will be identified in chapters 3 and 4 as $CD45^+CD64^+CD11c^{-/+}$ while ATDCs will be identified as $CD45^+CD64^-CD11c^+$.

Context for Chapter 3 – Features normally associated with obesity persist in visceral adipose tissue despite weight loss

Weight loss is often seen as the optimal resolution of obesity and obesity-associated comorbidities. However, some patients still retain a persistently elevated risk for cardiometabolic disease despite weight loss (125; 126; 128). Adipose tissue leukocytes are linked to obesity-associated insulin resistance and cardiometabolic disease development during obesity. However, few groups have attempted to investigate how adipose tissue leukocytes are altered during weight loss. Several recent studies have found that weight loss fails to resolve adipose tissue inflammation in mice and humans (125; 126; 129; 130), and suggest certain adipose tissue leukocyte populations remain activated despite weight loss. Persistent activation of adipose tissue leukocyte populations may provide a potential mechanism to explain elevated cardiometabolic disease risk after weight loss.

Our objective was to define the effects of weight loss on inflammatory leukocyte activation and composition within adipose tissue to understand the mechanisms by which metabolic inflammation persists. We identified long-term alterations in the composition of adipose tissue leukocytes including retention of proliferating $CD11c^+$ ATMs and a persistent activation state of ATMs despite weight loss. We also identified maintenance of obesity-associated derangements in eWAT structure and function after weight loss including fibrosis, crown-like structures, and altered adipogenic protein expression. The results from this project show that obesity imparts long-term, potentially permanent, alterations in eWAT that fail to resolve with weight loss (Figure 1-5). Understanding

which characteristics of obesity remain despite weight loss helps inform our understanding of the relationship between adipose tissue inflammation and metabolic function.
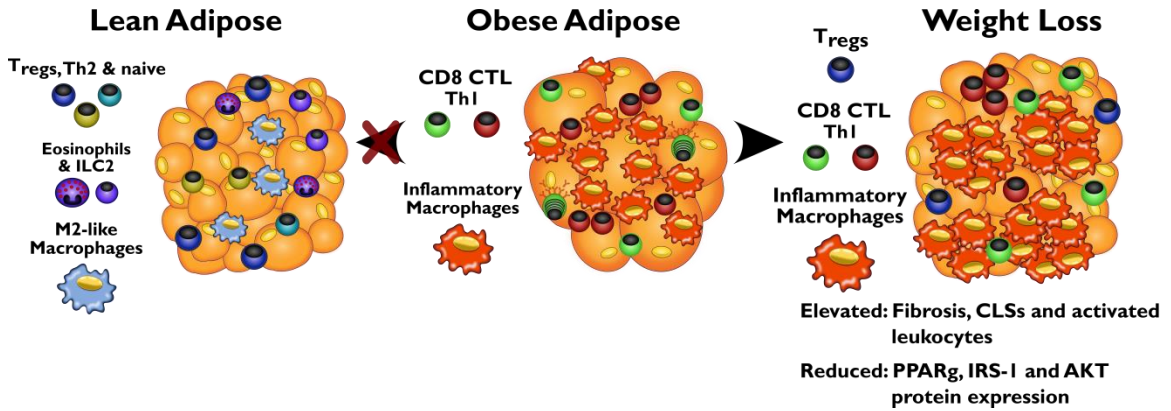
Figure 1-5 – Features normally associated with obesity persist in adipose tissue despite weight loss. After weight loss, adipose tissue of formerly obese mice fails to return to a lean-like state and, instead, maintains or develops several features normally only associated with chronically obese adipose tissue. These features include crown-like structures, increased leukocyte accumulation, inflammatory activation of resident leukocytes, and impaired adipogenic protein expression profile. PPARg = Peroxisome proliferator-activated receptor gamma; IRS-1 = Insulin receptor substrate 1; AKT = Protein kinase B (These are proteins important for adipocyte function and development).

Context for Chapter 4 – Formerly obese mice develop metabolic abnormalities faster than formerly lean mice after HFD re-challenge

Unfortunately, weight regain is a common occurrence in formerly obese subjects. An open question within the field is whether weight regain adversely alters metabolic health. Based on the findings of Chapter 3, we hypothesized there would be unique metabolic abnormalities in formerly obese mice that only manifest during weight regain (Figure 1-6). We sought to identify these potential metabolic abnormalities by re-exposing formerly obese mice with an additional HFD challenge. In chapter 4, I will present evidence suggesting that weight regain causes metabolic abnormalities to develop at a hastened rate in formerly obese mice due to unresolved effects that persist through weight loss. These findings could help identify unique health consequences of weight gain in formerly obese subjects which may require customized therapeutic intervention.
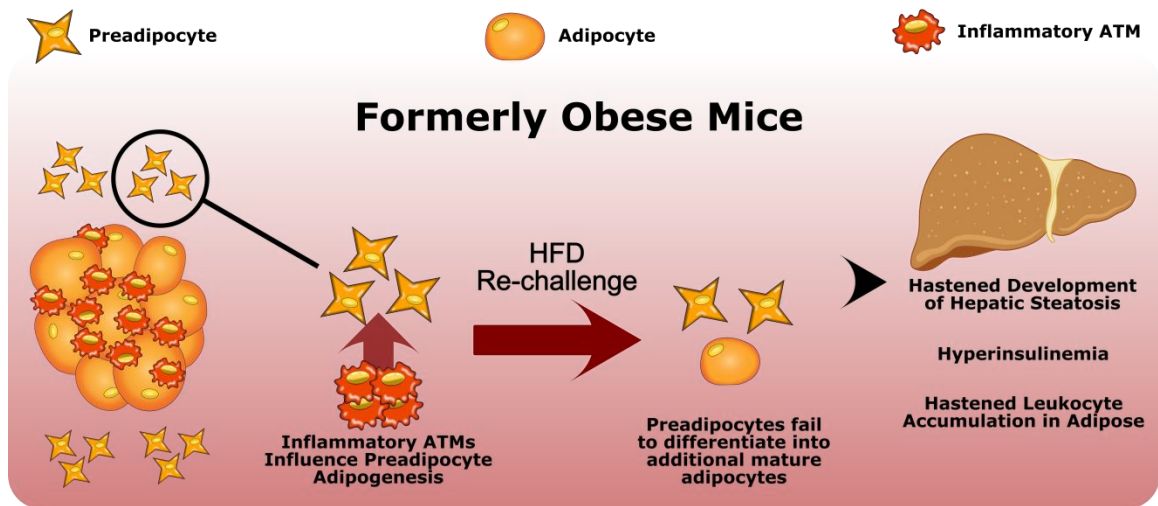
Figure 1-6 – Cartoon model depicting predicted metabolic perturbations after HFD re-challenge. Weight loss fails to fully resolve obesity-associated features within eWAT including the maintenance of pro-inflammatory ATMs. We hypothesize that these ATMs directly influence the adipogenic responsiveness of eWAT preadipocytes during HFD re-challenge of formerly obese mice. As a result, the eWAT tissue fails to respond due to a shortage of functional mature adipocytes. This encourages increased ectopic lipid deposition in organs such as liver and increases plasma insulin levels.

Chapter 2 – Adipose Tissue Dendritic Cells are Independent Contributors to Obesity-Induced Inflammation and Insulin Resistance

Abstract

Dynamic changes of adipose tissue leukocytes, including adipose tissue macrophages (ATM) and adipose tissue dendritic cells (ATDC), contribute to obesity-induced inflammation and metabolic disease. However, inability to clearly discriminate between ATDCs and ATMs in adipose tissue has limited progress in the field of immunometabolism. In this study, we utilize CD64 to distinguish ATMs from ATDCs and investigated the temporal and functional changes in these myeloid populations during obesity. Flow cytometry and immunolabeling demonstrated that the definition of ATMs as $CD45^+F4/80^+CD11b^+$ cells overlaps with other myeloid leukocytes while $CD45^+CD64^+$ is specific for ATMs. The expression of core dendritic cell genes were enriched in $CD11c^+CD64^-$ cells (ATDC), while core macrophage genes were enriched in $CD45^+CD64^+$ cells (ATM). $CD11c^+CD64^-$ ATDCs expressed MHCII and co-stimulatory receptors and had similar capacity to stimulate $CD4^+$ T cell proliferation as ATMs. ATDCs were predominantly $CD11b^+$ conventional DCs and made up the bulk of $CD11c^+$ cells in adipose tissue with moderate high-fat diet exposure. Mixed chimeric experiments with $Ccr2^{-/-}$ mice demonstrated that high-fat diet induced ATM accumulation from blood monocytes was dependent on CCR2, while ATDC accumulation was less CCR2-dependent. ATDC accumulation during obesity was attenuated in $Ccr7^{-/-}$ mice and was associated with decreased adipose tissue inflammation and insulin resistance. $CD45^+CD64^+$ ATMs and $CD45^+CD64^-CD11c^+$ ATDCs were also identified in human

obese adipose tissue and ATDCs were increased in subcutaneous adipose tissue compared to omental. These results support a revised strategy for unambiguous delineation of ATMs versus ATDCs, and suggest that ATDCs are independent contributors to adipose tissue inflammation during obesity.

Introduction

Obesity-induced inflammation is believed to be a potent contributing factor to the development of type 2 diabetes and metabolic dysfunction. Metabolic inflammation is driven largely by the induction of inflammation in adipose tissue of obese subjects and is regulated by a network of adipose tissue leukocytes (98; 131). The inflammatory components in adipose tissue include both innate and adaptive immune cells that undergo both qualitative and quantitative changes with obesity. Myeloid cells were among the first leukocytes identified as being deranged in adipose tissue and in the circulation of obese subjects (132). Obese children, as young as three years old, have increased circulating neutrophils indicating an early influence of obesity on myeloid cell regulation (133). Associations between classical monocytes (Ly6c^{hi} in mice and CD14$^+$CD16$^+$ in humans), adipose tissue macrophage content, and insulin resistance suggest a mechanistic contribution of myeloid cells to the development of metabolic disease with obesity (134; 135). Furthermore, obesity-induced activation of neutrophils and macrophages in adipose tissue are required for insulin resistance in obese mice and correlate with metabolic disease in humans (117; 136).

Adipose tissue macrophages (ATM) are a dominant innate immune cell in adipose tissue and can comprise up to 40% of the non-adipocyte stromal vascular fraction (SVF) in obese adipose tissue (119; 137; 138). Murine ATMs have been primarily defined as F4/80$^+$CD11b$^+$ and with obesity an F4/80$^+$CD11b$^+$CD11c$^+$ ATM population accumulates (119; 139). The importance of CD11c$^+$ ATMs has been emphasized in numerous studies in both mice and humans (135; 139; 140). Obesity increases blood monocyte recruitment into adipose tissue and induces pro-inflammatory activation and upregulation of CD11c (141). Ablation of CD11c$^+$ cells attenuates adipose tissue inflammation and improves glucose tolerance without changes in body weight (122; 142). CD11c$^+$ ATMs have been

described as having a metabolically active phenotype with lysosomal activation and characteristics of classically activated M1 macrophages (137; 138). In addition to classical innate immune cytokine production, ATMs express high levels of MHC class II and are active antigen presenting cells that shape the expansion of conventional Th1 CD4$^+$ T cells, induction of effector/memory T cells, and the attenuation of regulatory T cells (Tregs) (142-144).

The accumulation of CD11c$^+$ cells in adipose tissue suggests the possibility that adipose tissue dendritic cells (ATDC) may also play a role in obesity-associated inflammation. *Ex vivo,* ATDCs can induce a Th17 profile in T cells that may explain the associations between Th17 cytokines and insulin resistance (145). ATDCs can contribute to the regulation of adipose tissue expansion by controlling adipose tissue T cell clonal expansion (146). GM-CSF-dependent DCs have also been shown to contribute to adipose tissue expansion in lean animals (147). However, since CD11b and F4/80 expression overlaps between macrophages and DCs, it has been difficult to clarify the relative contribution of ATDCs towards adipose tissue inflammation. In mouse obesity models, ATDCs have been defined as CD11b$^+$CD11c$^+$, CD11c$^+$F4/80^{lo}, CD11c$^+$, or CD11c$^+$F4/80^{neg-lo} leukocytes depending on the study (145-150). Based on these definitions, conventional (cATDC) and plasmacytoid (pATDC; B220$^+$) ATDCs have been reported. Unfortunately, the degree of overlap with the previously defined CD11c$^+$ and CD11c$^-$ ATM has not been clarified.

Almost all studies of murine ATMs have utilized F4/80 as the primary marker despite its known expression on non-macrophage leukocytes such as DCs and eosinophils. The Immunologic Genome Consortium identified markers including CD64 and MerTK that improve the specificity of tissue macrophage phenotyping in several tissues (151). The use of CD64 has been useful in untangling macrophage and DC identity and diversity in the gut (152; 153). In this study, we used CD64 to revisit the F4/80 ATM phenotyping strategy in hopes of improving our understanding of the dynamics and functions of ATM and ATDC during obesity. We support the use of CD64 as a highly specific ATM marker and that CD64$^-$CD11c$^+$ labeling defines a pure population of bona-fide myeloid ATDC present in lean and obese states in both mice and

humans. We distinguish CD11c$^+$ ATMs and CD11c$^+$ ATDCs induced by obesity with distinct gene expression profiles and lipid storage capacity. Using competitive reconstitution experiments, CD11c$^+$ ATM accumulation was found to be CCR2-dependent while ATDC recruitment was only partially CCR2-dependent. With moderate high fat diet feeding, ATDC are the dominant CD11c$^+$ cell population induced in adipose tissue. Studies using $Ccr7^{-/-}$ mice reveal decreased ATDC content and mice were protected from insulin resistance development. This work increases the resolution by which adipose tissue myeloid cells can be identified and suggests that ATDCs are an independent contributor to obesity-induced adipose tissue inflammation.

Materials and Methods

Animal studies

CD45.1 and CD45.2 C57BL/6J mice, CC chemokine receptor (CCR) 7$^{-/-}$ (B6.129P2(C)-CCR7tm1Rfor/J), and OT-II (B6.Cg-Tg (TcraTcrb)425Cbn/J) mice were obtained from Jackson Laboratories. Ccr2$^{-/-}$ and Csf2$^{-/-}$ mice were kindly provided by Dr. Beth Moore and Dr. John Osterholzer at the University of Michigan, respectively. Male mice were *ad libitum* fed a control normal diet (ND; 4.09 kcal/g; 29.8% protein, 13.4% fat and 56.7% carbohydrate; PicoLab 5L0D, LabDiet) or fed a high-fat diet (HFD; 5.24 kcal/g; 20% protein, 60% fat and 20% carbohydrate; Research Diets) *ad libitum* beginning at 6 weeks of age. All animal experiments were approved by the University Committee on Use and Care of Animals at the University of Michigan and conducted in compliance with the Institute of Laboratory Animal Research Guide for the Care and Use of Laboratory Animals.

Bone marrow transplantation

Competitive bone marrow transplants were performed as described (154). Briefly, bone marrow cells were isolated from donor groups (CD45.1$^+$ CCR2$^{+/+}$ and CD45.2$^+$ CCR2$^{-/-}$) and mixed in a 1:1 ratio. Six week old CD45.1 mice were lethally irradiated

(900 Rad) and intravenously injected six hours after irradiation with 10×10^6 cells of the mixed bone marrow donor cells re-suspended in 150 μl of PBS. Bone marrow reconstitution efficiency was evaluated by examining peripheral blood leukocyte CD45.1$^+$:CD45.2$^+$ ratios at 6 weeks after transplantation, and recipient animals were fed either a ND or HFD for 15 weeks.

Human adipose tissue

Human omental and subcutaneous adipose tissues were collected intraoperatively from patients undergoing bariatric surgery at the University of Michigan and the Ann Arbor VA Hospital. All human use protocols were approved by the University of Michigan and Ann Arbor VA Hospital Institutional Review Boards.

Immunofluorescence microscopy

Immunofluorescence staining was performed as described (155) using the following antibodies: anti-CD64 (X54-5/7.1), anti-F480 (A3-1), anti-Mgl1 (MP23), anti-CD11c (N418), anti-Mac2 (M3/38), and anti-Caveolin (2297). Images were collected using an Olympus Fluoview 100 laser scanning confocal microscope.

SVF isolation and flow cytometry analysis

Stromal vascular fraction cells (SVF) were isolated as described previously (156). Cells were incubated in Fc Block for 10 min on ice and stained with indicated antibodies for 30 min at 4°C. Antibodies used for flow cytometry in this study are provided in Table 4. Live/dead fixable violet staining kits (Life Technology) and BODIPY (Life Technology) were used according to the manufacturers' instruction. Cells were analyzed on a FACSCanto II Flow Cytometer (BD Biosciences) using FlowJo 10.6 software (Treestar). For fluorescence-activated cell sorting (FACS), SVF were suspended in RPMI/2%HI-FBS and purified by FACSAria III (BD Biosceinces). Fluorescence minus

one controls were used to confirm SiglecF, Ly6G, and CD11c expression in SVF analyses in mice and humans in at least three independent experiments.

Microarray and real-time RT-PCR

Male C57BL/6 mice fed normal diet or HFD for 20 weeks were used for gene expression analysis in macrophages and dendritic cells. Cells were identified as macrophages ($CD45^+CD11c^+CD64^+$ and $CD45^+CD11c^-CD64^+$) or DC ($CD45^+CD11c^+CD64^-$) and sorted using a BD FACSAria III cell sorter. Microarray analyses were carried out as previously described (49). RNA was extracted using QIAzol (Qiagen) and amplified and hybridized on the Affymetrix Mouse Gene 2.1 ST array. RNA quality was assessed on Agilent Bioanalyzer Picochip. After quality control assessments probe sets with unadjusted p-value of 0.05 or less were identified. Differences in gene expression were identified and analysis was performed through the University of Michigan Microarray Core using affy, limman, and affy PLM packages of bioconductor implemented in the R statistical environment.

For real-time PCR, RNA from tissues and cells was prepared using RNeasy Midi Kits (QIAGEN), and cDNA was generated using high-capacity cDNA reverse transcription kits (Applied Biosystems). Real-time RT-PCR analyses were done in duplicate on the ABI PRISM 7900 Sequence Detector TaqMan System with the SYBR Green PCR kit as instructed by the manufacturer (Applied Biosystems). Primer sequences used for this study are shown in Table 5. Arbp or 18S was used as a housekeeping gene/internal standard for normalization. Relative expression was determined using standard $2^{-\Delta\Delta Ct}$ method.

CFSE dilution assay

Antigen-specific T cell activation assay was performed as previously described (144). Briefly, FACS-sorted cells were grown in 90-well U bottom plates, then pulsed with 100 µg/ml whole OVA (ThermoScientific). CD4$^+$ T cells were isolated from the spleen of OT-II mice using CD4+ T cell negative selection kites (Miltenyi Biotec). CD4$^+$ T cells were labeled with 2 µmol/L carboxy fluorescein succinimidyl ester (CFSE) and added to antigen-pulsed cells at a 1:1 ratio. After 5 days, T cells were stained for flow cytometry, and CFSE dilution was examined in viable CD3$^+$CD4$^+$ lymphocytes.

Metabolic evaluation

Body weights were measured weekly. Blood glucose and plasma insulin were measured by glucometer and an insulin ELISA kit (Crystal Chem), respectively.

Statistical Analysis

Data are expressed as means ± SEM. Statistical differences were assessed using a 2-tailed t test or analysis of variance (with Tukey's post-test analysis), using GraphPad Prism software. A p value of less than 0.05 was considered statistically significant.
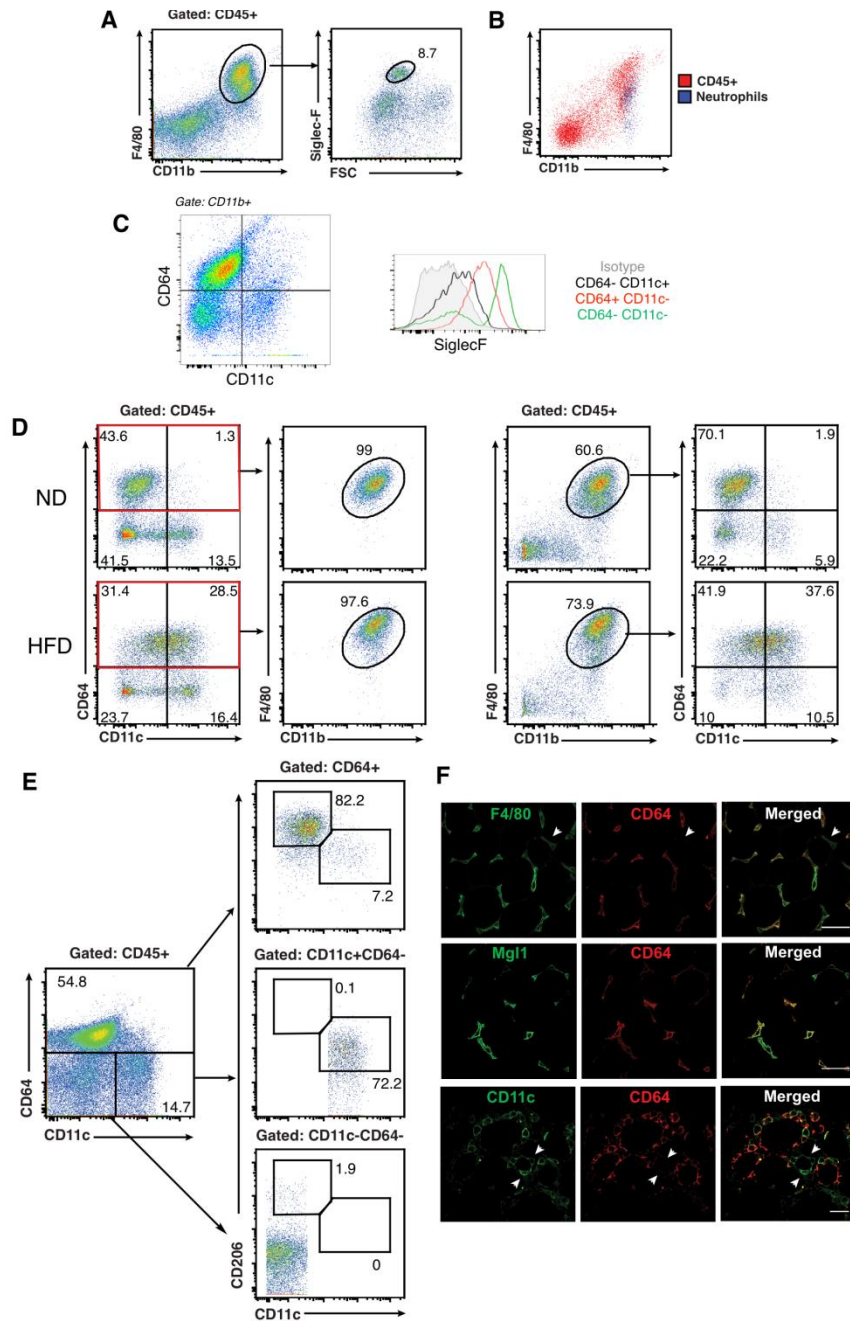
Figure 2-1 – CD64 is a specific ATM marker in lean and obese mice. Analysis of SVF from eWAT of C57BL/6 mice fed with ND or HFD for 20 weeks. (A) Flow cytometry analysis of eosinophils (siglec-F$^+$ and high side scatter) on CD11b$^+$F480$^+$ cells after gating CD45$^+$ stromal vascular fraction cells (SVF) from lean mice. (B) Overlap between F480$^+$ CD45$^+$ SVF cells (red) and neutrophils (blue) from obese mice. (C) Analysis of Siglec-F expression in CD64 stratified SVF cells. (D) Comparison of CD64 and F4/80 staining in SVF from ND and HFD fed mice. (E) Flow analysis of CD11c and CD206 expression in CD64$^+$ (top), CD11c$^+$CD64$^-$(middle) and CD11c$^-$CD64$^-$ (bottom) SVF cells from lean mice. (F) Immunofluorescence analysis of CD64$^+$ (red) cells in eWAT from lean (top 2 rows) and HFD-fed (bottom row) mice. Scale bar = 100 μm.

Arrowheads indicate CD64⁻ cells. Data are representative of at least three independent experiments with three mice per group.

Results

CD64 distinguishes ATMs from eosinophils, neutrophils, and ATDCs in lean and obese mice

Our group and others have defined ATM as CD45$^+$F4/80$^+$CD11b$^+$ cells in the SVF despite the potential for non-macrophage F4/80$^+$ cell contamination. Co-staining with markers for eosinophils (Siglec-F) and neutrophils (Ly6G) demonstrated that these cells are present within the CD45$^+$F4/80$^+$CD11b$^+$ fraction in both lean and obese mice (Figure 2-1A-B). We examined the utility of CD64 as a more specific marker of ATM in lean and obese (HFD fed for 10-12 weeks) mice. Adipose tissue eosinophils were CD64$^-$ in both lean and obese mice (Figure 2-1C) with CD64$^+$ macrophages showing intermediate SiglecF expression. Using CD64 and CD11c, lean mice demonstrated prominent populations of CD64$^+$CD11c$^-$ (putative ATMs) and CD64$^-$CD11c$^+$ cells (putative ATDCs) with rare CD64$^+$CD11c$^+$ cells (Figure 2-1D). In obese mice, there was an increase in CD64$^+$CD11c$^+$ (CD11c$^+$ ATMs) while distinct CD64$^+$CD11c$^-$ and CD64$^-$ CD11c$^+$ cells were still identifiable. All CD45$^+$CD64$^+$ cells expressed CD11b and F4/80, indicating that CD64 is capable of labeling cells that have been previously identified as CD45$^+$F4/80$^+$CD11b$^+$ ATM. However, >20% of CD45$^+$F4/80$^+$CD11b$^+$ cells in both lean and obese adipose tissue were CD64$^-$, further supporting the presence of non-macrophage cells within the F4/80$^+$ population.

F4/80$^+$CD11b$^+$ ATM in lean mice have high expression of markers for alternatively activated macrophages such as CD206 and CD301/Mgl1 (157). In lean mice 82% of the of the CD64$^+$ population were also CD206$^+$, with rare CD64$^-$CD11c$^-$CD206$^+$ cells identified (Figure 2-1E). The ability of CD64 to identify ATMs was further confirmed with immunofluorecence microscopy. There was co-localization of F4/80 and CD64 staining in lean mice, however F4/80$^+$ cells were also identified that did not stain for CD64. Co-localization between Mgl1 and CD64 staining was prominent in lean adipose tissue (Figure 2-1F). In obese mice, where CD11c$^+$ cells accumulate in adipose

32

tissue, co-localization between CD11c and CD64 was observed. However, distinct populations of CD11c$^+$ cells were identified that did not stain positive for CD64 in obese adipose tissue. Mac2 and CD64 staining showed significant overlap, especially in crown-like structures (CLS) where dense myeloid cell accumulation is known to occur.

Gene expression profiling supports distinguishing ATM and ATDC based on CD64

These initial studies suggest that ATMs are more stringently defined as CD45$^+$CD64$^+$CD11c$^{+/-}$ cells and may permit the delineation of a CD45$^+$CD64$^-$CD11c$^+$ ATDC population. To validate this, microarray analysis was performed on RNA from FACS sorted CD45$^+$CD64$^+$CD11c$^-$, CD45$^+$CD64$^+$CD11c$^+$, and CD45$^+$CD64$^-$CD11c$^+$ cells from adipose tissue of lean and obese mice. Due to low numbers, CD64$^+$CD11c$^+$ leukocytes from lean mice were not included in the analysis. When compared against the ImmGen core set of macrophage specific genes (151), CD64$^+$ cells were significantly enriched for macrophage-related genes in both lean and obese mice (Figure 2-2A). In contrast, expression of the core DC-related genes was highly enriched in CD64$^-$ cells in both lean and obese conditions (Figure 2-2B). Independent samples of FACS sorted CD64$^+$ and CD64$^-$ cells from adipose tissue confirmed these differences (Figure 2-2C). Core macrophage-related genes such as *Mertk* and *Camk1* were highly expressed in CD64$^+$ cells while DC-related genes *Flt3* and *Zbtb46* were enriched in CD64$^-$CD11c$^+$ cells.
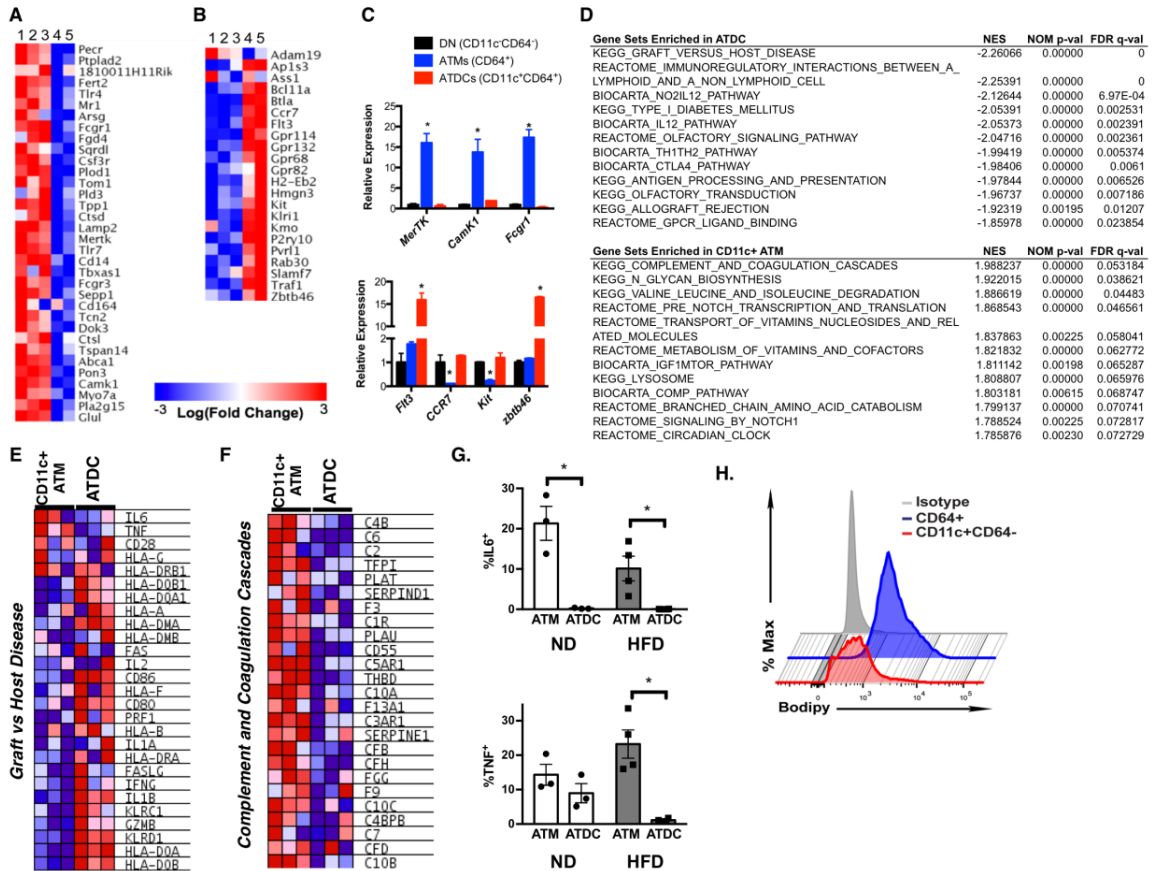
Figure 2-2 – Gene expression profiling of ATMs and ATDCs. Microarray analysis heat map of ImmGen (A) macrophage core signature genes and (B) DC core signature genes from adipose tissue myeloid cells. Lane 1: lean ATM CD11c$^-$CD64$^+$; lane 2: obese ATM CD11c$^-$CD64$^+$; lane 3: obese ATM CD11c$^+$CD64$^+$; lane 4: lean ATDC CD11c$^+$CD64$^-$; and lane 5: obese ATDC CD11c$^+$CD64$^-$. (C) Quantitative PCR analysis of macrophage-specific genes (upper panel) and DC-specific genes (lower panel) in CD11c$^-$CD64$^-$ double negative (DN), CD64$^+$ (ATM), and CD11c$^+$CD64- (ATDC) cells from eWAT of obese mice. (D) Gene Set Enrichment Analysis pathways enriched in ATDCs and CD11c$^+$ ATMs. Heat maps shown for differentially expressed genes for (E) graft-versus-host disease and (F) complement and coagulation cascade. (G) Intracellular cytokine staining for ATMs and ATDCs from ND and HFD fed mice eWAT. (H) Flow cytometry analysis of intracellular lipid content in CD64$^+$ ATMs and CD11c$^+$CD64$^-$ ATDCs from obese mice. Data are from two independent experiments with three mice per group. *$p < 0.05$.

Gene Set Enrichment Analysis was used to identify uniquely enriched networks in ATDCs and CD11c$^+$ ATMs in obese mice (Figure 2-2D). The top category for ATDCs was enrichment for genes involved in Graft vs Host Disease and interactions between antigen presenting cells and lymphoid cells. Examining this set showed that ATDCs are

enriched for the expression of cytokine genes including *Il2*, *Il1a, Ifng,* and *Il1b,* but not for *Il6* and *Tnfa* (Figure 2-2E-F). We confirmed this by intracellular cytokine staining that showed a higher number of IL-6$^+$ and TNFα^+ ATMs compared to ATDCs in lean and obese mice (Figure 2-2G). For CD11c$^+$ ATMs, Complement and Coagulation Cascade genes had the highest enrichment score along with genes involved in Glycan Biosynthesis and Lysosomes. A lipid-laden phenotype with activated lysosomes is associated with obesity and seen in obese rodent and human ATMs (115; 158). When ATMs and ATDCs from HFD fed mice were examined for lipid accumulation by BODIPY staining, ATMs had significantly higher BODIPY staining compared to ATDCs (Figure 2-2H).

ATDC are predominantly CD11b$^+$ conventional DCs

The surface marker profile of CD45$^+$CD64$^-$CD11c$^+$ ATDC was examined to further evaluate the phenotypes of ATDCs (Figure 2-3A). Both ATMs and ATDCs from lean mice express MHCII, CD40, CD80, and CD86. All of these antigen presenting cell (APC) markers were expressed at higher levels in ATMs compared to ATDCs, which suggests an immature phenotype of ATDCs in lean mice. With obesity, MHCII expression on ATDCs was significantly increased (Figure 2-3B). We have previously shown that ATMs are potent functional APCs. *In vitro* T cell stimulation assays were performed to compare ATM and ATDC APC function (Figure 2-3C). CFSE labeled CD4$^+$ T cells from OT-II mice were incubated with ATMs and ATDCs after loading with OVA (100 µg/ml). Both ATMs and ATDCs were able to stimulate T cell proliferation to a similar extent.
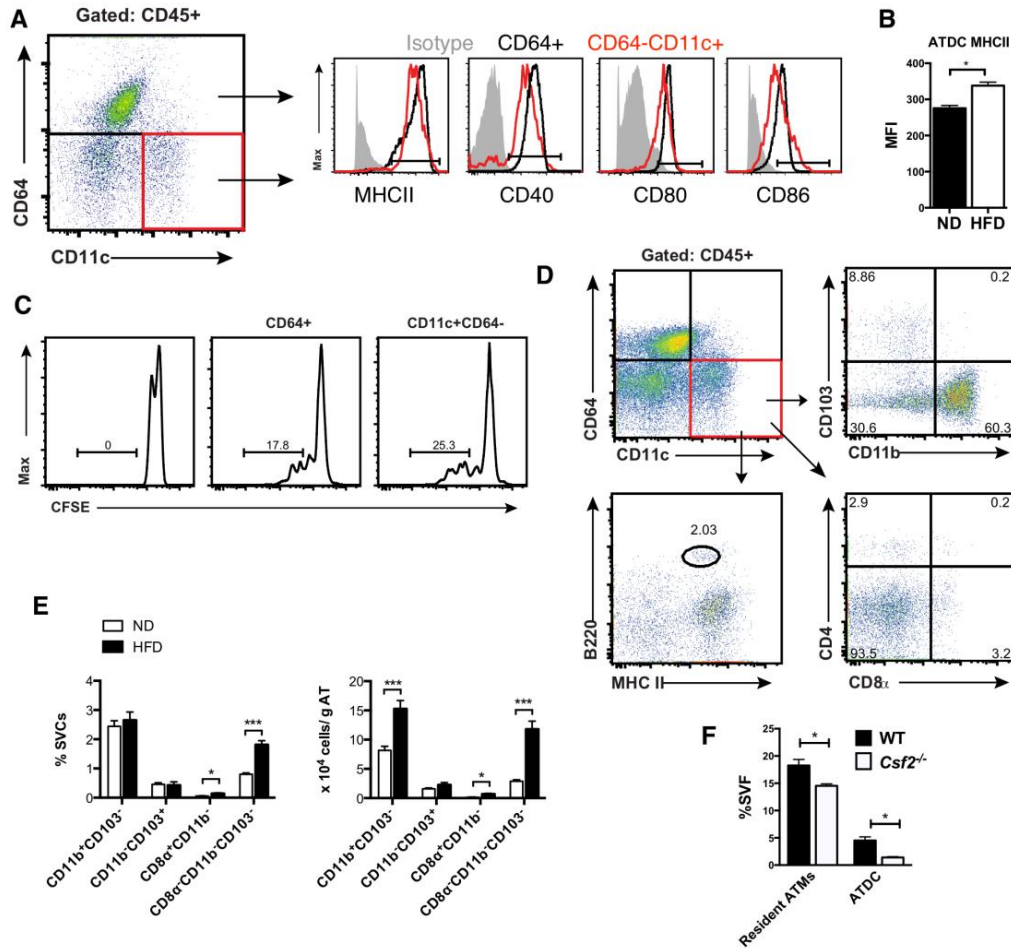
Figure 2-3 – Myeloid DCs predominate in adipose tissue. (A) Flow cytometry analysis of MHCII and costimulatory molecules in CD64$^+$ ATM (blue) and CD11c$^+$CD64$^-$ ATDC (red) from eWAT. (B) MHCII expression in ATDC in ND and HFD mice. (C) OTII-CD4$^+$ T cell proliferation after incubation with OVA-pulsed CD64$^+$ ATM (middle) and CD11c$^+$CD64$^-$ ATDC (right). One representative experiment from three independent replicates is shown. (D) ATDC subsets based on CD103, CD11b, CD4, CD8α, B220 and MHCII. (E) Quantitation of ATDC subsets in eWAT from ND- and HFD-fed mice. (F) Quantitation of ATM and ATDC in lean WT and *Csf2*$^{-/-}$ mice. *p < 0.05; ***p < 0.001.

Additional markers were used to identify ATDC subpopulations (Figure 2-3D). The majority of ATDCs in lean mice were CD11b$^+$ (>60%). Rare populations of CD103$^+$, B220$^+$, CD4$^+$, and CD8$^+$ ATDCs were also identified in lean mice suggesting that the majority of ATDCs are of the conventional CD11b$^+$ type. In obese mice, CD11b$^+$ myeloid cDCs remained the dominant ATDC type and the quantity of CD11b$^+$ ATDCs, normalized to adipose tissue weight, was increased by two-fold compared to lean mice

(Figure 2-3E). There was a small, but significant increase in $CD8a^+CD11b^-$ ATDC with HFD as well as a significant increase in ATDC that were negative for CD103, CD8 or CD11b. Consistent with the prominence of myeloid-derived $CD11b^+$ cATDCs, ATDC content was decreased in $Csf2^{-/-}$ mice (Figure 2-3F).

A. Epididymal WAT

B. Inguinal WAT

- CD64$^+$ CD11c$^+$ ATM
- CD64$^+$ CD11c$^-$ ATM
- CD64$^-$ CD11c$^+$ ATDC
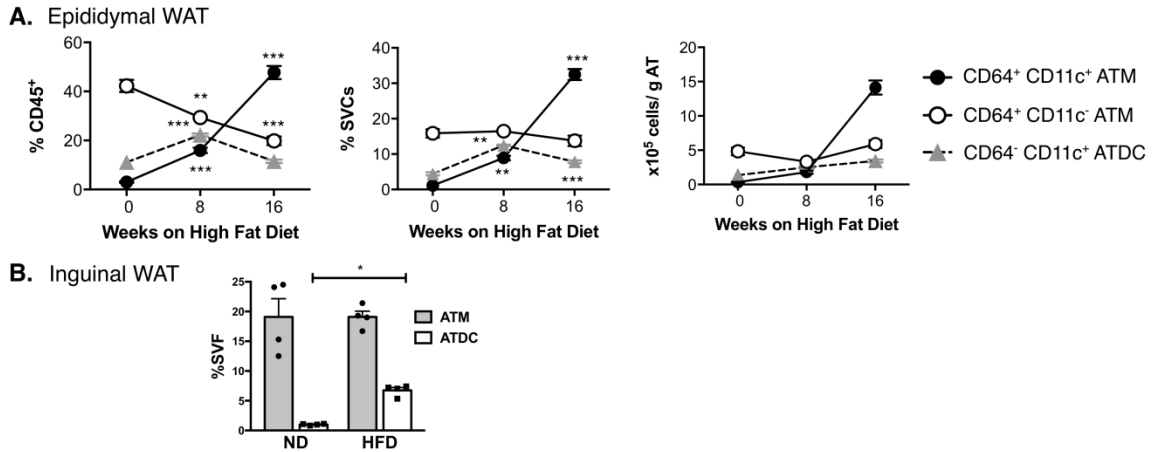
Figure 2-4 – Time course of ATM and ATDC accumulation in adipose tissue with HFD-induced obesity. C57BL/6 male mice were fed an HFD for various time periods (0, 8, and 16 wk). (A) eWAT SVFs quantified for CD11c$^+$ ATMs, CD11c$^-$ ATMs, and ATDCs by flow cytometry normalized for adipose tissue mass. (B) Quantitation of ATMs and ATDCs in iWAT at 16 wk of HFD. *p < 0.05, **p < 0.01, ***p < 0.001.

ATDC are a dominant CD11c$^+$ population with moderate high fat diet exposure

We next performed time course studies to examine the kinetics of accumulation of ATMs (CD11c$^+$ and CD11c$^-$) and ATDCs in gonadal/epididymal adipose tissue (eWAT) (Figure 2-4A). Mice were examined after 8 and 16 weeks of HFD feeding. 16 weeks of HFD induced a significant increase in body weight associated with eWAT hypertrophy and the development of fasting hyperglycemia (Data not shown). In lean mice, CD11c$^-$ ATMs were the dominant myeloid cell population as a percentage of all CD45$^+$ leukocytes. The majority of CD11c$^+$ cells in lean mice were ATDCs and not ATMs. With eight weeks of HFD, both CD11c$^+$ ATMs and CD11c$^+$ ATDCs increased in number. At this time point, ATDCs were still the larger CD11c$^+$ cell population in adipose tissue. 16 weeks of HFD exposure led to a substantial increase in CD11c$^+$ ATMs and the maintenance of a prominent population of ATDCs. Inguinal adipose tissue (iWAT) ATM content was not

significantly increased with HFD feeding (Figure 2-4B). However, there was a significant

induction of ATDCs in iWAT similar to what was seen in eWAT.
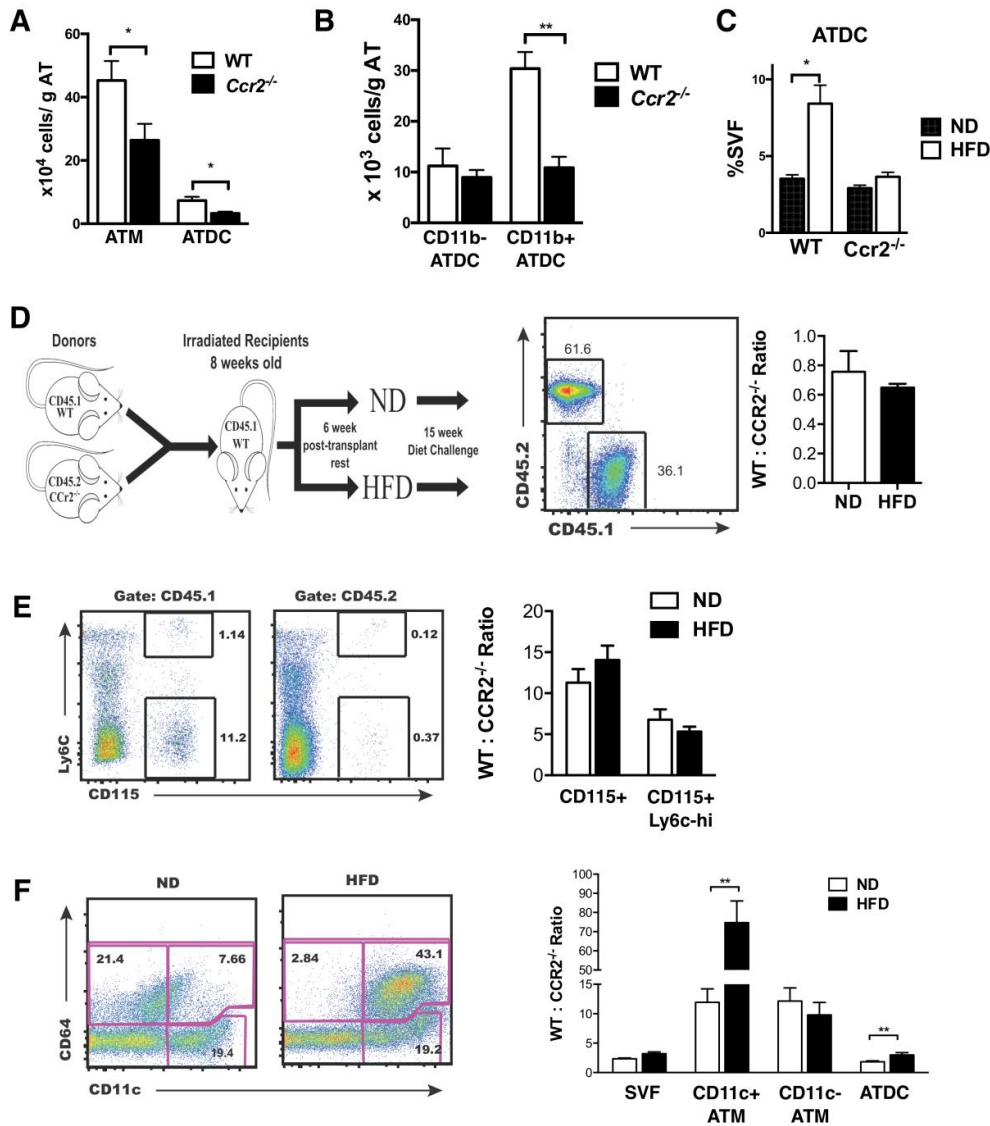
Figure 2-5 – CCR2 is required for obesity-induced CD11c$^+$ ATM and ATDC migration into adipose tissue. (A) Quantitation of CD11c$^+$ ATMs, CD11c$^-$ ATMs, and ATDCs in eWAT from WT and $Ccr2^{-/-}$ mice. (B) Quantitation of CD11b$^+$ and CD11b$^-$ ATDC subsets in eWAT from WT and $Ccr2^{-/-}$ mice. (C) ATM and ATDC content in WT and $Ccr2^{-/-}$ mice after 2 wk of ND or HFD feeding. (D) Diagram of mixed chimera experiment design. $Ccr2^{-/-}$ (CD45.2) and WT (CD45.1) bone marrow mixed in a 1:1 ratio before injection in irradiated recipients. Chimerism analysis of blood leukocytes is shown. (E) Frequency and ratio of CD45.1 (WT) and CD45.2 ($Ccr2^{-/-}$) in blood monocytes from lean and obese (15-wk HFD) chimeric mice. (F) Frequency and CD45.1/CD45.2 ratio in CD11c$^+$ ATMs, CD11c$^-$ ATMs, and ATDCs in eWAT. *p < 0.05, **p < 0.01 versus ND.

Differential recruitment dependence of CD11c$^+$ ATMs and ATDCs on CCR2 during diet-induced obesity

Monocyte recruitment is a primary mechanism by which CD11c$^+$ ATMs accumulate in adipose tissue during obesity (157; 159). Since our results suggest that the prior definition of F4/80$^+$CD11b$^+$CD11c$^+$ ATM is contaminated with ATDCs and other leukocytes, we revisited ATM and ATDC accumulation in *Ccr2$^{-/-}$* mice using CD64. *Ccr2$^{-/-}$* mice had significantly reduced ATM and ATDC compared to WT (Figure 2-5A). Specifically, CD11b$^+$ ATDC were decreased in *Ccr2$^{-/-}$* mice, but there were no differences in CD11b$^-$ ATDC (Figure 2-5B). With 2 weeks of HFD, we observed an increase in ATDC in WT, but not in *Ccr2$^{-/-}$* mice indicating that CCR2 is important for ATDC accumulation with short term HFD exposure (Figure 2-5C).

Since *Ccr2$^{-/-}$* mice have fewer circulating monocytes (159), it is difficult to discern whether ATM and ATDC accumulation in adipose tissue relies on *Ccr2* dependent signals for trafficking or is dependent on the size of the blood monocyte pool. To evaluate this, we used a mixed chimera model where lethally irradiated recipients were reconstituted with a 1:1 mixture of bone marrow cells from WT (CD45.1) and *Ccr2$^{-/-}$* (CD45.2) donor mice (Figure 2-5D). After reconstitution, the chimeras were fed ND or HFD for 16 weeks. Blood chimerism analysis was performed to evaluate the ratio of WT:*Ccr2$^{-/-}$* cells (CD45.1/CD45.2) relative to the BM input ratio of 1. Analysis of total peripheral blood leukocytes demonstrated a slight bias towards reconstitution with cells from *Ccr2$^{-/-}$* donors with the ratio of WT:*Ccr2$^{-/-}$* cells (CD45.1/CD45.2) less than 1 in both ND and HFD conditions. However, analysis of circulating CD115$^+$ monocytes demonstrated a significant increase in monocytes derived from WT compared to *Ccr2$^{-/-}$* mice with a WT:*Ccr2$^{-/-}$* ratio of 11.3 ± 1.6 (Figure 2-5E). Circulating WT derived cells dominated over *Ccr2$^{-/-}$* cells in both Ly-6c^{hi} and Ly-6c^{lo} blood monocyte subsets. This is consistent with the requirement of CCR2 to regulate monocyte exit from the bone marrow compartment into the circulation.

EWAT ATMs were also examined in the chimeras (Figure 2-5F). As expected, CD64$^+$ ATMs from ND fed mice were primarily CD11c$^-$ while HFD induced CD11c$^+$ ATM accumulation. In lean mice, the WT:$Ccr2^{-/-}$ ratio in both CD11c$^-$ and CD11c$^+$ ATMs was elevated (12.2 ± 2.2 and 11.9 ± 2.2, respectively) and was similar to what was observed in blood monocytes. This suggests that in a competitive reconstitution model both ATM subsets in lean mice may be dependent on circulating monocyte for reconstitution. In contrast, the WT:$Ccr2^{-/-}$ ratio of ATDCs in lean mice was significantly lower (1.8 ± 0.16) than what was observed in either ATMs or circulating monocytes. In obese mice, the WT:$Ccr2^{-/-}$ ratio of CD11c$^+$ ATMs was markedly increased (74.7 ± 11.7). This demonstrates that in the obese environment WT monocytes had a significant competitive advantage in trafficking to adipose tissue from the circulation compared to $Ccr2^{-/-}$ monocytes. In contrast, there was no change in the WT:$Ccr2^{-/-}$ ratio of CD11c$^-$ ATMs suggesting that any accumulation of CD11c$^-$ ATMs during obesity is CCR2 independent. While the WT:$Ccr2^{-/-}$ ratio of ATDCs was lower than that of blood monocytes in lean mice, there was a statistically significant increase in the WT:$Ccr2^{-/-}$ ratio in ATDCs (3.0 ± 0.4) in obese mice suggesting some ATDCs are dependent on CCR2 for trafficking to adipose tissue with obesity. However, the increased accumulation of ATDCs during obesity was less dependent on CCR2 than CD11c$^+$ ATMs (~1.6 fold increase for ATDCs versus ~6.3 fold increase for CD11c$^+$ ATMs). Overall this suggests that in chronic obesity, CCR2 signaling plays a critical role in regulating monocyte trafficking into obese adipose tissue to generate CD11c$^+$ ATMs and, to a lesser degree, ATDCs.

CCR7 is required for HFD-induced ATDC accumulation and insulin resistance.

The microarray analysis identified *Ccr7* as differentially expressed in ATDCs compared to ATMs. To evaluate whether CCR7 plays a role in the recruitment or maintenance of ATDCs in adipose tissue, age-matched male WT and *Ccr7*$^{-/-}$ mice were fed ND or HFD *ad libitum* for 8 weeks. This feeding duration was chosen based on our observation that 8 weeks led to increased ATDCs but minimal accumulation of CD11c$^+$ ATMs. In ND-fed mice, the quantity of CD11c$^+$ and CD11c$^-$ ATMs did not differ

between genotypes. However, $Ccr7^{-/-}$ mice had significantly fewer ATDCs compared to WT mice primarily due to a decrease in CD11b$^+$ ATDCs (Figure 2-6A-B). Eight-week HFD challenge induced CD11c$^+$ ATM and ATDC accumulation in both genotypes, but HFD-induced ATDC accumulation was significantly impaired in $Ccr7^{-/-}$ mice when normalized to adipose tissue weight (Figure 2-6C). CD11b$^+$ ATDCs in $Ccr7^{-/-}$ adipose tissue were ~50% lower than WT adipose tissue. Meanwhile, the quantity of CD11b$^-$ ATDCs was similar between genotypes (Figure 2-6D). After 8-weeks of HFD, $Ccr7^{-/-}$ mice had normal numbers of circulating monocytes and similar levels of Ly-6C^{hi} and Ly6C^{lo} monocytes compared to WT (Figure 2-6E). Importantly, there was no difference in the accumulation of splenic macrophages and DCs between genotypes (Figure 2-6F). These data suggest that HFD induces ATDC accumulation via CCR7-dependent increases in CD11b$^+$ ATDCs.
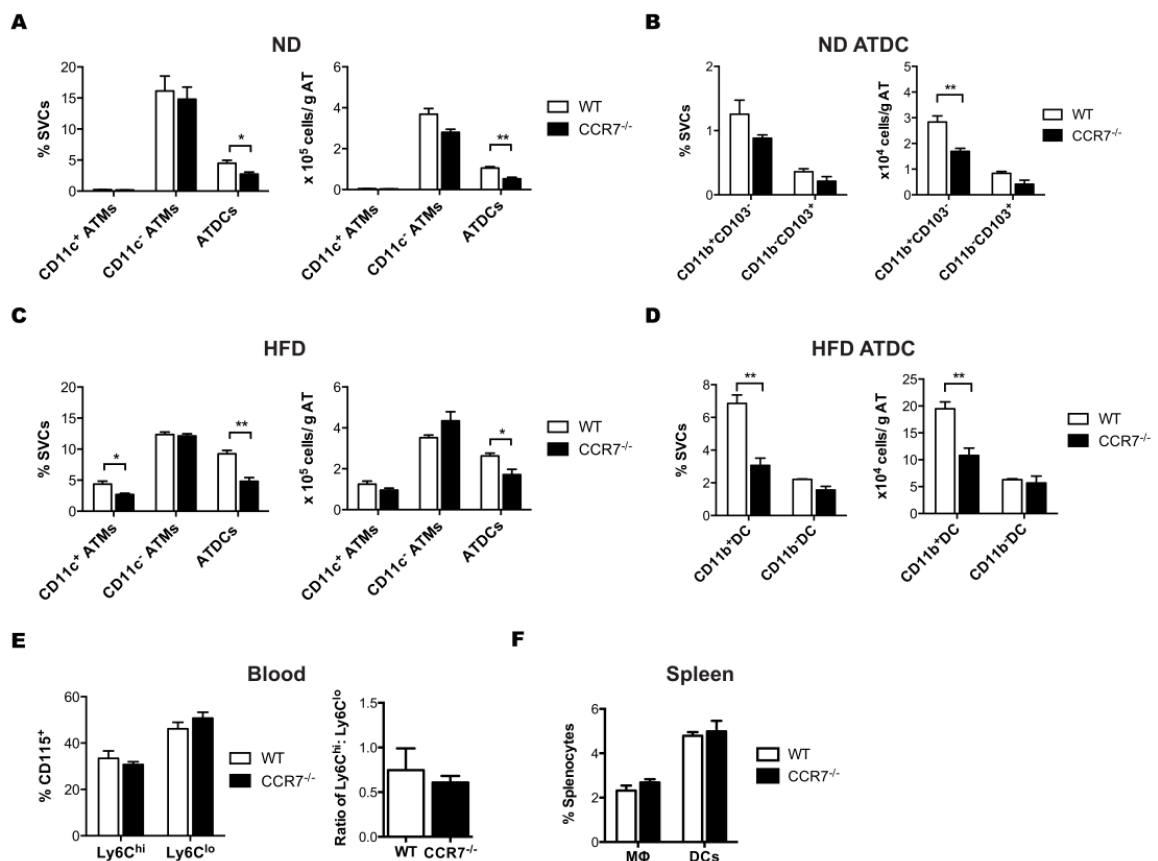
Figure 2-6 – CCR7 is required for ATDC accumulation during diet-induced obesity. (A) Quantitation of ATMs and ATDCs in eWAT from chow-fed WT and $Ccr7^{-/-}$ mice. (B) Quantitation of CD11b$^+$CD103$^-$ and CD11b$^-$CD103$^+$ ATDC subsets in eWAT from WT and

Ccr7^{−/−} mice. (C) Quantitation of CD11c^{+} ATMs, CD11c^{−} ATMs, and ATDCs in eWAT from WT and *Ccr7*^{−/−} mice fed HFD for 8 wk. (D) Quantitation of CD11b^{+} and CD11b^{−} ATDC subsets in eWAT from WT and Ccr7^{−/−} HFD-fed mice. (E) Frequency of Ly6^{hi} and Ly6^{lo} blood monocytes from WT and *Ccr7*^{−/−} mice. (F) Frequency of macrophages and DCs in spleen from WT and *Ccr7*^{−/−}. *p < 0.05, **p < 0.01.
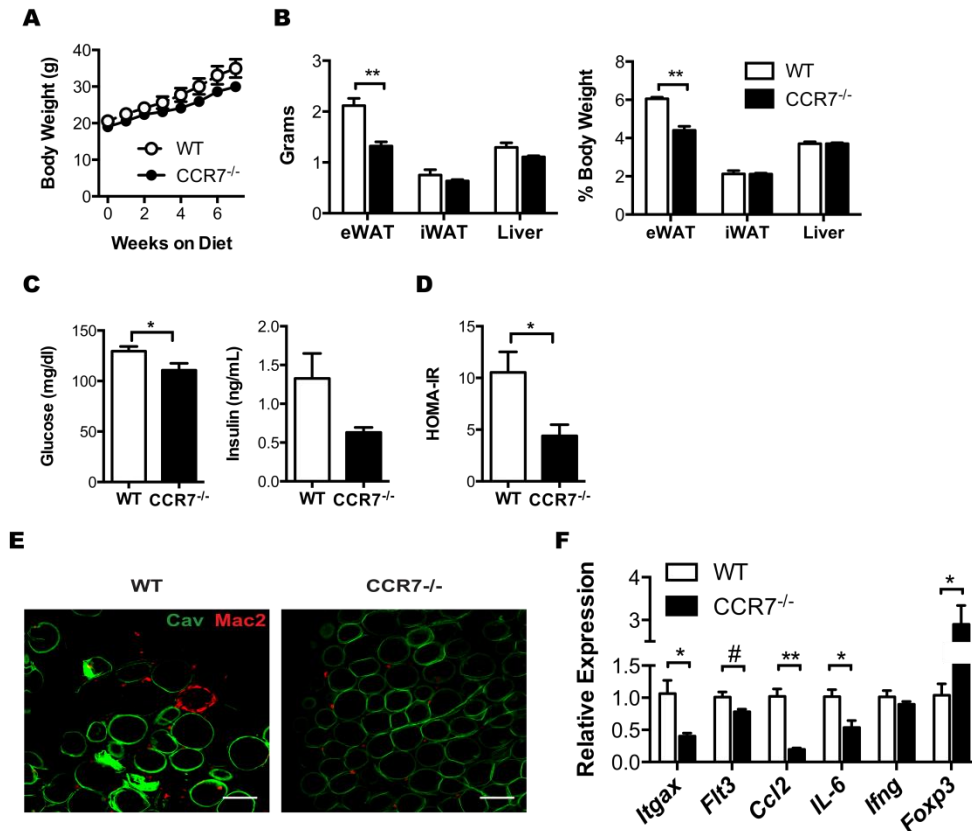
Figure 2-7 – CCR7-deficient mice are protected from HFD-induced insulin resistance and adipose tissue inflammation. (A) Body weights of WT and *Ccr7*^{−/−} mice during 8-wk HFD feeding. (B) Organ weights at the end of HFD exposure. (C) Fasting blood glucose and plasma insulin levels. (D) HOMA-IR in WT and *Ccr7*^{−/−} mice fed HFD for 8 wk. (E) Immunofluorescence imaging of Mac2^{+} ATM (red) and caveolin[+] adipocytes (green) in eWAT. Scale bar, 100 mm. (F) Expression of select immune-related genes in eWAT from HFD-fed WT and *Ccr7*^{−/−} mice. *p < 0.05, **p < 0.01, #p = 0.06.

We next examined the impact of *Ccr7* deficiency on HFD-induced insulin resistance and adipose tissue inflammation. Total body weight between the genotypes was not significantly different on HFD (Figure 2-7A). *Ccr7*^{−/−} mice had lower total eWAT weights (Figure 2-7B). Inguinal adipose tissue (iWAT) and liver weights were

similar between genotypes. Compared to WT mice, $Ccr7^{-/-}$ mice had lower fasting glucose levels and lower fasting insulin levels resulting in improved insulin sensitivity in $Ccr7^{-/-}$ mice based on the calculation of HOMA-IR (Figure 2-7C-D). Whole mount imaging of eWAT showed a significant accumulation of Mac2$^+$ cells in CLSs of WT eWAT, whereas CLSs were largely absent in $Ccr7^{-/-}$ eWAT (Figure 2-7E). Consistent with the flow cytometry data, gene expression of *Itgax* and *Flt3* were decreased in $Ccr7^{-/-}$ eWAT. In addition, *Ccl2* and *IL-6* expression were decreased and *Foxp3* expression was increased in $Ccr7^{-/-}$ eWAT (Figure 2-7F). Obese $Ccr7^{-/-}$ mice had increased adipose CD4$^+$ and CD8$^+$ cells suggesting that metabolic protection in these mice is not due to fewer T cells (data not shown). Overall, these data suggest that CCR7-dependent signals contribute to insulin resistance and adipose tissue inflammation by regulating ATDC content independently of ATMs.
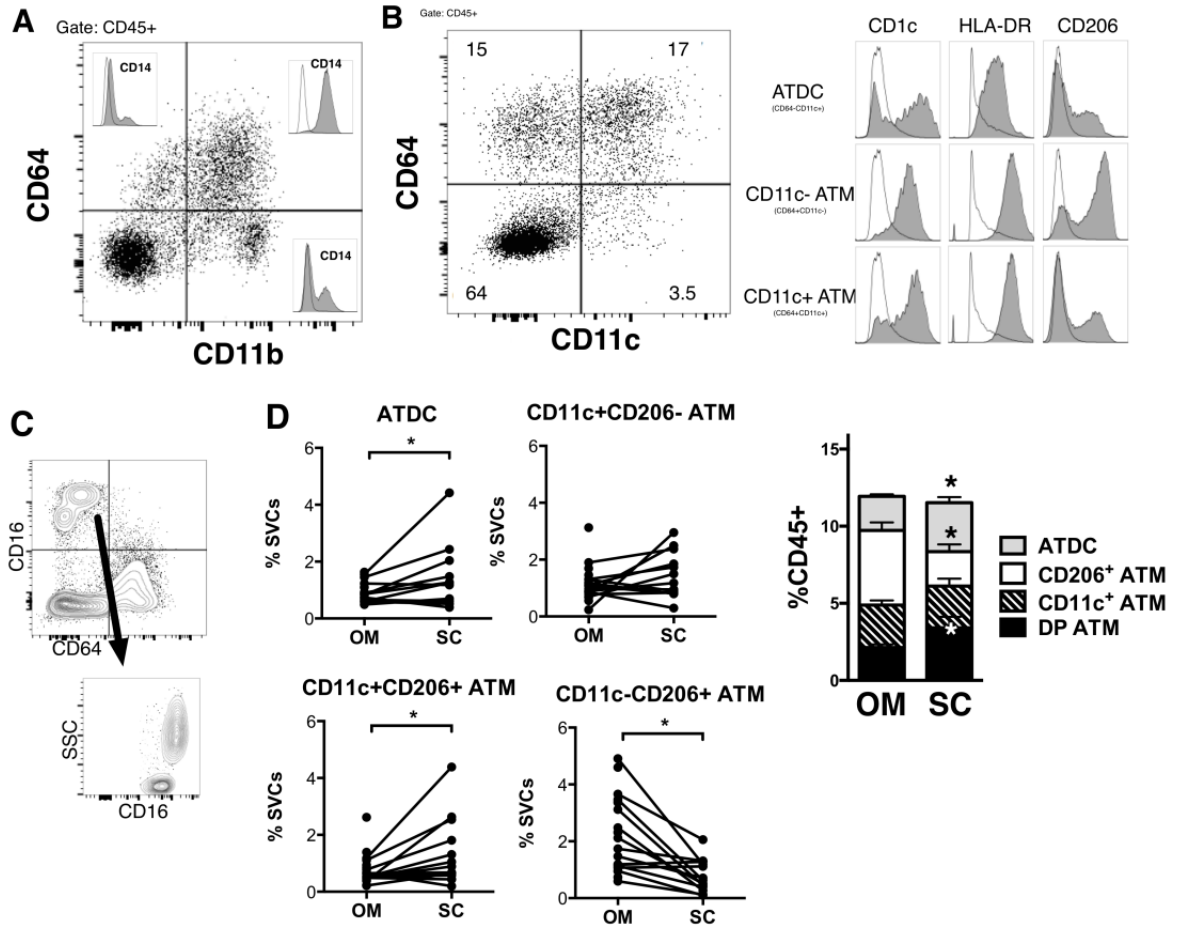
Figure 2-8 – CD64$^-$ CD11c$^+$ ATDCs are enriched in subcutaneous adipose tissue from obese humans. (A) SVF was isolated from human omental (OM) and subcutaneous adipose tissue, and analyzed by flow cytometry. Analysis of CD64-expressing cells and overlap with CD14 in OM. A representative plot of three independent experiments is shown. (B) Marker expression of CD64$^-$ CD11c$^+$ ATDCs, CD64$^+$ CD11c$^-$ ATMs, and CD64$^+$ CD11c$^+$ ATMs in OM. (C) Contour plot showing CD16 and CD64. (D) Frequency of ATDCs, CD11c$^+$CD206$^-$ ATMs, CD11c$^+$CD206$^+$ ATMs, and CD11c$^-$CD206$^+$ ATMs in paired OM and subcutaneous adipose tissue from obese patients (n = 10–14). *p < 0.05 versus OM.

CD64$^-$ ATDC are enriched in subcutaneous adipose tissue from obese humans

A range of markers have been used to quantify human ATMs in published studies and many rely on CD14 as an ATM marker despite the demonstration of CD14$^+$ DCs (160). We therefore wanted to evaluate the utility of CD64 in delineating ATMs from ATDCs in human samples. Multi-color flow cytometry was performed on SVF cells from subcutaneous and omental/visceral adipose tissue (OM) from obese subjects undergoing

bariatric surgery. Using CD64, a major population of $CD45^+CD11b^+CD64^+$ cells was identified with minor populations of $CD45^+CD11b^+CD64^-$ and $CD45^+CD11b^-CD64^+$ cells (Figure 2-8A). $CD45^+CD11b^+CD64^+$ stained uniformly positive for $CD14^+$. However, a minor population of $CD14^+$ cells was observed in the $CD45^+CD11b^+CD64^-$ and $CD45^+CD11b^-CD64^+$ populations. Using CD64 and CD11c, we identified $CD64^+CD11c^+$, $CD64^+CD11c^-$ and $CD64^-CD11c^+$ myeloid leukocyte populations (Figure 2-8B). All 3 populations expressed CD1c and HLA-DR. However, $CD45^+CD64^-CD11c^+$ cells had the highest CD1c expression and moderate HLA-DR expression compared to the $CD45^+CD64^+$ population. CD206 was primarily expressed on $CD64^+CD11c^-$ cells, consistent with mouse studies suggesting this is the phenotype of resident ATMs in lean adipose tissue. $CD64^+$ cells were $CD16^-$ in human adipose tissue and $CD64^-CD16^+$ cells were a mix of monocytes and neutrophils based on side scatter (Figure 2-8C). Overall this suggests that human ATDCs can be defined as $CD64^-CD11c^+$ as we observed in mice.

We next examined the proportion of ATDC ($CD64^-$) and ATM ($CD64^+$) subsets in paired samples from subcutaneous and omental depots (Figure 2-8D). $CD11c^+CD206^+$ ATMs were enriched in subcutaneous compared to omental adipose tissue, while $CD11c^-CD206^+$ ATMs were lower in subcutaneous adipose. The frequency of ATDCs was higher in subcutaneous compared to omental adipose tissue. Collectively these results indicate that ATDCs are enriched in the subcutaneous adipose tissue of obese humans.

Discussion

There is considerable interest in the contribution of myeloid cells to obesity-induced inflammation and metabolic disease pathogenesis. Unfortunately, the adipose tissue myeloid cellular network is complex and we lack good markers for properly delineating the relatively contributions of the adipose-resident leukocytes. The primary goal of this study was to identify a better marker for identifying ATMs from other leukocyte populations including ATDCs. By using CD64 as a macrophage-specific marker, our primary findings suggest that defining ATMs as $F4/80^+CD11b^+$ leukocytes fails to exclude other myeloid cell types. In particular, we found the

45

F4/80$^+$CD11b$^+$CD11c$^+$ cell subset was contaminated with ATDCs. ATDCs comprise a significant portion of the total myeloid network in adipose tissue and this contamination may substantially confound results obtained when using F4/80 as an ATM-specific marker. A secondary goal was to use this newly identified marker to examine how ATM and ATDC accumulation is regulated during obesity. ATDC accumulation appears to be regulated by different chemotactic cues compared to ATMs. ATDCs were found to be CCR7-dependent with *Ccr7*$^{-/-}$ mice having fewer ATDC and being protected from obesity-induced inflammation and insulin resistance. On the other hand, ATM accumulation with obesity was confirmed to be primarily CCR2-depdendent.

ATMs have been defined almost exclusively as F4/80$^+$CD11b$^+$ by our group and others (117; 158; 161). Our experiments suggest that some studies may need to be re-evaluated and that some changes originally attributed to the F4/80$^+$CD11b$^+$CD11c$^+$ ATM population may actually be accounted for by changes in ATDCs. In addition, our experiments suggest that the use of CD11c as a single marker to define ATDC, which has been utilized by some groups, is inadequate given the clear identification of CD11c$^+$ ATMs (149). Our studies agree with the results of the ImmGen Consortium supporting the specificity of CD64 as a marker of tissue macrophages (150; 151). In addition, we have extended their results to the study of obese mouse models and obese human adipose tissue and support the specificity of CD64 as a marker of ATMs in both contexts.

Our observation that ATDCs increase with early obesity and are a dominant CD11c$^+$ population in adipose tissue with moderate HFD may be important for the control of adaptive immunity during obesity. Eight weeks of HFD correlates with major alterations in adaptive immunity including accumulation and activation of both CD8$^+$ and CD4$^+$ adipose tissue T cell populations (50; 109; 110). *Ccr7*$^{-/-}$ mice had fewer ATDCs and showed metabolic improvement after eight weeks of HFD which suggests that ATDC signals may be important for promoting metabolic derangement in the early stages of obesity development. CD4$^+$ and CD8$^+$ T cell populations were actually increased in *Ccr7*$^{-/-}$ mice which indicate metabolic improvement was not due to reduced T cell numbers in the relative absence of ATDCs. Ablation of CD11c$^+$ cells has been found to improve glucose intolerance partially by deactivating T cells in adipose tissue (142). Whether this

is due to alterations in ATMs, ATDCs, or both will have to be examined in future studies. We have previously shown that ATMs are required for T cell activation in adipose tissue using *LysM*-Cre mice, but the results from this current study indicate that we can't eliminate the possibility of ATDCs contributing to this effect. ATDCs and ATMs may independently direct adaptive immune responses during obesity given the potent antigen presentation capabilities of both populations (122; 142).

Our observation of protection from insulin resistance in $Ccr7^{-/-}$ mice agrees with recent reports and identifies loss of the ATDC population as a primary mechanism for this effect (162). *CCR7* was identified in a module of signal transduction genes that were downregulated with weight loss after bariatric surgery that was disconnected from T cell signaling genes (163). The functional profile of ATDC in the setting of obesity may be strikingly different from that of CD11c$^+$ ATM. Unlike ATM, lysosomal and lipid storage are not induced in ATDC with obesity. Instead, pathways related to antigen presentation and cytokine signaling remain elevated in ATDC suggesting that they have an independent contribution to the adipose tissue immune activation environment.

The protective effect of *Ccr2* deficiency in adipose tissue inflammation has been supported by several studies (159; 164; 165). However, separating the defects in circulating monocytes in $Ccr2^{-/-}$ mice from the defects in migration into peripheral tissues in this model is a challenge (166). Our competitive bone marrow experiments demonstrate that $Ccr2^{+/+}$ monocytes have an advantage for recruitment from the circulation into adipose tissue compared to $Ccr2^{-/-}$ monocytes independent of effects on the quantity of circulating monocytes. This supports findings showing CD11c$^+$ ATM recruitment is CCR2-dependent. Our results also suggest that some conventional ATDC are recruited to adipose tissue by CCR2-dependent mechanisms as well. However, the relative CCR2-dependency was much lower for ATDC recruitment and suggests that ATDC are not likely monocyte derived. ATDC accumulation may instead be dependent on recruitment of pre-DC populations from the circulation or proliferation *in situ*.

Overall, our studies clarify the somewhat confusing literature on CD11c expression in adipose tissue myeloid cells. We propose that there are three primary myeloid cell populations in adipose tissue: CD45$^+$CD64$^+$CD11c$^-$ ATMs present in lean

adipose, recruited CD45$^+$CD64$^+$CD11c$^+$ ATMs, and CD45$^+$CD64$^-$CD11c$^+$ ATDCs that are predominantly CD11b$^+$ conventional ATDC. Importantly, these observations extend to human adipose tissue and help inform future studies. ATDCs are not a minor population and can be as numerous as ATMs depending on the depot. The elevated number of ATDCs in human subcutaneous adipose tissue may explain the lower inflammatory capacity of this depot. Whether or not human subcutaneous ATDCs are similar in function to human omental ATDCs will be examined in future studies. An additional limitation is the lack of samples from lean individuals for comparison and that, too, is the topic of ongoing studies by our group. Clarifying the landscape of functional antigen presenting cells in adipose tissue may advance our understanding of the mechanisms by which inflammation and leukocyte activation is controlled in adipose tissue.

Table 4 – Antibodies used for flow cytometry this chapter

Antibody	Clone	Company
Anti-mouse		
CD11b	M1/70	eBioscience
CD11c	N418	eBioscience
CD45.2	104	eBioscience
CD45.1	A20	eBioscience
CD64	X54-5/7.1	BD Biosciences
MHC I-A/I-E	M5/114.15.2	eBioscience
F4/80	BM8	eBioscience
CD206	MR5D3	AbD Serotec
Siglec-F	E50-2440	BD Biosciences
Ly6G	RB6-8C5	eBioscience
CD40	1C10	eBioscience
CD80	16-10A1	eBioscience
CD86	GL1	eBioscience
CD103	2E7	eBioscience
CD4	RM4-5	eBioscience
CD8a	53-6.7	eBioscience
B220	RA3-6B2	eBioscience
CD115	AFS98	eBioscience
Ly6C	AL21	BD Biosciences
Anti-human		
CD206	15-2	Biolegend
CD11c	3.9	Biolegend
CD11b	44	BD Biosciences
CD14	RMO52	Beckman
CD45	HI30	eBioscience
CD1c	F10/21A3	BD Bioscience
CD64	10.1	eBioscience

Table 5 – Sequences for RT-PCR primers used in this chapter

Gene	Primer	Sequence
Arbp	Forward	AGA TTC GGG ATA TGC TGT TGG C
	Reverse	TCG GGT CCT AGA CCA GTG TTC
18S	Forward	TTG ACG GAA GGG CAC CAC CAG
	Reverse	GCA CCA CCA CCC ACG GAA TCG
Flt3	Forward	GAG CGA CTC CAG CTA CGT C
	Reverse	ACC CAG TGA AAA TAT CTC CCA GA
Mertk	Forward	CAG GGC CTT TAC CAG GGA GA
	Reverse	TGT GTG CTG GAT GTG ATC TTC
Camk1	Forward	AAG CAG GCG GAA GAC ATT AGG
	Reverse	AGT TTC TGA GTC CTC TTG TCC T
Zbtb46	Forward	AGA GAG CAC ATG AAG CGA CA
	Reverse	CTG GCT GCA GAC ATG AAC AC
Fcgr1	Forward	AGG TTC CTC AAT GCC AAG TGA
	Reverse	GCG ACC TCC GAA TCT GAA GA
kit	Forward	GCC ACG TCT CAG CCA TCT G
	Reverse	GTC GCC AGC TTC AAC TAT TAA CT
Ccr7	Forward	TGT ACG AGT CGG TGT GCT TC
	Reverse	GGT AGG TAT CCG TCA TGG TCT TG
Itgax	Forward	CTG GAT AGC CTT TCT TCT GCT G
	Reverse	GCA CAC TGT GTC CGA ACT C
Ccl2	Forward	TTA AAA ACC TGG ATC GGA ACC AA
	Reverse	GCA TTA GCT TCA GAT TTA CGG GT
Il6	Forward	TAG TCC TTC CTA CCC CAA TTT CC
	Reverse	TTG GTC CTT AGC CAC TCC TTC
Ifng	Forward	ATG AAC GCT ACA CAC TGC ATC
	Reverse	CCA TCC TTT TGC CAG TTC CTC
Foxp3	Forward	CCC ATC CCC AGG AGT CTT G
	Reverse	ACC ATG ACT AGG GGC ACT GTA

Chapter 3 – Macrophage Proliferation Sustains Adipose Tissue Inflammation in Formerly Obese Mice

Portions of this chapter have been published:

Abstract

Obesity causes dramatic pro-inflammatory changes in the adipose tissue immune environment, but relatively little is known regarding how this inflammation responds to weight loss. To understand the mechanisms by which meta-inflammation resolves during weight loss (WL), we examined adipose tissue leukocytes in mice after withdrawal of high-fat diet. After 8 weeks of WL, mice achieved similar weights and glucose tolerance as age-matched lean controls but showed abnormal insulin tolerance. Despite fat mass normalization, total and CD11c$^+$ adipose tissue macrophage (ATM) content remained elevated in WL mice for up to 6 months and was associated with persistent fibrosis in adipose tissue. ATMs, but not adipose tissue dendritic cells, in formerly obese mice demonstrated a pro-inflammatory profile including elevated expression of IL-6, TNFα, and IL-1ß. T cell deficient $Rag1^{-/-}$ mice showed a similar degree of ATM persistence as WT mice, but with reduced inflammatory gene expression. Proliferation was identified as the predominant mechanism by which ATMs are retained in adipose tissue with WL. Our study suggests that weight loss does not completely resolve obesity-induced ATM activation which may contribute to the persistent adipose tissue damage and reduced insulin sensitivity observed in formerly obese mice.

Introduction

Obesity induces a state of chronic low-grade inflammation characterized by qualitative and quantitative changes in the leukocytes of metabolic tissues including the hypothalamus, liver, and adipose tissue (98; 167; 168). In particular, inflammation within visceral adipose tissue of obese mice and humans has been shown to be associated with diabetes and contribute to the development of insulin resistance, with multiple cellular sources contributing to the inflammatory environment including adipocytes, stromal cells and leukocytes (113; 114). In mice, a pro-inflammatory CD11c$^+$ macrophage population accumulates in visceral adipose tissue during obesity and assumes a metabolically activated phenotype that is associated with development of systemic insulin resistance (51; 137; 138). Recruitment of circulating bone marrow-derived monocytes as well as proliferation contribute to CD11c$^+$ adipose tissue macrophage (ATM) accumulation and maintenance (124; 159; 169). Adipose tissue T (ATT) cell-dependent signals have also been shown to promote CD11c$^+$ ATM accumulation and inflammation with obesity (109; 112).

While there is a fairly detailed understanding of how adipose tissue inflammation is generated with obesity, relatively few details are known regarding how adipose tissue leukocytes respond to weight loss following obesity. Previous studies have shown varying degrees of change in adipose tissue inflammation after weight loss through different regimens. Interventions such as caloric restriction or bariatric surgery can improve metabolic dysfunction and reduce markers of inflammation within adipose tissue (170-172). However, several studies suggest that weight loss may not fully resolve adipose tissue inflammation and insulin sensitivity. Inflammation-related gene expression in subcutaneous adipose tissue of formerly obese human subjects remains high compared to lean individuals (126; 129). Similar results have been observed in mice where weight loss has been shown to be associated with a persistent expression of inflammatory cytokines such as IL-6, IL-1β and TNFα in adipose tissue (125; 130; 173; 174). Schmitz *et al* recently demonstrated weight loss improved glucose tolerance but incompletely resolved adipose tissue inflammation and insulin sensitivity in mice and humans (125). Few studies have specifically examined how weight loss influences the quantity and quality of adipose tissue leukocytes. Weight cycling in mice suggests IFNγ-expressing T

cells accrue during successive high-fat diet exposures indicating an incomplete resolution of lymphocyte activation with weight loss (175). Weight loss has also been shown to induce short term ATM recruitment in response to lipolytic signals (176).

Understanding the cellular and molecular events that reshape adipose tissue leukocytes during the resolution of obesity may identify pathways important in promoting weight loss and improvements in insulin resistance. Therefore, our objective was to perform a detailed investigation into the effects of weight loss on inflammatory leukocyte activation and composition within adipose tissue to understand the mechanisms by which metabolic inflammation may resolve. We found weight loss improved glucose tolerance, however abnormal systemic and visceral adipose tissue insulin resistance persisted. This was associated with long-term alterations in the composition of adipose tissue leukocytes including retention of proliferating CD11c$^+$ ATMs, expansion of adipose tissue lymphocytes, and a persistent activation state of ATMs despite weight loss. Understanding which inflammatory characteristics of obesity remain despite weight loss helps inform our understanding of the relationship between adipose tissue inflammation and metabolic function.

Materials and Methods
Animals and Animal Care

Male Rag1$^{-/-}$ (B6.129S7-Rag1tm1Mom/J) and C57BL/6J mice were purchased from Jackson Laboratory. Mice were started at 6 weeks of age on control diet (LabDiet PicoLab 5L0D 4.09kcal/gm 29.8% protein, 13.4% fat, 56.7% carbohydrate) or high-fat diet (Research Diets D12492, 5.24kcal/gm 20% protein, 60% fat, 20% carbohydrate).

Glucose tolerance tests (GTT) and insulin tolerance tests (ITT) were performed after 6 hour fasting. Mice were injected IP with D-glucose (0.7 g/kg) for GTTs and human recombinant insulin (1 U/kg) for ITTs. Insulin and Leptin measured by ELISA (Crystal Chem). Energy metabolism was measured using Comprehensive Lab Animal Monitoring System analysis (CLAMS, Columbus Instruments) and body composition measured by NMR (Minispec LF90II, Bruker Optics). All mice procedures were

approved by the University of Michigan Committee on Use and Care of Animals and were conducted in compliance with the Institute of Laboratory Animal Research Guide for the Care and Use of Laboratory Animals.

Isolation of Adipose Tissue SVF and Flow Cytometry

Excised adipose tissue was digested in RPMI with 0.5% BSA and 1 mg/ml type II collagenase for 25 min at 37 °C and the stromal vascular fraction was separated from adipocytes by centrifugation. The following antibodies were used for flow cytometry: anti-CD45 (30-F11), anti-CD3e (145-2C11), anti-CD4 (GK1.5), anti-CD8a (53-6.7), anti-Foxp3 (FJK-16s), anti-IFNγ (XMG1.2), anti-Ki67 (SolA15), anti-TNFα (MP6-XT22), anti-CD40 (1C10), anti-CD80 (16-10A1), anti-CD86 (GL1), anti-CD11c (N418) (eBioscience), anti-IL-6 (MP5-20F3) and CD64 (X54-5/7.1) (BD Pharmingen). Analysis was performed on a BD FACSCanto II and sorting was performed on a FACSAria III (BD Biosciences).

Gene expression analysis and microarray

RNA was extracted from adipose using Trizol LS (Life Technologies) and cDNA generated using High Capacity cDNA Reverse Transcription Kit (Applied Biosystems). SYBR Green PCR Master Mix (Applied Biosystems) and the StepOnePlus System (Applied Biosystems) were used for real-time quantitative PCR. *Gapdh* expression was used as an internal control for data normalization. Samples were assayed in duplicate and relative expression was determined using $2^{-\Delta\Delta}$ CT method. For microarray experiments, analysis was done using Mouse Gene ST 2.1 plate and WT-Pico kit (Affymetrix, Santa Clara, CA). Expression values were calculated using a robust multi-array average. Data were filtered to remove probesets with a variance over all samples of less than 0.1 and then fit to a linear model (177; 178). The false discovery rate was set at an adjusted P value of 0.05. Oligo_1.24.2 and limma_3.16.7 packages from Bioconductor were used for data analysis in the R statistical environment (R version 3.0.0 2013-04-03).

Primer sequences used for this study are provided in Table 6.

Immunoblotting

Adipose tissue was homogenized in RIPA lysis buffer with phosphatase inhibitors (Roche). Protein concentration was determined using Bio-Rad Protein Assay Dye Reagent. Proteins were labeled and visualized using Odyssey infrared imaging system (Li-Cor Bioscience). Antibodies used for immunoblotting: anti-PPARγ(81B8), anti-IRS-1, anti-Phospho-Akt (Ser473), anti-AKT, anti-Adiponectin(C45B10), anti-Caveolin(D46G3) (Cell Signaling Technology) and anti-β-Actin(AC-40) (Sigma-Aldrich).

Glycerol Release, Collagen Quantification and Cytokine Array

Stimulated release of glycerol was performed on minced 100mg pieces of adipose cultured five hours ± isoproterenol (1μM) according to manufacturer's instructions for Glycerol Detection Kit for Explants (ZenBio). Explants were cultured in serum-free AIM V media with AlbuMax and BSA (Life Technologies). Additional samples were hydrolyzed in 6M HCl according to manufacturer's instructions for Total Collagen Assay Kit (Cedarlane Labs, QuickZyme BioSciences). Culture supernatant glycerol and adipose hydroxyproline content was measured using colorimetry. Mouse Cytokine Antibody Array (R&D Systems) was used to evaluate cytokine output from adipose tissue explants after 48 hours and pooled from 3 samples. Quantitation by ImageJ after background subtraction and normalization to reference controls.

Immunohistochemistry and Immunofluorescence

Ki67 IHC and H&E sections were performed by the University of Michigan's Comprehensive Cancer Center Histology Core. Picosirius red stain kit was used following kit manufacturer instructions (Polysciences Inc). Antibodies used for

immunofluorescence include: polyclonal anti-caveolin (BD Pharmingen) and anti-Mac2 (Galectin-3) (eBioM3/38) (eBioscience).

PKH26 labeling of macrophages in vivo

PKH26 cell linker kit for phagocytic cell labeling (Sigma-Aldrich) was used for *in vivo* macrophage labeling experiments per manufacturer instructions. Briefly, 500μl of a 1μM solution of PKH26 dye mixed with diluent was injected into two sets of ND and 12 week HFD fed mice intraperitoneally before weight loss. The first set was euthanized one day later to check labeling efficiency and the second set after weight loss (8wk); PKH26 uptake was evaluated using flow cytometry.

Statistical Analyses

All values are reported as mean ± SEM unless otherwise noted. Statistical significance of differences between ND controls and other diet groups were determined using unpaired two-tailed Student's t-test or one-way ANOVA for multiple groups with Fisher's least significant difference test for planned statistical comparisons, unless otherwise noted, to ND using GraphPad Prism V6.05.
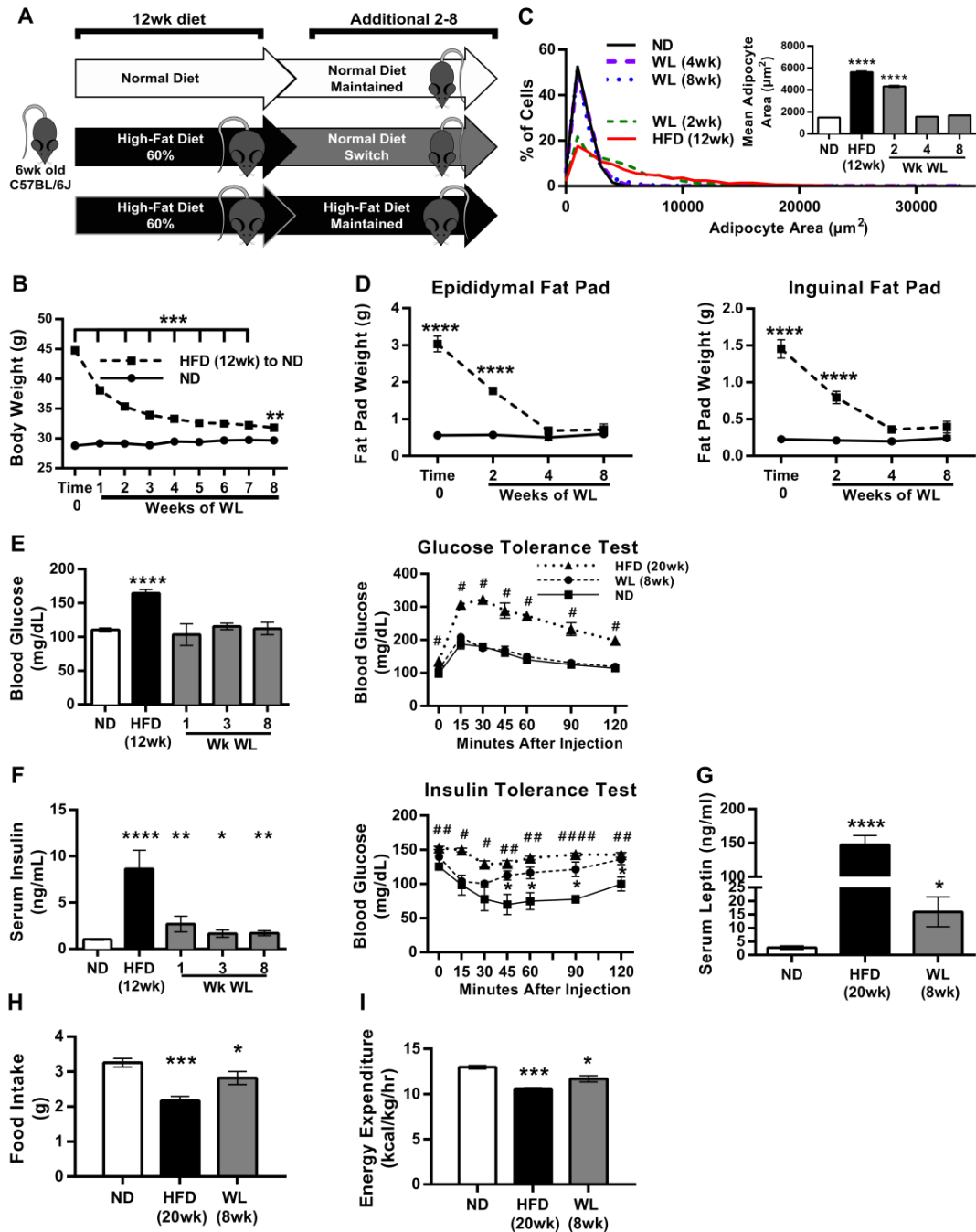
Figure 3-1 – Glucose tolerance normalization but persistently elevated insulin with weight loss. (A) Cartoon showing obesity induction and weight loss model. (B) Body weight curve after weight loss (n ≥ 12 ND, n ≥ 16 WL). (C) Adipocyte-size distribution and average adipocyte size. (D) Fat weight curve after weight loss (n = 4). (E) Fasted blood glucose and glucose tolerance after weight loss (n ≥ 4, # refer to HFD vs ND). (F) Fasted serum insulin (n ≥ 4) and insulin tolerance after weight loss (n = 4, $ refer to HFD versus ND while * refer to WL versus ND). (G) Fasted serum leptin concentrations (n = 8). H and I: Food intake measures (H) and energy expenditure (I) (n = 4). $^{#,*}p < 0.05$, $^{##,**}p < 0.01$, $^{***}p < 0.001$, $^{####,****}p < 0.0001$; significance compares to ND control group unless otherwise indicated.

57

Results

Withdrawal of high-fat diet decreases adiposity and improves glucose tolerance but not insulin tolerance in mice

We established a model of weight loss based on the withdrawal of high-fat diet (HFD). Male C57BL/6J mice were fed high-fat diet (HFD 60% kcal fat) or normal diet (ND, 13.5% kcal fat) for 12 weeks. Obese mice were then either maintained on HFD or switched to ND to induce weight loss over a period of 2-24 weeks (Figure 3-1A). After 8 weeks diet-switch, body weight of weight loss (WL) mice decreased ~28% from 44.8g (SD ± 2.8) to 31.8g (SD ± 2.3) and was similar to age-matched ND fed mice (29.6g (SD ± 1.8) (Figure 3-1B). Body composition analysis showed no significant differences in percentage fat and lean mass between ND and WL mice (data not shown). Epididymal (eWAT) and inguinal (iWAT) white adipose tissue mass and eWAT adipocyte size normalized by 4 weeks off HFD (Figure 3-1D, 3-1C).

To assess metabolism after weight loss, GTTs and ITTs were performed. After 8 weeks of weight loss fasting glucose and glucose tolerance decreased to levels similar to ND mice (Figure 3-1E). Fasting serum insulin levels decreased, but remained elevated compared to ND controls (Figure 3-1F). ITTs revealed improvement in insulin sensitivity in WL mice compared to HFD, but insulin tolerance remained abnormal compared to ND mice (Figure 3-1F). Leptin levels were lower in WL mice compared to HFD, but remained elevated compared to ND (Figure 3-1G). Food intake and energy expenditure increased in WL mice compared to HFD mice, but remained lower than ND fed controls (Figure 3-1H-I). The respiratory exchange ratios for ND and WL mice were not significantly different, and were both higher than HFD mice. No differences in physical activity were noted between groups. Overall, these studies demonstrated that formerly obese mice retained persistent abnormalities in insulin sensitivity despite normalization of body weight, fat mass, and glucose tolerance.
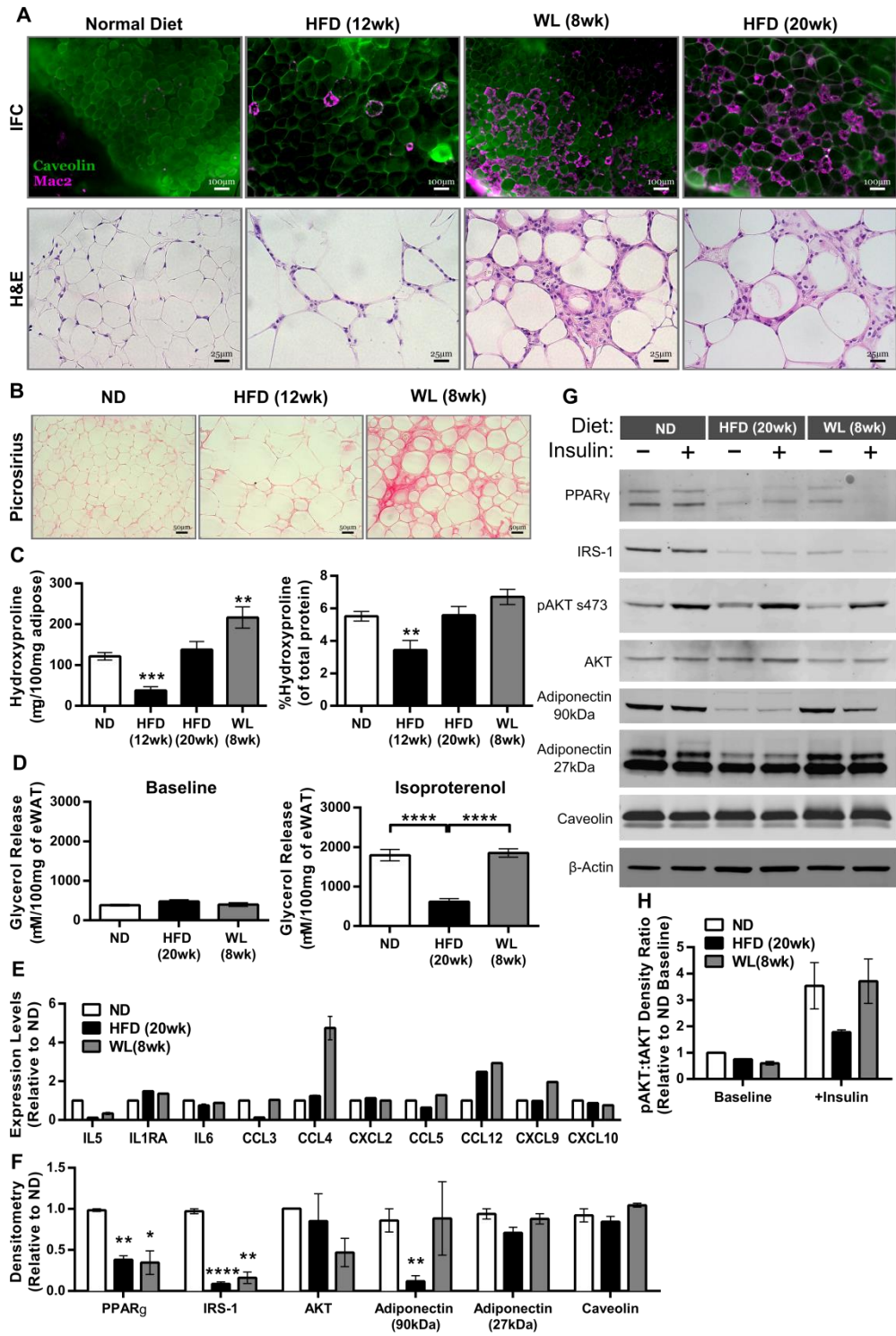
Figure 3-2 – Epididymal adipose tissue maintains features associated with obesity despite weight loss. (A) Immunofluorescence and H&E stained epididymal adipose (eWAT) slides representative for each diet condition showing CLS development and maintenance. (B) Picrosirius red staining of eWAT slides representative of diet conditions. (C) Hydroxyproline quantification of eWAT (n ≥ 4). (D) Isoproterenol stimulated glycerol release from whole eWAT

explants (n = 8). (E) eWAT explant multiplex cytokine array (n=2 per condition). (F) Quantification of densitometry measurements from immunoblots of whole eWAT (n = 2 ND, n = 4 HFD & WL; ANOVA with Dunnet's multiple comparisons. (G) Representative immunoblots from mice injected IP with or without 1U/kg insulin for 10 minutes with 2 mice pooled per lane. (H) Phosphorylated AKT s473 relative to total AKT from immunoblots (n = 2 for baseline and n = 3 for insulin administered = +insulin). $^{*}p < 0.05$, $^{**}p < 0.01$, $^{***}p < 0.001$, $^{****}p < 0.0001$; significance compares with the ND-fed control group.

Measures of adipose tissue dysfunction persist despite weight loss after HFD

We next evaluated if adipose tissue structure normalized with weight loss concomitant with the normalization of depot mass. Crown-like structures (CLS), a characteristic histologic feature of obese adipose tissue, were induced with 12 weeks of HFD. Despite weight loss CLS remained a prominent feature of eWAT and were similar in quantity to mice maintained on HFD for 20 weeks (Figure 3-2A). Picrosirius red staining demonstrated an association between CLS persistence and adipose tissue fibrosis in WL mice (Figure 3-2B). Biochemical quantification of hydroxyproline content in adipose tissue supported this finding of increase fibrosis (Figure 3-2C).

We next examined several measures of adipocyte function in WL mice. To assess lipolysis, explant baseline glycerol release was examined and found to be similar between ND, 20wk HFD and 8wk WL explants (Figure 3-2D). Isoproterenol-stimulated glycerol release was decreased in HFD mice compared to ND mice and was restored after weight loss. Cytokine release was assessed in eWAT explants by cytokine arrays (Figure 3-2E). Adipose tissue secretion of CCL3, CCL4, CCL5, and CXCL9 was increased in WL eWAT compared to HFD. IL-1RA and CCL12 were increased in both HFD and WL mice compared to ND mice.

Immunoblots demonstrated decreases in PPARγ, IRS-1, and total Akt protein expression in eWAT from HFD and WL mice compared to ND (Figure 3-2F-G). Caveolin and 27kDa adiponectin were similar between groups. Adipose AKT serine 473 phosphorylation (pAKT) was decreased in HFD and WL mice at baseline (Figure 3-2G-H), but pAKT in WL mice was not significantly different from ND mice after insulin injection. Overall, these data demonstrate that formerly obese mice demonstrate

persistent derangements in adipose tissue architecture, fibrosis, adipogenic protein expression, and cytokine production.

ATMs maintain a pro-inflammatory profile despite weight loss

Flow cytometry was used to profile adipose tissue leukocyte changes with weight loss. The percentage of CD45$^+$ cells in the stromal vascular fraction (SVF) of eWAT was increased with HFD. WL mice had fewer CD45$^+$ leukocytes in the SVF than HFD mice but remained increased compared to ND mice despite similar adipose tissue weights. ATMs (CD45$^+$ CD64$^+$ (179)) were reduced with weight loss, but remained significantly elevated compared to ND when expressed as either total ATM per eWAT pad, ATMs per gram eWAT or as a frequency of CD45$^+$ leukocytes (Figure 3-3B-D). While total ATM content was reduced with weight loss, the frequency of CD11c$^+$ ATMs remained consistently elevated (Figure 3-2E), indicating that formerly obese mice have long-term perturbations in ATM composition.

During obesity, CD11c$^+$ ATMs express a pro-inflammatory gene expression profile (49; 138). To see if CD11c$^+$ ATMs from WL mice retained pro-inflammatory characteristics, FACS sorted ATMs were evaluated using gene expression microarrays. Microarrays revealed that all ATMs during obesity and after weight loss, regardless of CD11c (M1-like marker) or CD301 (M2-like marker) expression, had similar gene expression profiles and were thus combined for the following analyses. Pathway analysis identified enrichment of genes involved in Cytokine-Cytokine Receptor Interaction (mmu04060) and Chemokine Signaling Pathway (mmu04062) in ATMs from WL mice compared to ND mice (180). WL ATMs maintained a pro-inflammatory expression profile compared to ND mice including increased *Il-1β, Il-6, Tnfα, Cxcl1, Ccl4, Ccl5, Ccl11 and Ccl12* (Figure 3-3F). Intracellular cytokine labeling of non-stimulated ATMs verified increased IL-6 (Figure 3-3G) and TNFα (Figure 3H) protein expression despite weight loss. Immunofluorescence localization of active IL-1β revealed enrichment surrounding CLS in HFD mice that was sustained after weight loss (Figure 3-3I). Overall this

demonstrates a persistence of pro-inflammatory ATMs in WL mice and suggests that weight loss is insufficient to deactivate ATMs.

Adipose tissue physiologic and immune cell perturbations persist as long as six months off high-fat diet

To establish how long the effects of obesity might persist in adipose tissue after weight loss, we extended our weight loss model to 24 weeks off HFD. Body weights in 24wk WL mice were 35.8g (SD ± 1.3) compared to HFD at 60.8g (SD ± 4.3) and ND mice at 32.8g (SD ± 1.2) (Figure 3-4A), while eWAT weight completely normalized (Figure 3-4B). Total ATM and CD11c$^+$ ATM content remained significantly elevated compared to ND and comparable to 8wk WL mice (Figure 3-4C-D). Overall the data indicate prolonged maintenance of leukocyte population changes induced by obesity despite weight loss. Immunofluorescence revealed continued maintenance of CLS (Figure 3-4F). However, H&E staining revealed these CLS were surrounded by less dense collagen deposition than CLS found in 8wk WL mice. 24wk WL mice also no longer retained the abnormal systemic insulin responsiveness (Figure 3-4E) observed in 8wk WL mice.

We next evaluated if the degree of ATM persistence is dependent on the duration of HFD exposure prior to diet switch. Mice were placed on HFD for 6, 9 or 12 weeks prior to switching to ND for 8 weeks. All HFD groups gained weight (6wk: 37.45g SD ± 3.5, 9wk: 38.6g SD ± 3.6, and ND: 23.67 SD ± 0.9), but 6wk and 9wk HFD groups gained less than 12wk HFD mice (46.6g ± 2.0) (Figure 3-4G). After weight loss, eWAT weights in all HFD durations were similar to ND controls (Figure 3-4H). Total ATM content after weight loss was higher than age-matched ND mice and increased with longer time spent on HFD (Figure 3-4I). CD11c$^+$ ATMs after weight loss in 6wk and 9wk HFD mice remained slightly increased compared to ND controls (Figure 3-4J). However, mice fed HFD for 12 weeks prior to weight loss had significantly more CD11c$^+$ ATMs after weight loss than the groups exposed to HFD for shorter times. Immunofluorescence after weight loss revealed fewer CLS in 6wk HFD and 9wk HFD mice (Figure 3-4K)

compared with 12wk HFD (Figure 3-2A). These data indicate that the degree to which ATMs and CD11c$^+$ ATMs persist in adipose tissue after weight loss is dependent on the duration of HFD or degree of adiposity prior to weight loss intervention.

Weight loss does not alter ATM in inguinal adipose tissue and improves liver steatosis

Subcutaneous inguinal white adipose tissue (iWAT) was also evaluated to determine how this adipose tissue depot responds to weight loss. iWAT weights remained significantly elevated after weight loss compared to ND mice (Figure 3-5A). WL mice had fewer CD45$^+$ leukocytes in iWAT than HFD mice and were similar to ND (Figure 3-5B). Total ATMs trended towards being increased in HFD and WL mice but were not significantly different from ND (Figure 3-5C). The frequency of all ATMs and CD11c$^+$ ATMs were not increased in HFD or WL mice compared to ND (Figure 3-5D-E). Histology revealed little or no CLS and fibrosis in iWAT of HFD or WL mice (Figure 3-5F). Overall the results indicate immune infiltration to murine iWAT during obesity is blunted compared to eWAT and remains low with weight loss. Liver histology revealed that steatosis, which is after 12wk HFD, resolved in WL mice (Figure 3-5G).
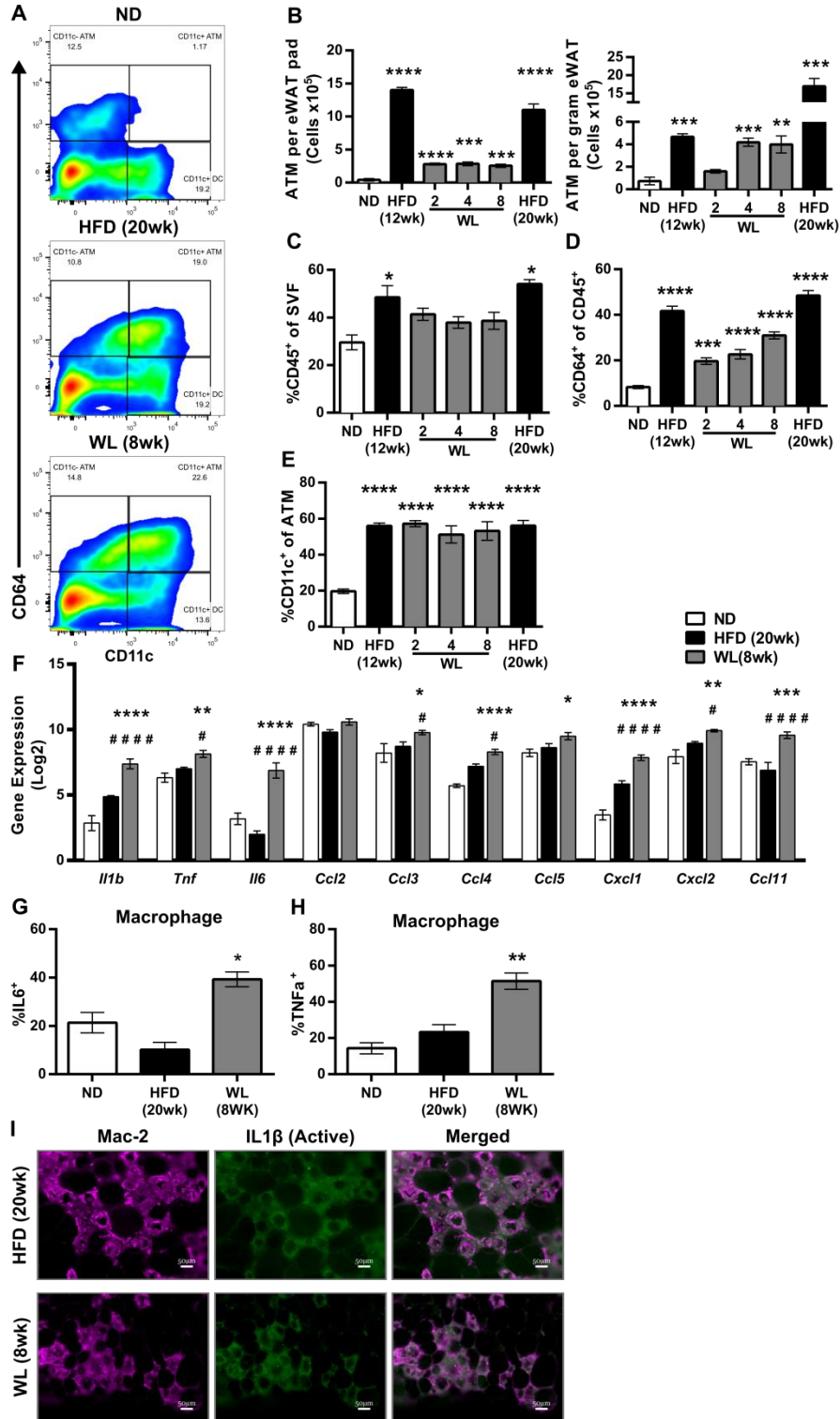
Figure 3-3 – Maintenance of inflammatory CD11c$^+$ adipose macrophages despite weight loss. (A) Representative flow plots showing our macrophage (CD45$^+$CD64$^+$) and dendritic cell (CD45$^+$CD64$^-$CD11c$^+$) gating strategy. (B) Total ATM content per eWAT pad (left) and ATM content per gram of eWAT (right) (n = 4). (C) Frequency of CD45$^+$ immune cells of all eWAT

SVF (n ≥ 4). (D) Frequency of CD64$^+$ ATM of all CD45$^+$ SVF (n ≥ 4). (E) Frequency of CD11c$^+$ ATM of all CD45$^+$CD64$^+$ ATM (n ≥ 4). (F) Gene expression of select immune genes from microarrays of flow sorted ATMs (two-way ANOVA with Dunnett's multiple comparisons, α = 0.05). #Significance comparing WL to HFD groups. Intracellular cytokine staining of unstimulated SVF showing (G) IL6 protein expression and (H) TNFα protein expression from eWAT ATM (n = 4). (I) Immunofluorescence from eWAT showing cleaved IL1β deposition surrounding CLS in mice during obesity and after weight loss. *p < 0.05, **p < 0.01, ***p < 0.001 and ****p < 0.0001; significance compares with the ND-fed control group unless otherwise indicated

Increased IFNγ production potential of adipose T cells after weight loss

Cross-talk between macrophages and T cells is critical for the activation of both cell types in obesity (142; 181). We evaluated co-stimulatory marker expression on eWAT ATMs from WL mice. Relative to the ND control group, *Cd40* expression is reduced in ATMs sorted from HFD mice but increased in ATMs from WL mice (Figure 3-6A). Weight loss induced *Cd80* expression in ATMs (Figure 3-6B) while *Cd86* was reduced in both HFD and WL ATMs compared to ND controls (Figure 3-6C). Surface expression of these markers was assessed using flow cytometry. CD40$^+$ and CD80$^+$ ATMs were significantly higher in WL mice compared to ND mice, while CD86$^+$ ATMs were elevated in both ND and WL mice (Figure 3-6D).

We next investigated how weight loss influenced adipose tissue T cells (ATT). Similar to ATMs, conventional CD4$^+$ T cell and CD8$^+$ T cell numbers increased with obesity (Figure 3-6E). CD4$^+$ ATT cells decreased after 2 weeks and transiently increased 4 weeks after diet switch. CD8$^+$ ATT cells were decreased in WL mice, but remained significantly elevated compared to ND up to 8 weeks after diet switch (Figure 3-6F). Total Foxp3$^+$ regulatory ATT cell numbers were also increased with obesity and returned to levels similar to ND mice by 8 weeks of weight loss (Figure 3-6G).

Figure 3-4 – Obesity-induced effects can persist in adipose as long as six months after HFD removal. (A) Body weight and (B) eWAT weight of mice after 24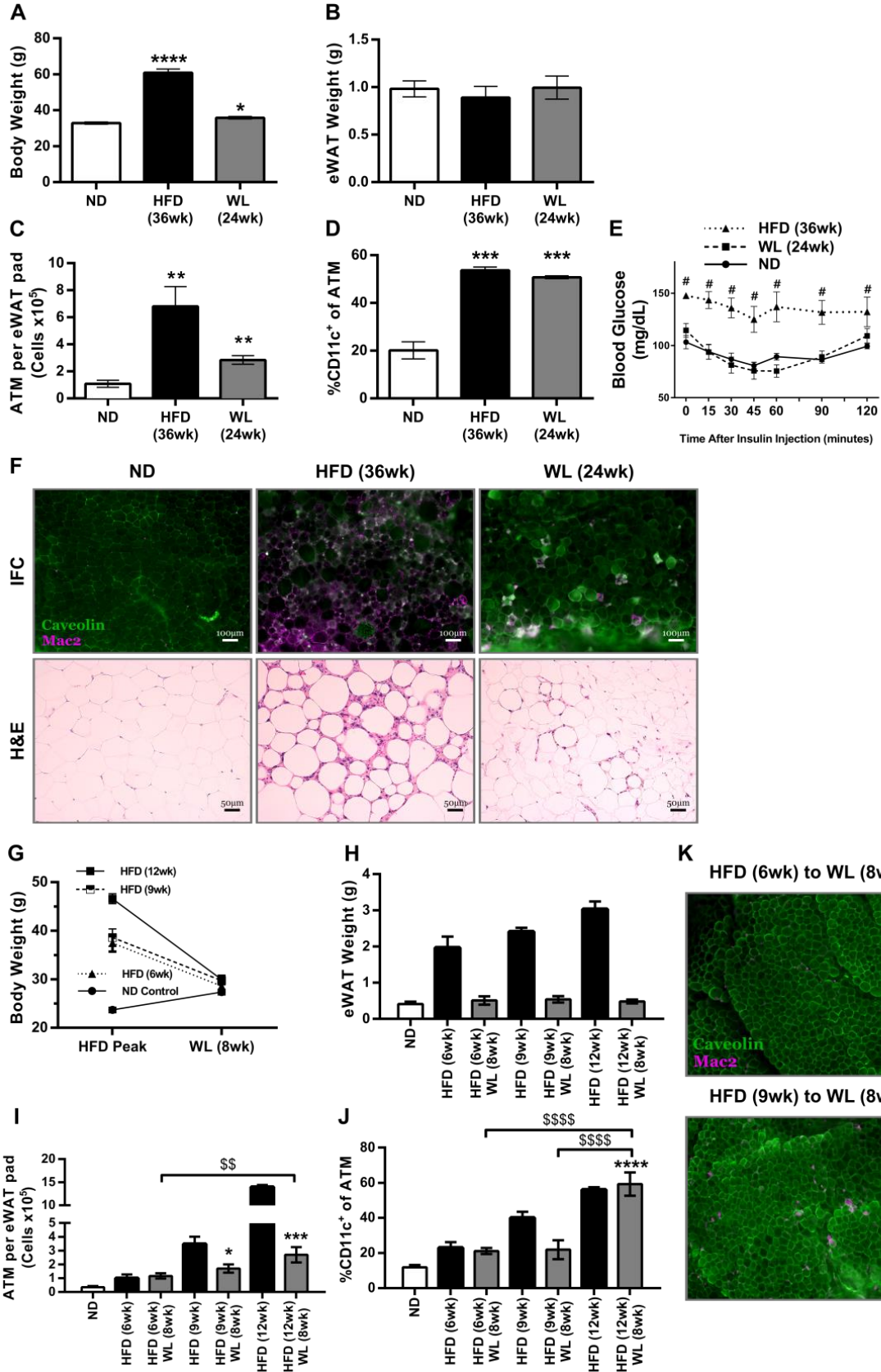 weeks of WL along with respective controls (n = 4). (C) Total $CD45^+CD64^+$ ATM content per eWAT pad for six-month weight loss mice (n = 4). (D) Frequency of $CD11c^+$ ATM of all $CD45^+CD64^+$ ATM (n = 4). (E) GTT (n = 4, #Significance compares HFD with ND). (F) Immunofluorescence and hematoxylin & eosin stained slides representative for each diet condition showing CLS development and maintenance. (G) Body weight and (H) eWAT weight of mice after weight loss from 6, 9 or 12 weeks HFD feeding groups (n = 4). (I) Total $CD45^+CD64^+$ ATM content per eWAT pad for short-term HFD fed mice (n = 4). (J) Frequency of $CD11c^+$ ATM of all $CD45^+CD64^+$ ATM (n = 4). H-J ANOVA with Tukey multiple comparisons ($\alpha = 0.05$) was used to compare WL averages to each other and to the ND-fed group; HFD points were not included in analysis. (K) Immunofluorescence representative images from eWAT showing macrophage accumulation. $^*p < 0.05$, $^{\$\$,**}p < 0.01$, $^{***}p < 0.001$ and $^{\$\$\$\$,****}p < 0.0001$; significance compares with the ND-fed control group unless otherwise indicated

Obesity promotes type-1 polarization of T cells within adipose tissue and IFNγ has been implicated in the development of insulin resistance (111; 182-184). Evaluation of IFNγ expression by flow cytometry demonstrated a reduction in the percentage of $IFN\gamma^+CD4^+$ and $INF\gamma^+CD8^+$ ATTs in HFD compared to ND mice (Figure 3-6H-I). Decreased per cell IFNγ expression was also observed in obese mice. The frequency of $IFN\gamma^+ CD4^+$ ATT cells returned to ND levels after 2 weeks of weight loss. The frequency of $IFN\gamma^+ CD8^+$ ATT cells returned to ND levels after 4 weeks of weight loss and was increased after 8 weeks. These data suggest that continued activation of $CD4^+$ and $CD8^+$ ATT cells occurs in adipose tissue in the setting of weight loss.

T cells contribute to ATM activation with weight loss, but are not required for macrophage accumulation

Given the increase in ATT with weight loss, we evaluated if T cells were required for the persistence of ATMs in formerly obese mice. T and B cell deficient $Rag1^{-/-}$ mice and WT controls were fed HFD for 12 weeks and then switched to ND (Figure 3-7A). $Rag1^{-/-}$ mice weighed less than WT mice prior to diet switch. Surprisingly, $Rag1^{-/-}$ WL mice had significantly worse glucose tolerance compared with $Rag1^{-/-}$ ND controls despite similar body weights (Figure 3-7B) which contrasts with the normalized GTTs of WT WL mice (Figure 3-1E). Similar to WT mice, $Rag1^{-/-}$ mice had significantly elevated

total and CD11c$^+$ ATMs despite 8 weeks of weight loss (Figure 3-7C-D). Crown-like structures persist in WT and *Rag1*$^{-/-}$ WL mice as assessed by histology (Figure 3-7H-I and 3-8A).
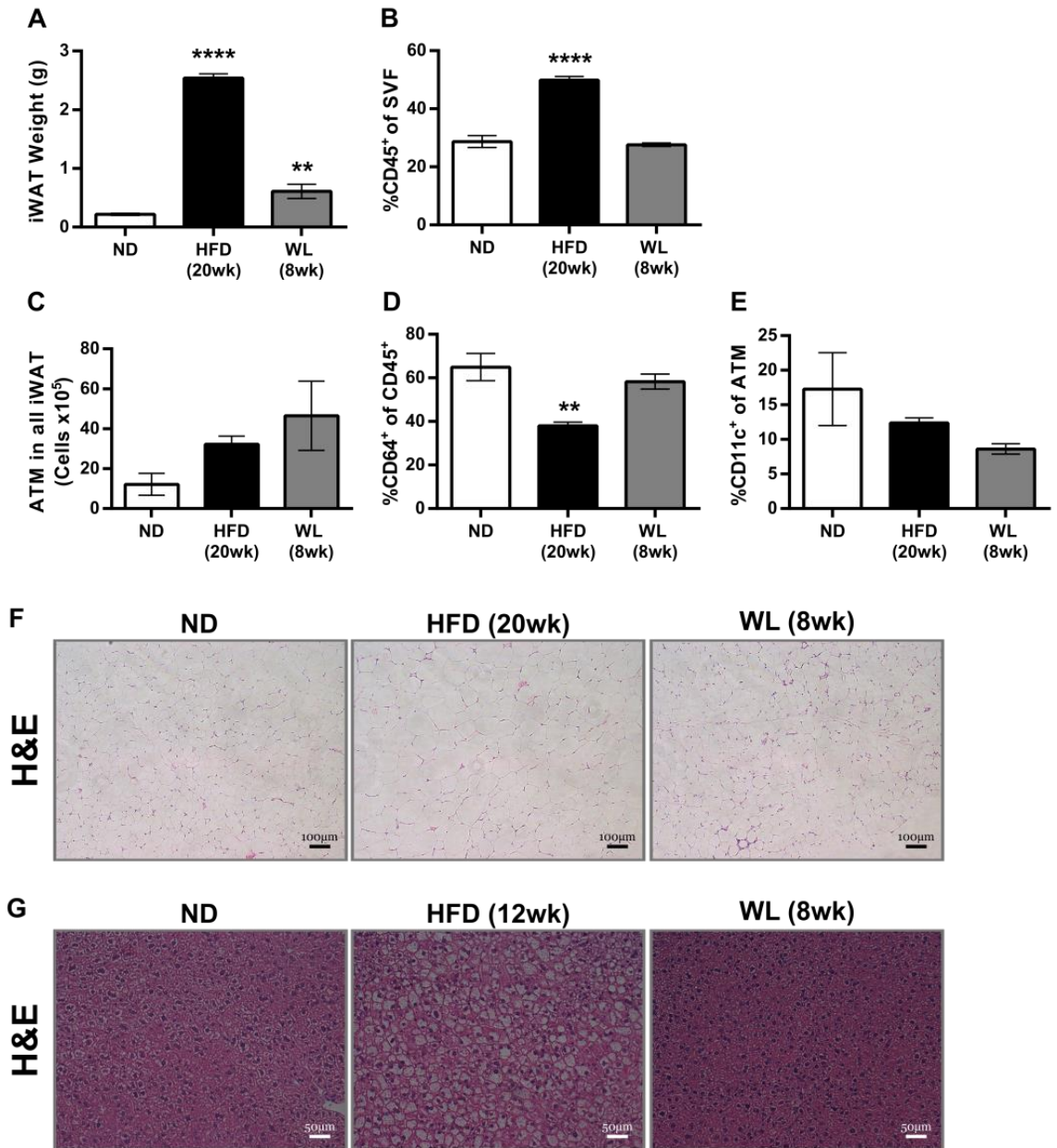
Figure 3-5 – Inguinal adipose tissue and liver changes with weight loss. (A) Inguinal white adipose tissue (iWAT) weights. (B) Frequency of CD45$^+$ leukocytes of total iWAT SVF. (C) Total CD45$^+$CD64$^+$ ATM in iWAT. (D) Frequency of ATM of all CD45$^+$ iWAT SVF leukocytes. (E) Frequency of CD11c$^+$ cells of all ATM (n = 4 for A-E). (F) H&E stained iWAT and (G) liver slides. **p < 0.01 and ****p < 0.0001, significance compares with the ND-fed control group.
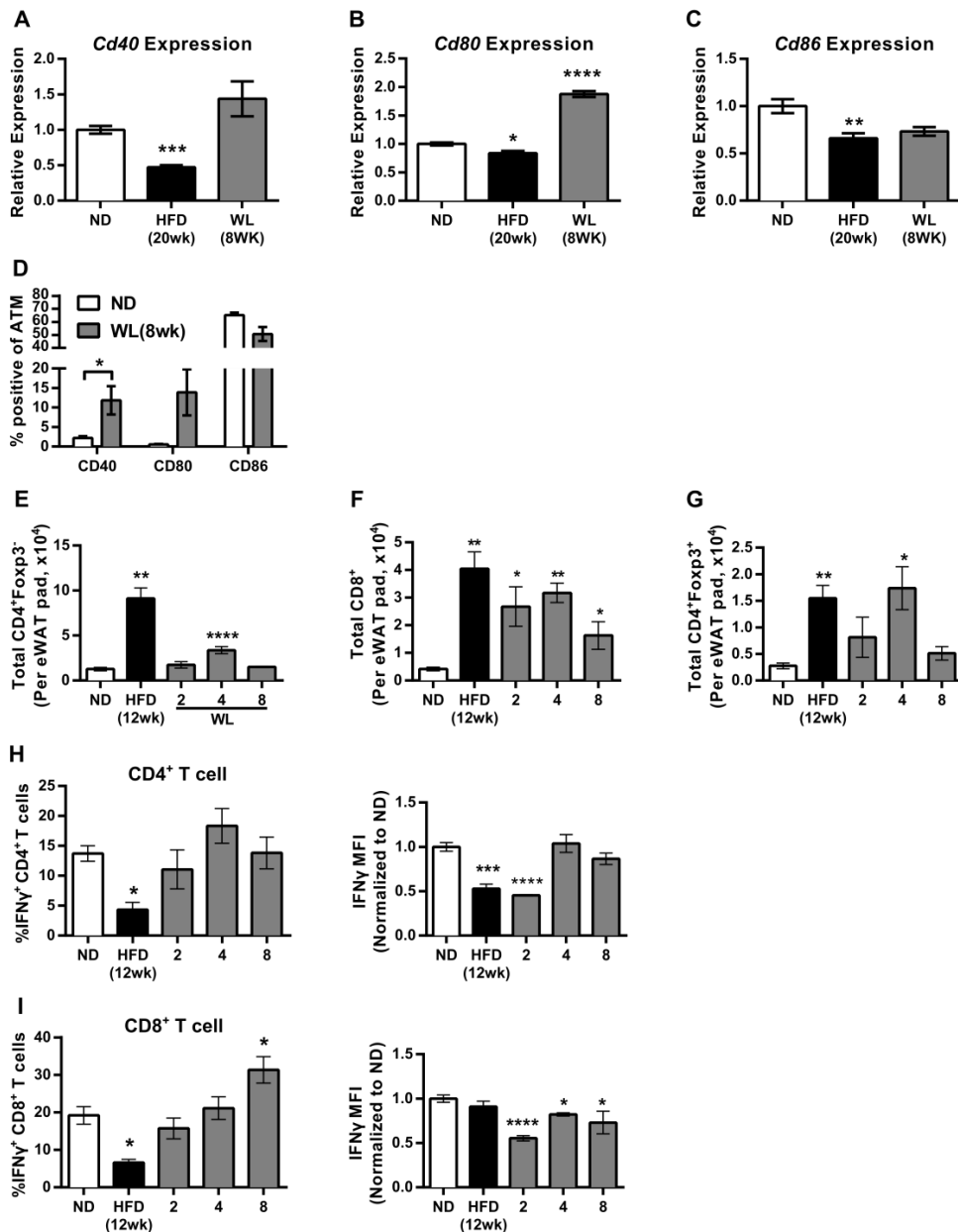
Figure 3-6 – Adipose tissue T cell activation with weight loss. Quantitative RT-PCR from flow sorted ATMs of mice evaluating (A) CD40, (B) CD80 and (C) CD86 gene expression (ATMs pooled from a total of 12 mice from the ND and HFD groups and 6 mice from the WL group; ND n = 4, HFD n = 4, WL n = 2). (D) Surface marker expression of *Cd40*, *Cd80*, and *Cd86* evaluated by flow cytometry (n = 4). Total ATT cell count per eWAT pad evaluated by flow cytometry for (E) conventional CD4$^+$ T cells, (F) CD8$^+$ T cells and (G) Foxp3$^+$CD4$^+$ T regulatory cells (n ≥ 4 for E-G). Intracellular cytokine stain on phorbol myristic acetate and ionomycin

stimulated SVF to evaluate IFNγ production potential from (H) CD4$^+$ T cells and (I) CD8$^+$ T cells. *p < 0.05, **p < 0.01, ***p < 0.001, ****p < 0.0001; significance compares with the ND-fed control group.
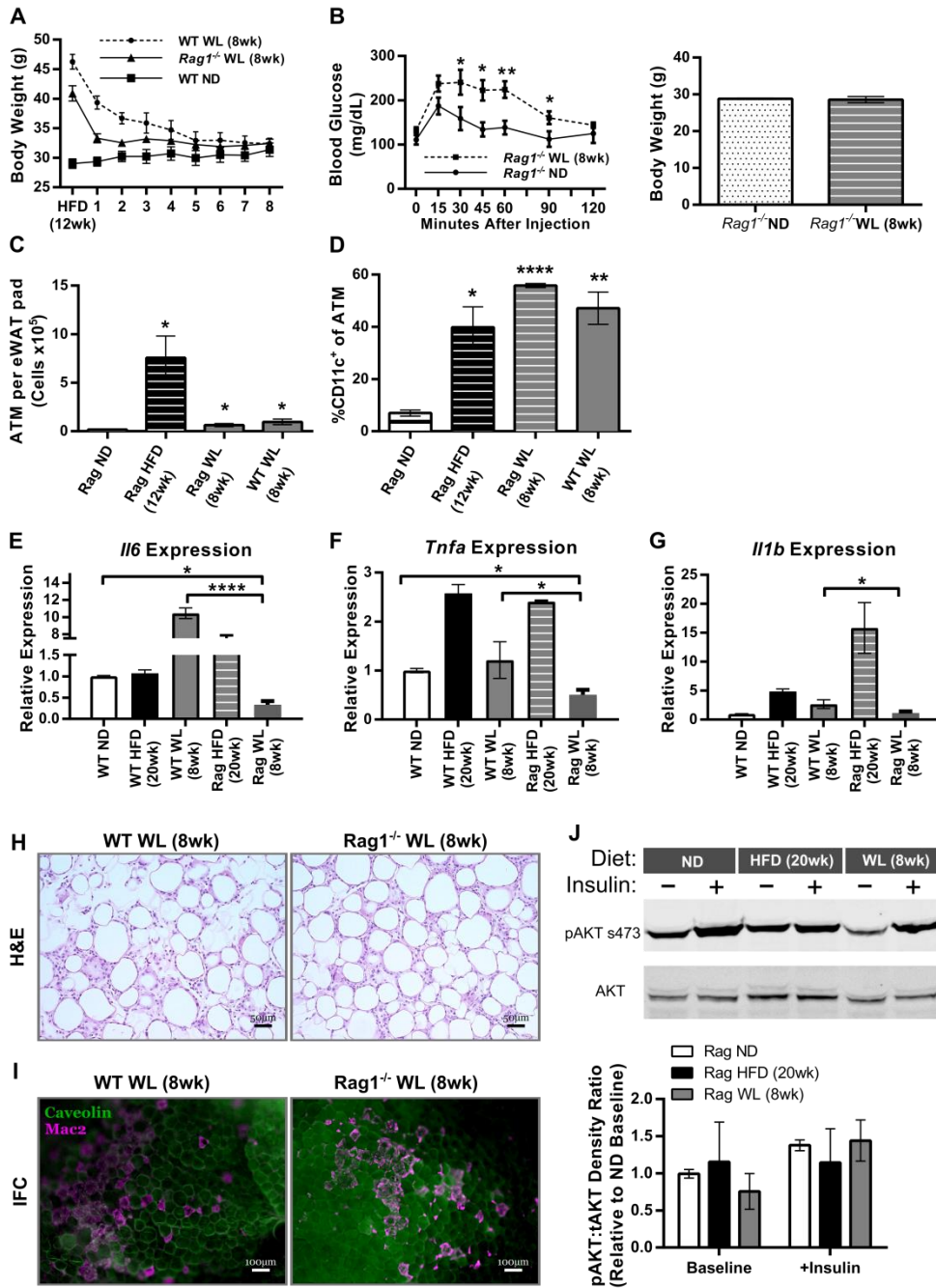
Figure 3-7 – T cells are not required for CD11c$^+$ macrophage accumulation but may control inflammatory activation state. (A) Body weight curves during weight loss (n ≥ 4). (B) Glucose tolerance in *Rag1$^{-/-}$* knockout mice after weight loss (left) and normalization of total body weight (right) (n = 4). (C) Total CD45$^+$CD64$^+$ ATM content per eWAT pad for *Rag1$^{-/-}$* mice (n ≥ 4). (D) Frequency of CD11c$^+$ ATM of all CD45$^+$CD64$^+$ ATM (n ≥ 4). Quantitative RT-PCR from flow

sorted ATMs evaluating (E) *Il6*, (F) *Tnfα* and (G) *Il1β* gene expression (ATMs pooled from a total of 12 mice from the ND and HFD groups and 6 mice from the WL group; WT ND n = 4, WT HFD n = 4, WT WL n = 2, Rag WL n = 4. (H) H&E stained slides and (I) immunofluorescence representative images showing CLS development and maintenance despite weight loss. *p < 0.05, **p < 0.01 and ****p < 0.0001; significance compares with the ND-fed control group unless otherwise indicated.

To evaluate the contribution of T and B cells towards ATM pro-inflammatory activity during weight loss, we assessed gene expression from flow sorted ATMs in WT and $Rag1^{-/-}$ WL mice. *Il6, Tnfa* and *Il1b* were all increased in HFD-fed $Rag1^{-/-}$ mice, but were significantly reduced in $Rag1^{-/-}$ WL mice compared to WT WL mice (Figure 3-7E-G). $Rag1^{-/-}$ adipose insulin signaling was evaluated. Relative to ND mice, baseline pAKT was decreased in $Rag1^{-/-}$ WL mice. However, similar to WT mice, pAKT was not significantly different from ND mice after insulin injection in $Rag1^{-/-}$ WL mice (Figure 3-7J). Given the accumulation of CLSs and fibrosis in $Rag1^{-/-}$ mice during obesity and weight loss (Figure 3-7H-I and Figure 3-8A), we decided to further investigate adipogenic gene and protein expression in whole eWAT tissue. Analysis revealed similar gene expression profiles between WT and $Rag1^{-/-}$ mice during obesity and weight loss for all genes evaluated (Figure 3-8B). Immunoblots revealed reduced protein expression for IRS1, PPARγ, and AKT in $Rag1^{-/-}$ mice during HFD feeding (Figure 3-8C-D). Similar to WT eWAT tissue, expression of these proteins were reduced with HFD and remained significantly reduced despite weight loss in $Rag1^{-/-}$ mice. Taken together, the data show that T cells are not essential for the maintenance of CD11c$^+$ ATMs or the continual development of adipose derangement with weight loss in WT mice. However, signals from lymphocytes appear to contribute to the ongoing pro-inflammatory activation of ATMs in formerly obese mice.

ATM after weight loss are derived primarily from macrophages present during obesity and maintained through proliferation

We next examined the mechanisms responsible for ATM persistence during weight loss. To determine if recruitment was a significant contributor to ATM

maintenance during weight loss, we employed PKH26 pulse-labeling in ND and HFD mice prior to diet switch. This method labels tissue macrophages, but not blood monocytes, allowing identification of recruited ATMs as PKH26$^-$ cells (49). Twelve-week HFD and ND controls were injected IP with PKH26. Labeling efficiency of ATMs assessed one day after PKH26 injection was similar in lean and obese mice (Figure 3-9A-B). The frequency of PKH26$^+$ ATMs was examined after 8 weeks and was lower in ND mice compared to HFD or WL groups demonstrating a higher rate of ATM retention in HFD and WL mice (Figure 3-9C). The data indicate that new monocyte recruitment may not be the primary mechanism for maintenance of CD11c$^+$ ATMs during weight loss.

Reduced apoptosis was also considered as a potential mechanism of ATM maintenance. ATM annexin V labeling was significantly reduced in HFD mice and after one week of diet-switch compared to ND mice indicating these ATMs had a relatively low level of apoptosis which may contribute to ATM maintenance in eWAT of HFD and WL mice (Figure 3-9D). This is surprising given the reduction in total ATM content observed during the early stages of weight loss (Figure 3-3D) and suggests ATM exfiltration may be responsible for the decrease.

Another mechanism for how total numbers of ATMs may be sustained without continual recruitment is proliferation. We evaluated ATM proliferation by Ki67 expression. IHC demonstrated an increase in Ki67$^+$ nuclei surrounding CLS in 8wk WL mice compared to 12wk HFD and comparable to 20wk HFD mice (Figure 3-9E-F) suggesting a continual increase in proliferating cells despite WL. Flow cytometry demonstrated that >90% of the Ki67$^+$ cells in the SVF were CD45$^+$ leukocytes (Figure 3-9G). ATMs made up >50% of these Ki67$^+$ SVF cells in both HFD and WL mice, and both were significantly elevated compared with ND controls (Figure 3-9H). The overall frequency of Ki67$^+$ ATMs in HFD and WL mice was also significantly higher than ND (Figure 3-9I). Specifically, our data demonstrates that the frequency of Ki67$^+$CD11c$^+$ ATMs in HFD and WL mice was significantly elevated compared to Ki67$^+$CD11c$^-$ ATMs (Figure 3-9J). Collectively, the data indicate that CD11c$^+$ ATM maintenance during weight loss may primarily be due to a combination of increased proliferation and reduced apoptosis.

Adipose tissue dendritic cell dynamics during obesity and weight loss

We also evaluated adipose tissue dendritic cell populations (ATDC) during obesity and weight loss to compare and contrast with ATMs. Similar to ATMs, ATDCs accumulate in eWAT with obesity and, though reduced, remain significantly elevated after weight loss when compared to ND mice (Figure 3-10A). However, the overall number of eWAT ATDCs was substantially less than ATMs during obesity and after weight loss. Microarray analysis of sorted eWAT ATDC populations from both ND and 20wk HFD mice revealed similar expression levels of pro-inflammatory cytokines *Il1b*, *Tnf* and *Il6* (Figure 3-10B). Intracellular cytokine staining was also done with ATDCs and showed little to no expression of TNFα and IL6 during obesity and weight loss (Figure 3-10C-D), which was in stark contrast to what was observed in ATMs (Figure 3-3G). Fewer ATDCs expressed surface co-stimulatory markers (Figure 3-10E) compared to ATMs (Figure 3-6A-D) as well. A majority of eWAT ATDCs were found to express Ki67 during obesity and weight loss (Figure 3-10F). However, ATMs were still found to be the dominant Ki67$^+$ population within the SVF and the overall frequency of Ki67$^+$ ATDCs was not different between ND, HFD and WL conditions.
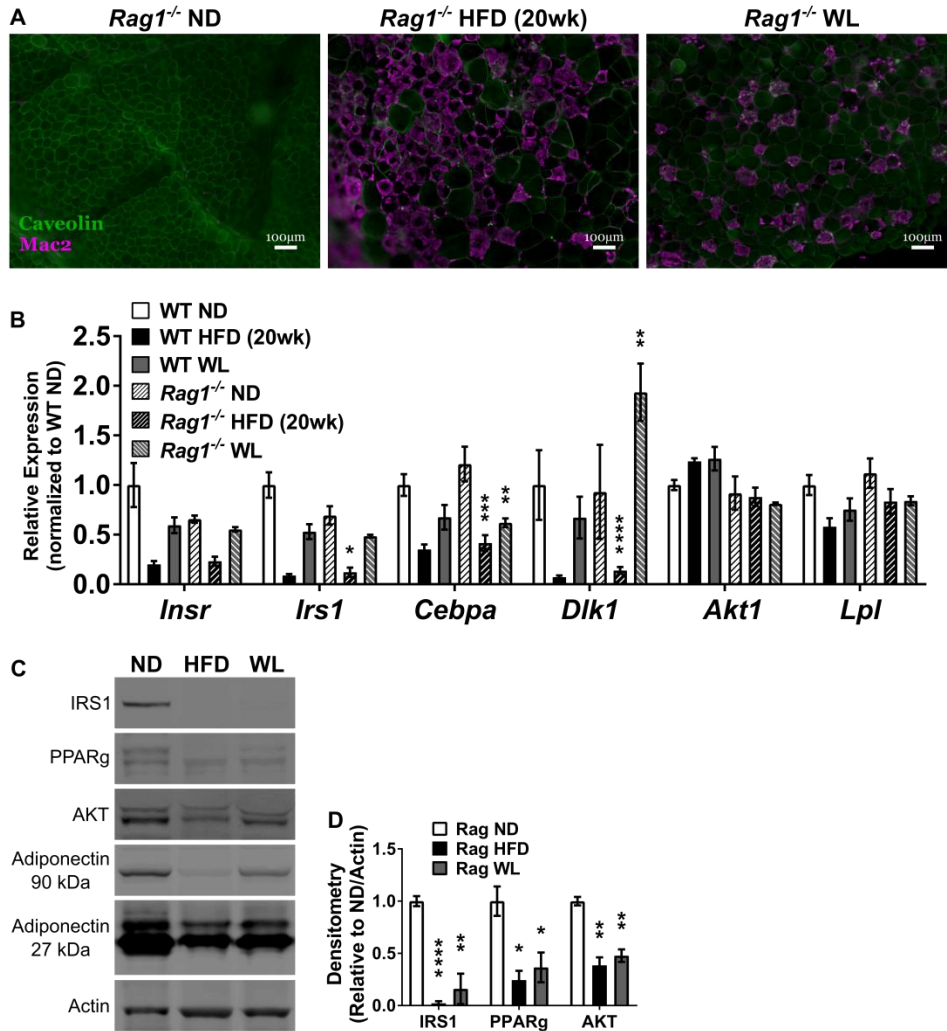
Figure 3-8 – *Rag1*$^{-/-}$ mice show altered eWAT gene and protein expression during obesity and weight loss similar to WT mice. (A) Immunofluorescence images showing CLS development in eWAT tissue after 20 weeks HFD and weight loss. (B) Comparison of eWAT gene expression between WT and *Rag1*$^{-/-}$ mice normalized to WT ND. (C) Immunoblots showing protein expression changes during obesity and weight loss in whole eWAT tissue and (D) quantification of relative densitometry measures from immunoblots. $^{*}p < 0.05$, $^{**}p < 0.01$, $^{***}p <0.001$, and $^{****}p < 0.0001$. For B and D significance compares with the *Rag1*$^{-/-}$ ND-fed control group.
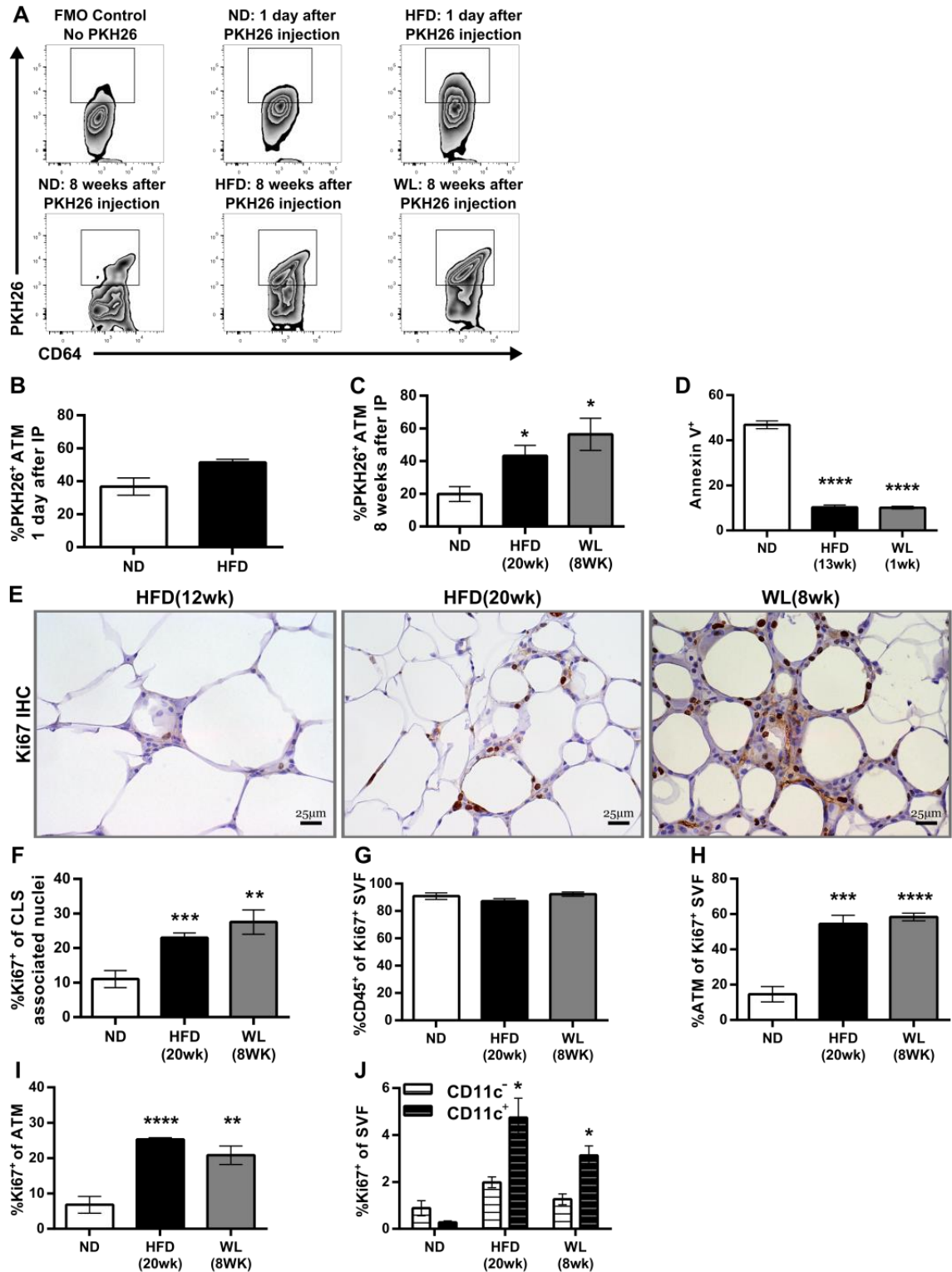
Figure 3-9 – Macrophages are maintained through increased proliferation and reduced apoptosis. Mice were injected with PKH26 intraperitoneally after 12 weeks of HFD exposure along with aged-matched ND controls. (A) Representative flow cytometry plots gated on CD45$^+$CD64$^+$ ATM showing PKH26$^+$ cells one day after injection, 8 weeks after injection and a

fluorescence minus one control for PKH26. Frequency of PKH26$^+$ ATM either (B) one day after injection or (C) 8 weeks after injection. (D) Annexin V staining of SVF as evaluated by flow cytometry (n = 4). (E) Representative Ki67 immunohistochemistry slides and (F) Quantification of Ki67$^+$ nuclei surrounding CLS from the IHC images (n ≥ 7). (G) Flow cytometric analysis showing frequency of all Ki67$^+$ SVF that were CD45$^+$ immune cells (n = 4). (H) Frequency of all Ki67$^+$ cells that were ATMs (n = 4). (I) Frequency of all ATMs that were Ki67$^+$ (n = 4). (J) Frequency of Ki67$^+$ CD11c$^-$ (white) or ki67$^+$ CD11c$^+$ (black) ATM as a percent of all SVF (n = 4). *p < 0.05, **p < 0.01, ***p < 0.001, ****p < 0.0001; significance compares with the ND-fed control group except in J; significance values for (J) compare CD11c$^+$ with CD11c$^-$.
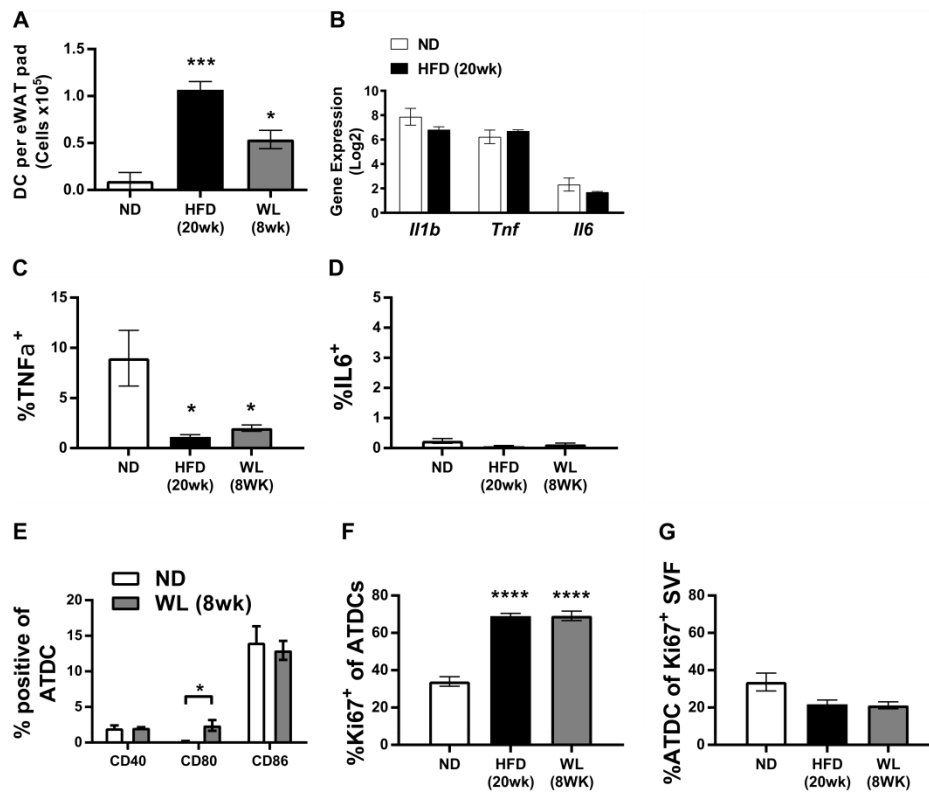
Figure 3-10 – Adipose tissue dendritic cells have a less-inflammatory profile than ATMs during obesity and weight loss. (A) Total adipose tissue dendritic cells (ATDC) in eWAT. (B) Gene expression as evaluated by microarray on FACS sorted ATDCs from eWAT of lean and obese mice. Frequency of ATDCs expressing (C) TNFα and (D) IL6 as determined by flow analysis of intracellular cytokine labeled SVF. (E) Surface labeling of co-stimulatory markers on ATDCs from eWAT tissue of ND and WL mice. (F) Frequency of all ATDCs which are also Ki67$^+$ and (G) frequency of all Ki67$^+$ SVF that are ATDCs. *p < 0.05, ***p < 0.001, ****p < 0.0001; significance compares with the ND-fed control group.

Discussion

In this study, we used a mouse model of weight loss to understand leukocyte dynamics in adipose tissue of formerly obese mice. Our major finding is that chronic

obesity leads to long term alterations in adipose tissue leukocyte populations associated with persistent abnormalities in insulin tolerance that persist despite weight loss. Maintenance of CD11c$^+$ ATMs was observed as long as six months after HFD was stopped. ATMs, but not ATDCs, in WL mice retained a pro-inflammatory profile with elevated cytokine (IL-6, IL-1β and TNFα) and costimulatory marker expression. Adipose tissue T cells were required for ATM activation, but not required for sustaining ATMs in abdominal depots.

ATMs were sustained in formerly obese mice primarily through local proliferation and decreased apoptosis and not ongoing recruitment of blood monocytes. The mechanism(s) for ATM proliferation induction and maintenance remains unclear at this time, but potential mechanisms include MCP-1 and IL-4 (169; 185). Our findings are in agreement with other studies suggesting that weight loss only partially improves adipose tissue inflammation after it is established (125; 130; 173; 174). The transient increase and persistence of CLSs that we observe in this study is more robust than reported in other studies. One potential difference is our use of 60% HFD for 12 weeks, a widely used model of chronic over-nutrition (48; 49; 51; 87; 112). We found that the leukocyte changes observed after removal of HFD were dependent on the duration of HFD feeding and, potentially, body fat percentage. We focused on the inflammatory activation of individual leukocyte subsets because of a lack of studies comparing the activation profiles of sorted ATMs and T cells after weight loss. We observed reduced *Tnfα* and *Il1β* in WL ATMs compared to ATMs residing in mice maintained on HFD in agreement with other observations (51). However, *Il6* expression was substantially increased and we found the overall expression of inflammatory cytokines and chemokines from ATMs remained significantly elevated in WL mice compared to ND mice. Overall, our observations significantly support and critically extend an evolving paradigm demonstrating that obesity imparts lasting changes which fail to fully resolve with weight loss. Clinical studies have found persistent subcutaneous adipose inflammation in humans after weight loss despite improvements in insulin sensitivity improvements (125; 126; 130; 186).

We also observed a persistent decrease in systemic insulin sensitivity in WL mice associated with adipose tissue architectural changes, elevated ATM content, and fibrosis in agreement with other recent studies (51; 125; 126). Several proteins involved in adipocyte differentiation and insulin signaling were substantially reduced in formerly obese mice despite return to normal weight. Interestingly, the 24 week weight loss experiment shows that adipose tissue fibrosis can be cleared with time (Figure 3-4F). It's worth speculating that retained ATMs may also have beneficial functions related to resolving the excess extracellular matrix deposition consistent with the role macrophages play in wound healing and matrix remodeling (187; 188). Further investigation is necessary to determine whether ATMs have potentially beneficial functions within adipose tissue in addition to known deleterious activity.

Given the connection between antigen presenting cells and T cell activation in adipose tissue, we evaluated T cell changes with weight loss (111; 181; 184). Weight cycling was shown to alter T cell composition in adipose tissue (175) and we observed dynamic changes in adipose tissue T cells in our model as well. IFNγ$^+$ T cells, particularly CD8$^+$ T cells, were retained during weight loss. However, experiments in $Rag1^{-/-}$ mice revealed that T cells were not required for CD11c$^+$ ATM recruitment and maintenance. After weight loss, $Rag1^{-/-}$ mice remained glucose intolerant which may relate either to ongoing adipose tissue inflammation due to lack of regulatory T cells (50), or due to dysfunction in other metabolic tissues such as islets or the liver. Our findings also indicate that lymphocyte signals are necessary for the inflammatory maintenance of ATMs during weight loss but are not necessary for pro-inflammatory activation of ATMs during HFD-induced obesity. This suggests lymphocyte-derived stimulatory signals (i.e. CD40L or IFNγ) could be targeted to attenuate inflammation while still preserving beneficial ATM functions but that active obesity may limit the potential efficacy. Innate lymphocyte populations, such as NK cells, should also be carefully investigated during obesity and weight loss to determine how they may influence the adipose tissue inflammatory state. It's also important to note publications which have found potentially neutral or even beneficial effects of inflammation for regulating adipose tissue function. Thermoneutrality, for example, potentiates adipose tissue inflammation and ATM accumulation without abnormalities in glucose regulation (189). Low-level adipose

inflammation has even been found to be important for maintaining metabolic homeostasis and adipogenesis (87). Overall the literature indicates the role played by adipose tissue inflammation is complex with both detrimental and potentially beneficial effects on adipose tissue function.

Clinical studies have shown persistent risk for cardiometabolic disease development in formerly obese adults (125; 126; 128). Our study suggests obesity elicits damage responses in adipose that persist despite weight loss which may contribute to this risk. We posit that maintenance of these features within adipose, particularly inflammation, could contribute to the persistence of metabolic disease risk observed in formerly obese patients. It will be critical to compare our results obtained from using dietary manipulation with the induction of weight loss by other mechanisms such as bariatric surgery which may impart different outputs in the inflammatory state of adipose tissue (190). A potential weakness of this study is that our weight loss protocol did not use isocaloric diets and did not control for food intake by pair-feeding. Our paradigm was designed to mimic current weight loss strategies that use reduced calorie diet meal replacement to achieve weight loss. We believe this paradigm offered the best potential for reversal of obesity-associated features. It's possible, though we believe unlikely, that maintaining HFD but using caloric restriction to induce weight loss may show improved resolution. Future work will continue to investigate the physiological consequences of these maintained features. In particular, we would be interested in identifying whether formerly obese mice have altered physiologic responses in response to certain stimuli such as HFD re-challenge. An additional limitation was the inability to evaluate additional adipose-resident leukocyte populations, such as B cells and NK cells, which may influence the overall inflammatory state of adipose tissue during both obesity and weight loss. We hope the results from this study invigorate interest for evaluating changes in, and functions of, these other populations during obesity and weight loss.

Table 6 – Sequences for RT-PCR primers used in this chapter.

Gene	Forward Primer	Reverse Primer
Cd40	TGTCATCTGTGAAAAGGTGGTC	ACTGGAGCAGCGGTGTTATG
Cd80	ACCCCCAACATAACTGAGTCT	TTCCAACCAAGAGAAGCGAGG
Cd86	TGTTTCCGTGGAGACGCAAG	TTGAGCCTTTGTAAATGGGCA
Tnfa	ACGGCATGGATCTCAAAGAC	AGATAGCAAATCGGCTGACG
Il1b	AAATACCTGTGGCCTTGGGC	CTTGGGATCCACACTCTCCAG
Il6	AGTGAGGAACAAGCCAGAGC	CATTTGTGGTTGGGTCAGG

Chapter 4 – Weight Regain in Formerly Obese Mice Hastens the Development of Hepatic Steatosis and Reveals Impaired Adipose Tissue Function

Abstract

Cycles of weight loss and regain are common in people attempting to lose excess adiposity. We sought to investigate the impact of weight regain in formerly obese mice on metabolic health, adipose tissue architecture, and stromal cell function. A diet-switch model was employed for obesity induction, weight loss, and weight regain in mice. Epididymal white adipose tissue of formerly obese mice failed to expand in response to repeat exposure to high-fat diet and retained elevated numbers of macrophages and T cells. Weight regain was associated with hyperinsulinemia and disproportionally elevated liver mass, hepatic triglyceride content, and serum transaminase concentrations. These effects occurred despite an extended six month weight loss cycle and demonstrate that formerly obese mice maintain durable alterations in their physiological response to weight regain. Epididymal adipose tissue of formerly obese mice secreted factor(s) that actively inhibited adipogenesis of 3T3-L1 preadipocytes suggesting a potential mechanism to explain failed epididymal adipose tissue expansion during weight regain. These data indicate that metabolic and physiologic abnormalities manifest in formerly obese mice during weight regain as a result of unresolved effects that persist through weight loss.

Introduction

Obesity is associated with increased risk for a number of co-morbidities including insulin resistance, type 2 diabetes, and cardiovascular disease. Weight loss, through caloric restriction or bariatric surgery, improves metabolic dysfunction and can reduce inflammation within adipose tissue (170-172). Unfortunately, long-term maintenance of even 10% weight loss is difficult, with only around 20% of people able to maintain this reduction beyond one year (191; 192). Even bariatric surgery, which can achieve

81

dramatic initial weight loss effects, has highly variable long-term weight management success with substantial variation in long-term weight loss outcomes (193; 194). One study found over 48% failure rate in long-term weight loss management after gastric banding procedures, with over 60% failure rates in patients originally lost to short-term follow-up (195). Weight regain, regardless of the method used for initial weight loss, is a common occurrence.

An open question within the field is whether weight regain and weight cycling adversely alters metabolic health. The majority of recent research suggests that weight cycling is not associated with increased metabolic risk factors in humans when compared to those that remain overweight or obese (196-198). For example, analysis from the Action for Health in Diabetes (Look AHEAD) clinical trial found no negative associations between regaining weight versus having lost no weight at all when comparing HbA1c, blood pressure, HDL cholesterol, and blood triglycerides (199). However, few studies have evaluated metabolic parameters and altered physiological responses during the active weight regain cycle or examined the long-term effects on adipose tissue function and architecture. Rodent studies have found altered fatty acid metabolism and increased lipoprotein lipase, serum triglycerides, and serum cholesterol during high-fat diet (HFD) re-feeding beyond what was observed in rodents consistently fed HFD *ad libitum* (200-202). Weight cycling can also increase inflammatory markers within adipose tissue and has been associated with insulin resistance (175; 203). These findings suggest metabolic perturbations could exist that only clearly manifest during weight regain in formerly obese subjects.

In support of this possibility, recent research suggests that weight loss is not capable of fully resolving life-long metabolic syndrome risk or reducing markers of adipose tissue dysfunction. Inflammatory gene expression within the adipose tissue of formerly obese human subjects remains high compared to lean subjects (126; 129). Results from mouse studies show similar persistent expression of inflammatory cytokines in adipose tissue despite weight loss including IL-6, IL-1β and TNFα (125; 130; 173; 174; 204). It was recently demonstrated that weight loss incompletely resolved adipose tissue inflammation and insulin sensitivity in both mice and humans (125). Our group

recently reported that inflammatory CD11c$^+$ macrophages are maintained within adipose tissue despite extended weight loss along with persistent impairment in insulin tolerance (204).

In this study, we sought to identify metabolic and inflammatory perturbations associated with early weight gain in formerly obese mice compared with lean or obese mice. We found that the epididymal white adipose tissue (eWAT) of formerly obese mice had impaired expansion and reduced lipid storage capacity with HFD re-feeding. This effect persisted despite an extended six month period off HFD for the weight loss cycle. After weight regain, mouse eWAT was found to secrete factors that actively inhibited *in vitro* adipogenesis and lipid storage in 3T3-L1 cells. This failure for eWAT to expand was associated with increased hepatic triglyceride storage and elevated transaminase levels in serum after weight regain. We believe there may be certain unique metabolic abnormalities that develop at a hastened rate in formerly obese subjects during weight regain as a result of unresolved effects that persist despite weight loss.

Materials and Methods

Animals and Animal Care

Male C57BL/6J mice were purchased from Jackson Laboratory. Six-week old male mice were fed control normal diet (ND; LabDiet PicoLab 5L0D 4.09 kcal/gm 29.8% protein, 13.4% fat, 56.7% carbohydrate) or high-fat diet (HFD; Research Diets D12492, 5.24 kcal/gm 20% protein, 60% fat, 20% carbohydrate).

Glucose tolerance tests (GTT) and insulin tolerance tests (ITT) were performed after 6 hours fasting. Mice were injected IP with D-glucose (0.7 g/kg) for GTTs and human recombinant insulin (1 U/kg) for ITTs. Glucose was measured using FreeStyle Lite blood glucose monitoring system. Insulin was measured by ELISA (Crystal Chem). Energy metabolism was measured using Comprehensive Lab Animal Monitoring System analysis (CLAMS, Columbus Instruments). All mouse procedures were approved by the University of Michigan Committee on Use and Care of Animals and were conducted in

compliance with the Institute of Laboratory Animal Research Guide for the Care and Use of Laboratory Animals.

Gene expression analysis

RNA was extracted from adipose using Trizol LS (Life Technologies) and cDNA generated using High Capacity cDNA Reverse Transcription Kit (Applied Biosystems). SYBR Green PCR Master Mix (Applied Biosystems) and the StepOnePlus System (Applied Biosystems) were used for real-time quantitative PCR. *Gapdh* expression was used as an internal control for data normalization. Samples were assayed in duplicate and relative expression was determined using $2^{-\Delta\Delta}$ CT method.

Primers used in this study are listed in Table 7.

Immunoblotting and Immunofluorescence

Adipose tissue was homogenized in RIPA lysis buffer with phosphatase inhibitors. Protein concentration was determined using Bio-Rad Protein Assay Dye Reagent. Proteins were labeled and visualized using Odyssey infrared imaging system (Li-Cor Bioscience). Antibodies used for immunoblotting: PPARγ (81B8), IRS-1, Phospho-Akt (Ser473), AKT, Adiponectin (C45B10) (Cell Signaling Technology) and β-Actin (AC-40) (Sigma-Aldrich).

Whole-mount adipose tissue explantsfixed overnight in a 2% paraformaldehyde solution were used for immunofluorescence. Antibodies used for immunofluorescence: caveolin (BD Pharmingen) and Mac2 (Galectin-3) (eBioM3/38) (eBioscience).

Isolation of Adipose Tissue Stromal Vascular Fraction and Flow Cytometry

Excised adipose tissue was digested in RPMI with 0.5% BSA and 1 mg/ml type II collagenase for 25 min at 37°C and the stromal vascular fraction (SVF) was separated

from adipocytes by centrifugation. The following antibodies were used for flow cytometry: CD45 (30-F11), CD3e (145-2C11), CD4 (GK1.5), CD8a (53-6.7), CD11c (N418), Sca-1 (Ly-6A/E) (D7), CD31 (390) (eBioscience), PDGFRα (RM0004-3G28) (Abcam), and CD64 (X54-5/7.1) (BD Pharmingen). Analysis was performed using a BD Biosciences FACSCanto II and FlowJo v.10 (Treestar).

Explant Conditioned Media

200mg epididymal adipose tissue explants were cultured in serum-free AIM V media with AlbuMax and BSA (Life Technologies) to create conditioned media (CM). For CM treatment, confluent 3T3-L1 cells were treated with a 1:1 mixture of CM and MDI differentiation media (final concentration 0.5mM methylisobutylxanthine, 1μM dexamethasone and 10μg/mL human recombinant insulin in DMEM); after 3 days media was replaced with another 1:1 mixture of CM and insulin medium (10μg insulin in DMEM). For cytokine and chemokine treatments 3T3-L1 cells were treated during both phases of differentiation. For TNFα neutralizing experiments CM was treated 1 hour with 100 ng/mL blocking antibody before using the CM in 3T3-L1 differentiation cultures at a final concentration of 50ng/mL (D2H4 mAb, CST). Chemokine treatments were performed at 10ng/mL (PeproTech).

Mouse Cytokine Antibody Array (R&D Systems) was used to evaluate cytokine output from adipose tissue explants after 48 hours conditioning and samples were pooled from 3 mice. Quantitation by ImageJ after background subtraction and normalization to reference controls.

Liver Triglyceride Quantification

Approximately 100mg frozen liver samples were homogenized in 300μL lysis buffer (10% NP-40, 50mM Tris-HCl pH 7.5 and 100mM NaCl) and 200μL chloroform was added before drying in a vacuum concentrator. Lipids were extracted using 400μL chloroform and transferred to new tubes for drying. Lipids were reconstituted with 1mL

85

per 100mg tissue of a butanol mixture (6% butanol, 3.33% Triton-X100 and 0.66% Methanol) and quantified using the Infinity™ Triglyceride Quantification Kit (Thermo Scientific).

Statistical Analyses

All values are reported as mean ± SEM unless otherwise noted. Statistical significance of differences were determined using unpaired two-tailed Student's t-test or one-way ANOVA for multiple groups using Fisher's least significant difference test for planned statistical comparisons. All relative gene expression data was compared using two-way ANOVA with Dunnett's multiple comparisons correction. All analysis was performed using GraphPad Prism V6.05.

Results

High-fat diet re-challenged mice have greater than anticipated increases in body weight but reduced eWAT mass

Weight loss was modeled based on the withdrawal of high-fat diet (HFD) from diet-induced obese mice (204). Male C57BL/6J mice were fed HFD (60% kcal fat) or ND (13.5% kcal fat) for 12 weeks. Obese mice were then maintained on HFD or switched to ND for 8 weeks to induce weight loss. After weight loss, mice were then re-challenged with HFD for 6 weeks (RC HFD). Age-matched control mice included: a) a group continuously fed HFD long-term for all 26 weeks (LT HFD); and b) mice fed ND for the first 20 weeks followed thereafter by short-term HFD challenge for the final 6 weeks (ST HFD) (Figure 4-1A).

After weight loss, body weight was 32.1g (SD ± 1.45) and was similar to age-matched ND mice 30.35g (SD ± 1.11) (Figure 4-1B). After HFD re-challenge the body weight of RC HFD mice was significantly elevated (52.68g SD ± 1.52) compared to ST HFD mice (43.85 SD ± 5.21), but RC HFD mice were not significantly different from LT HFD mice (52.0 SD ± 4.0) (Figure 4-1C). Energy metabolism analysis of mice after

weight loss showed a small, but significant, reduction in total energy expenditure in weight loss mice compared to ND mice which was further reduced in mice fed HFD for 20 weeks (Figure 4-1D). One week after initiating HFD re-challenge, RC HFD mice had higher food intake than ST HFD and LT HFD mice (Figure 4-1E). The reduced energy expenditure and increased HFD intake likely explains the significantly elevated body weight of RC HFD mice compared to ST HFD mice.

GTTs and ITTs were performed during HFD re-challenge to assess metabolic differences between ST HFD and RC HFD mice. GTTs were similar between RC HFD and ST HFD mice after 2 weeks and 4 weeks of HFD (Figure 4-1F-G). Fasted blood glucose and serum insulin were also measured after 6 weeks of HFD re-challenge. RC HFD mice had a trend towards reduced fasting blood glucose levels compared to ST HFD mice, but this did not reach significance (Figure 4-1H). Serum insulin levels were significantly increased in RC HFD mice and similar to levels measured in LT HFD mice (Figure 4-1I). ITTs revealed comparable insulin sensitivity between ST HFD and RC HFD mice and impaired insulin tolerance in LT HFD mice (Figure 4-1J).

Despite increased body weights, the epididymal white adipose tissue (eWAT) in RC HFD mice was paradoxically smaller than ST HFD mice and made up a smaller percentage of total body weight (Figure 4-1K-L). The eWAT adipocyte size distribution from both ST HFD and RC HFD mice were not different (Figure 4-1M). These curves were similar to LT HFD (not shown), and the average adipocyte size in ST HFD, RC HFD and LT HFD were not significantly different from each other (Figure 4-1M). Overall, the data suggest reduced eWAT mass was not due to a deficiency in individual adipocyte lipid storage capacity and may, instead, be due to a difference in adipocyte number.
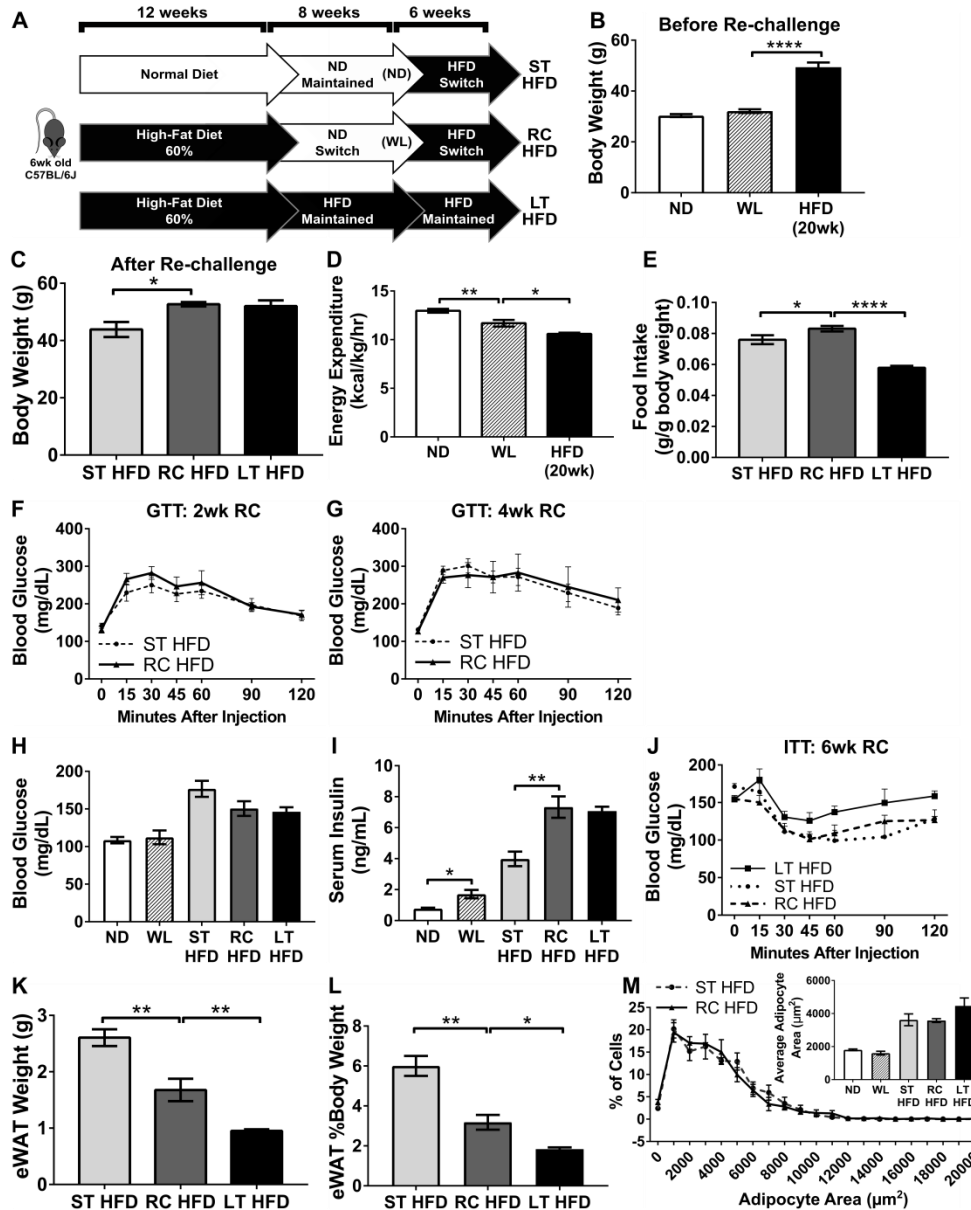
Figure 4-1 – Weight loss and HFD re-challenge model. (A) Cartoon showing obesity induction, weight loss and HFD re-challenge model. Body weights after (B) weight loss and (C) HFD re-challenge. (D) Energy expenditure after weight loss and (E) food intake one week after starting HFD re-challenge phase. (F-G) Glucose tolerance testing at 2 and 4 weeks of HFD re-challenge. (H) Fasted blood glucose, (I) fasted serum insulin and (J) insulin tolerance after 6 weeks of HFD re-challenge. (K) Total epididymal WAT (eWAT) weight and (L) eWAT as a percent of total body weight with (M) eWAT adipocyte size distribution. [*]p < 0.05, [**]p < 0.01, [****]p <0.0001; significance was only compared for ST HFD versus RC HFD, LT HFD versus RC HFD, ND versus WL or WL versus HFD (20wk).

eWAT of formerly obese mice had deranged protein and gene expression profiles after HFD re-challenge

To better understand why the eWAT depots of RC HFD were resistant to expansion after HFD re-challenge we examined adipose tissue histology of all groups. We previously reported that the eWAT of formerly obese mice retain many features associated with chronic obesity including increased fibrosis, continual crown-like structure (CLS) development, and maintenance of pro-inflammatory leukocytes despite weight loss (204). As anticipated, histology and immunofluorescence of RC HFD and LT HFD eWAT revealed substantial CLS presence and leukocyte infiltration while ST HFD mice had minimal identifiable CLS (Figure 4-2A). Adipocytes are critically dependent on expression of key genes encoding proteins for insulin signaling (*Insr*, *Irs1*, *Akt,* and *Glut4*) as well as transcription factors important for adipogenesis and mature adipocyte function (*Cebpa* and *Pparg*) (205). Immunoblots of eWAT revealed reductions in proteins associated with mature differentiated adipocytes including PPARγ, IRS-1, and AKT in RC HFD and LT HFD mice compared to ST HFD mice (Figure 4-2B-C). Gene expression analysis showed reduced expression of *InsrI, Irs1*, *Cebpa*, *Pref1* and *Glut4* in ST HFD, LT HFD, and RC HFD eWAT compared to ND mice. RC HFD and LT HFD gene expression was further reduced compared to ST HFD for these same genes with significant reductions observed for *Cebpa*, *Pref1* and *Glut4* (Figure 4-2D).
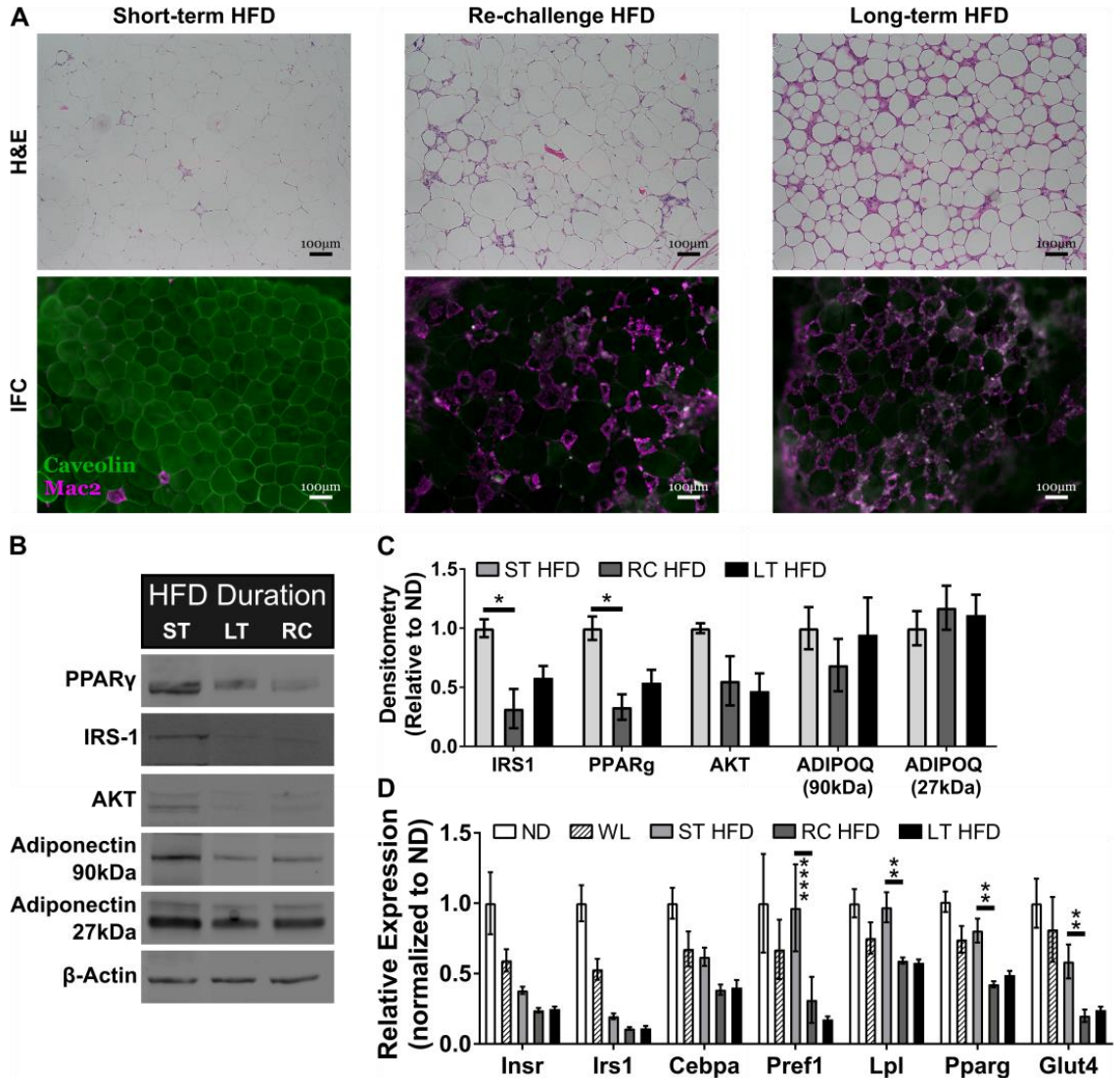
Figure 4-2 – HFD re-challenge increases epididymal adipose tissue crown-like structures and reduces expression of proteins essential for mature adipocyte development and function. (A) Immunofluorescence and H&E stained eWAT slides representative for each diet condition showing CLS development and maintenance. (B) Representative immunoblots from eWAT showing select adipocyte maturation and insulin signaling proteins. (C) Quantification of densitometry measurements from immunoblots of whole eWAT. (D) Expression of select adipocyte maturation genes from eWAT. Two-way ANOVA with Dunnett's multiple comparisons for D. $^{*}p < 0.05$, $^{**}p < 0.01$, $^{****}p < 0.0001$, significance was only compared for ST HFD versus RC HFD, LT HFD versus RC HFD or ND versus WL.
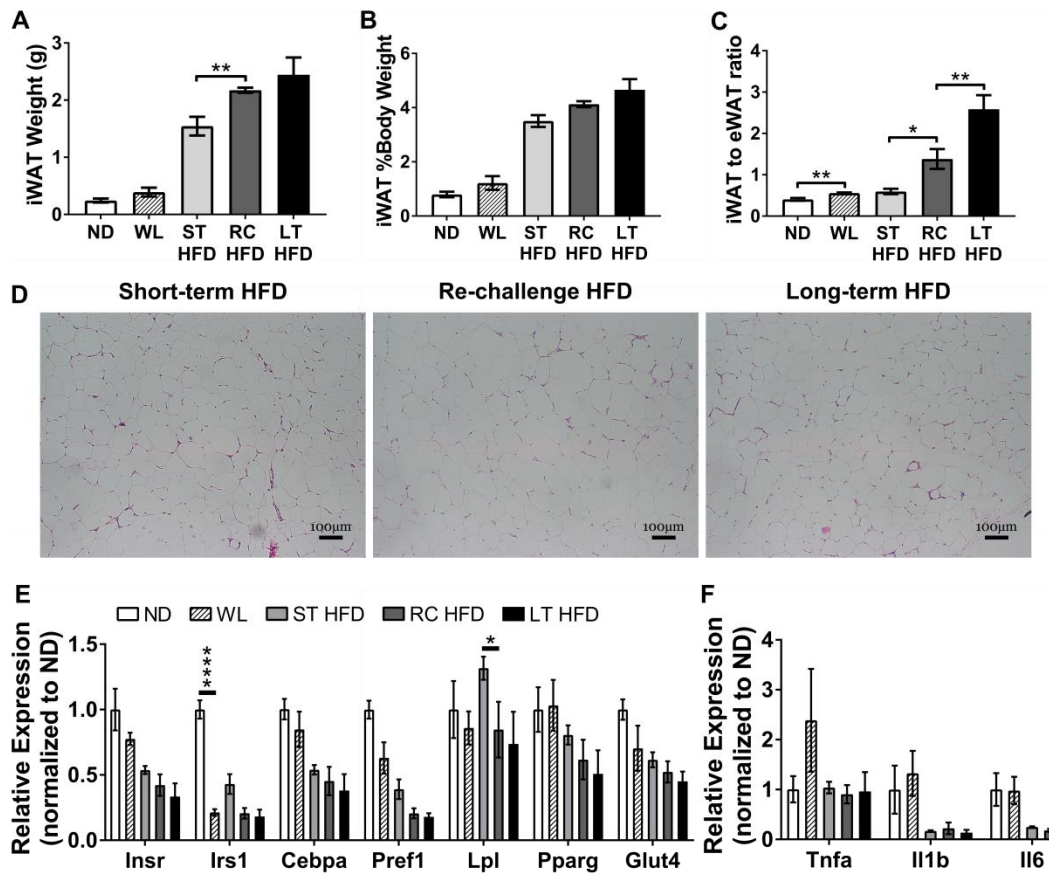
Figure 4-3 – Inguinal adipose tissue shows resistance to derangement with HFD re-challenge. Inguinal WAT (iWAT) (A) weight, (B) iWAT as percent of total body weight and (C) ratio of iWAT to eWAT after HFD re-challenge. (D) H&E stained iWAT slides representative for each diet condition showing limited crown-like structures. (E) Expression of select adipocyte maturation genes from whole iWAT. (F) Expression of select inflammatory cytokine genes from whole iWAT. $^{*}p < 0.05$, $^{**}p < 0.01$, $^{****}p < 0.0001$, significance was only compared for ST HFD versus RC HFD, LT HFD versus RC HFD or ND versus WL.

Inguinal subcutaneous adipose tissue has increased mass after HFD re-challenge but is protected from the deranged features found in eWAT

To identify depot specific effects of weight regain, we evaluated subcutaneous inguinal WAT (iWAT) architecture and gene expression. Total iWAT weight was increased in RC HFD mice, compared to ST HFD, and was similar to LT HFD. However, as a percent of total body weight, iWAT was not significantly different between HFD

91

groups (Figure 4-3A-B). When iWAT weight was compared to eWAT weight, ST HFD had similar ratios to what was observed in ND and WL mice. In contrast, RC HFD and LT HFD had significantly greater iWAT to eWAT ratios (Figure 4-3C), suggesting a different pattern of adipose tissue depot lipid storage. Histology revealed no substantial differences in tissue structure or CLS development between diet groups in iWAT (Figure 4-3D). Gene expression from iWAT revealed HFD induced reductions in most mature adipocyte genes compared to ND control, but no significant differences between ST HFD, RC HFD and LT HFD groups were observed except for *Lpl* which was increased in ST HFD iWAT (Figure 4-3E). Inflammatory cytokine gene expression was also evaluated in iWAT revealing no significant differences between ST HFD, RC HFD and LT HFD mice (Figure 4-3F). Overall, in contrast to eWAT, iWAT expansion in RC HFD mice was not significantly impaired compared to ST HFD mice and was associated with a lack of CLS development.

HFD re-challenge increased hepatic steatosis and serum markers of liver dysfunction

Liver histology from ND and WL mice was similar showing resolution of hepatic steatosis after 8 weeks off of HFD (Figure 4A). By histology, RC HFD mice had significantly elevated hepatic lipid involvement compared to ST HFD and similar to LT HFD mice (Figure 4-4A-B). Liver weights were significantly elevated in RC HFD mice compared to ST HFD mice both in absolute and relative liver mass (Figure 4-4C-D). As a result, total hepatic triglyceride content was more than 2 fold higher in RC HFD and LT HFD mice when compared to ST HFD (Figure 4-4E-F). Serum triglyceride concentrations were similar between ST HFD, RC HFD, and LT HFD mice (Figure 4-4G). Serum aspartate aminotransferase (AST) and alanine aminotransferase (ALT) levels were quantified as markers of liver stress and damage. RC HFD mice had significantly elevated levels of both markers with more than two-fold higher serum ALT concentrations than ST HFD mice (Figure 4-4H). Overall, these results show that despite the same duration of HFD exposure as ST HFD mice, RC HFD mice have significantly elevated hepatic steatosis and hepatic dysfunction.
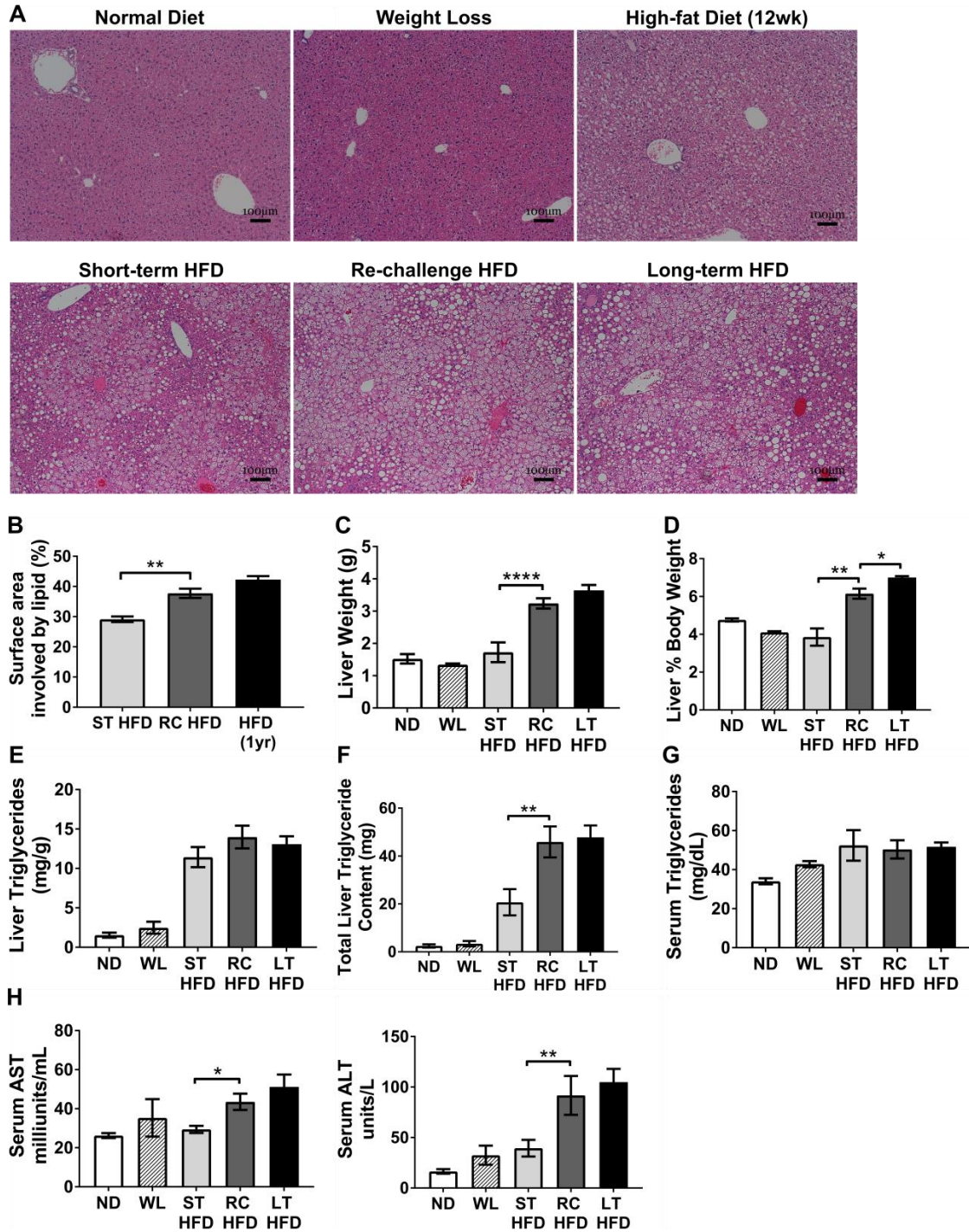
Figure 4-4 – Increased liver steatosis and signs of liver damage with HFD re-challenge. (A) Representative H&E stained slides from livers showing steatosis development and (B) percent of surface area with lipid involvement from H&E images. (C) Liver weight and (D) liver as a percent of total body weight. (E) Liver triglyceride concentration and (F) total liver triglyceride content. Serum concentrations for (G) triglyceride, (H) aspartate aminotransferase (AST, left) and alanine aminotransferase (ALT, right). $^*p < 0.05$, $^{**}p < 0.01$, $^{****}p < 0.0001$, significance was only compared for ST HFD versus RC HFD, LT HFD versus RC HFD or ND versus WL.
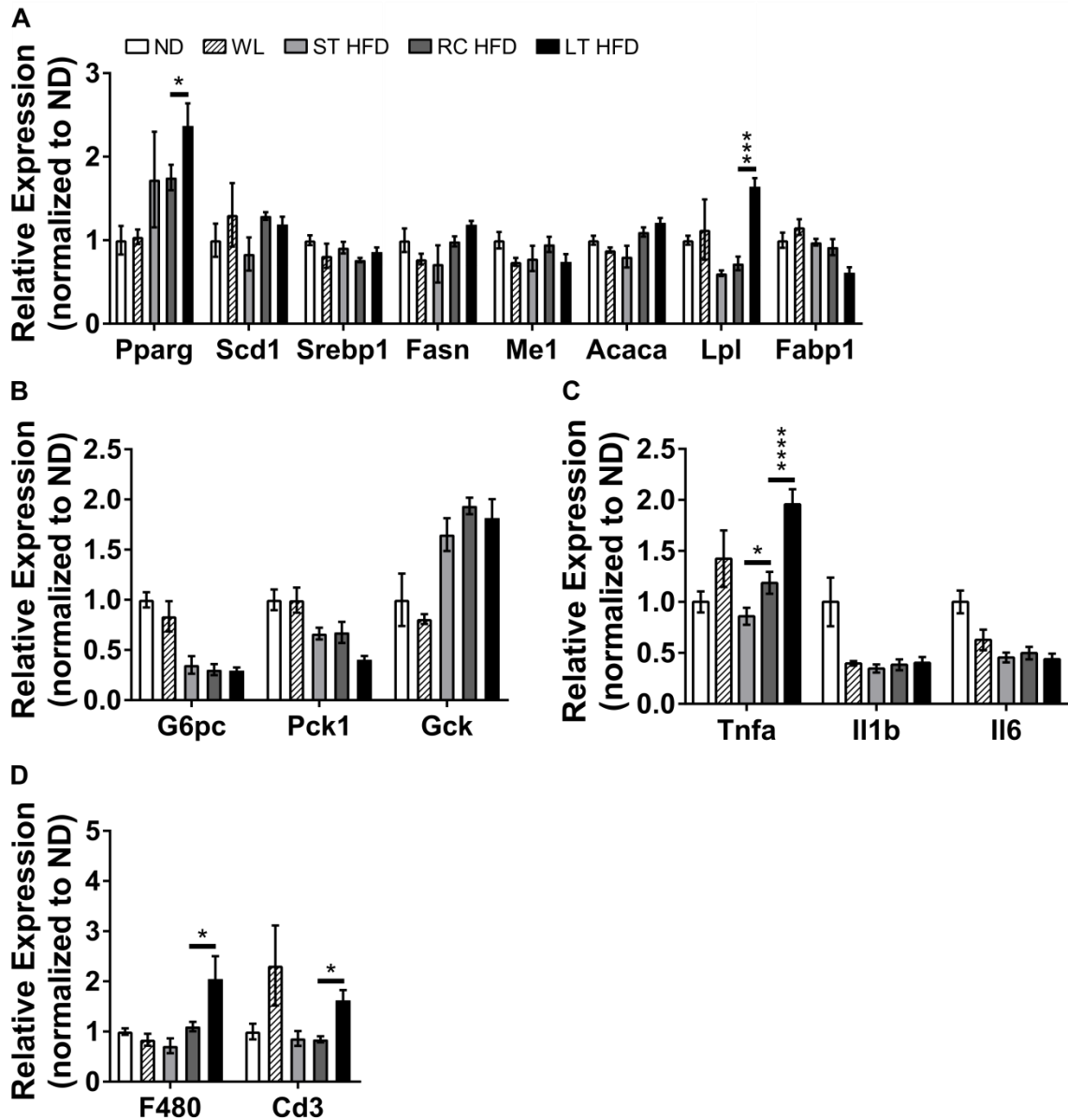
Figure 4-5 – Liver lipid metabolism and lipogenesis gene expression is not significantly different between ST HFD and RC HFD mice groups. Gene expression for select liver (A) lipid metabolism, (B) glucose metabolism, (C) inflammatory cytokine genes, and (D) leukocyte genes. $^{*}p < 0.05$, $^{***}p < 0.001$, $^{****}p < 0.0001$, significance was only compared for ST HFD versus RC HFD, LT HFD versus RC HFD or ND versus WL.

To determine if the increased hepatic triglyceride content was due to increased liver lipogenesis, we evaluated a number of hepatic lipid and glucose metabolism genes.

Compared to ST HFD and RC HFD mice, LT HFD induced *Lpl* and *Pparg* expression but showed no significant differences in expression *of Scd1, Srebp1, Fasn, Me1, Acaca, Fabp1, G6pc, Pck1, or Gck*. No differences were observed in the expression of genes involved in lipid metabolism between RC HFD and ST HFD liver samples (Figure 4-5A-B). Liver inflammatory gene expression did reveal significantly increased expression of *Tnfa* in RC HFD and LT HFD mice, but no differences in *Il1b* and *Il6* expression was observed (Figure 4-5C). Leukocyte gene expression for *F480* and *Cd3* was elevated in LT HFD mice but was not significantly different between ST HFD and RC HFD mice (Figure 4-5D). These results suggest that the increased hepatic triglyceride storage was not the result of increased *de novo* lipogenesis in liver.

The effects observed with HFD re-challenge are retained despite extended time removed from HFD for the weight loss cycle

To evaluate the durability of the effects of prior obesity, we extended the weight loss cycle to 24 weeks and then re-challenged mice with HFD for 6 weeks (Ex-RC HFD) (Figure 4-6A). Age-matched mice were maintained on extended ND (Ex-ST HFD) and extended HFD (Ex-LT HFD) were used for controls. After HFD, the Ex-RC HFD group weighed significantly more than age-matched Ex-ST HFD mice and significantly less than Ex-LT HFD mice (Figure 4-6B). EWAT was reduced in Ex-RC HFD and Ex-LT HFD mice compared to Ex-ST HFD mice in both total mass and as a percent of body weight (Figure 4-6C-D). EWAT immunofluorescence revealed increased CLS in Ex-RC HFD and Ex-LT HFD mice compared to Ex-ST HFD mice (Figure 4-6E). Gene expression of eWAT revealed no significant differences between diet conditions for evaluated adipocyte maturation genes (Figure 4-6F). IWAT weight was not significantly different between Ex-RC HFD and Ex-ST HFD mice but both were less than Ex-LT HFD (Figure 4-6G-H). Fasting blood glucose of Ex-RC HFD mice was significantly elevated compared to Ex-LT HFD mice, but not when compared to Ex-ST HFD mice (Figure 4-6I).

95

Liver histology revealed substantial lipid involvement with all three diet conditions (Figure 4-7A). Total liver weight, and liver weight as a percent of body weight, was significantly elevated in Ex-RC HFD and Ex-LT HFD mice compared to Ex-ST HFD (Figure 4-7B-C). Liver triglycerides were increased in the Ex-RC HFD and Ex-LT HFD mice compared to Ex-ST HFD mice (Figure 4-7D-E). Liver gene expression revealed no significant differences between groups for lipid and glucose metabolism genes assessed (Figure 4-7F-G). Overall the results show that increasing the ND-switch time from 8 weeks to 24 weeks did not improve eWAT lipid storage capability nor reduce liver steatosis development with HFD re-challenge.

Epididymal adipose tissue leukocyte content is increased after HFD re-challenge

Flow cytometry revealed increased total leukocyte accumulation in the eWAT stromal vascular fraction (SVF) of RC HFD compared to ST HFD but less than what was observed in LT HFD mice (Figure 4-8A). The total number of eWAT adipose tissue macrophages (ATM) was also significantly increased in RC HFD mice as well as the frequency of CD11c$^+$ ATM (Figure 4-8B-C). Analysis of adipose tissue T cell populations showed a non-significant increase of total T cell content in RC HFD mice. However, there was a significantly higher frequency of CD8$^+$ T cells in RC HFD mice compared to ST HFD mice (Figure 4-8D-F). EWAT inflammatory cytokine gene expression showed *Tnfα* was increased in RC HFD and LT HFD mice compared to ST HFD, but *Il1β* and *Il6* expression did not differ between groups (Figure 4-8G). Overall, the results suggest that HFD re-challenge promotes increased inflammation and accelerated accumulation of leukocytes within eWAT.
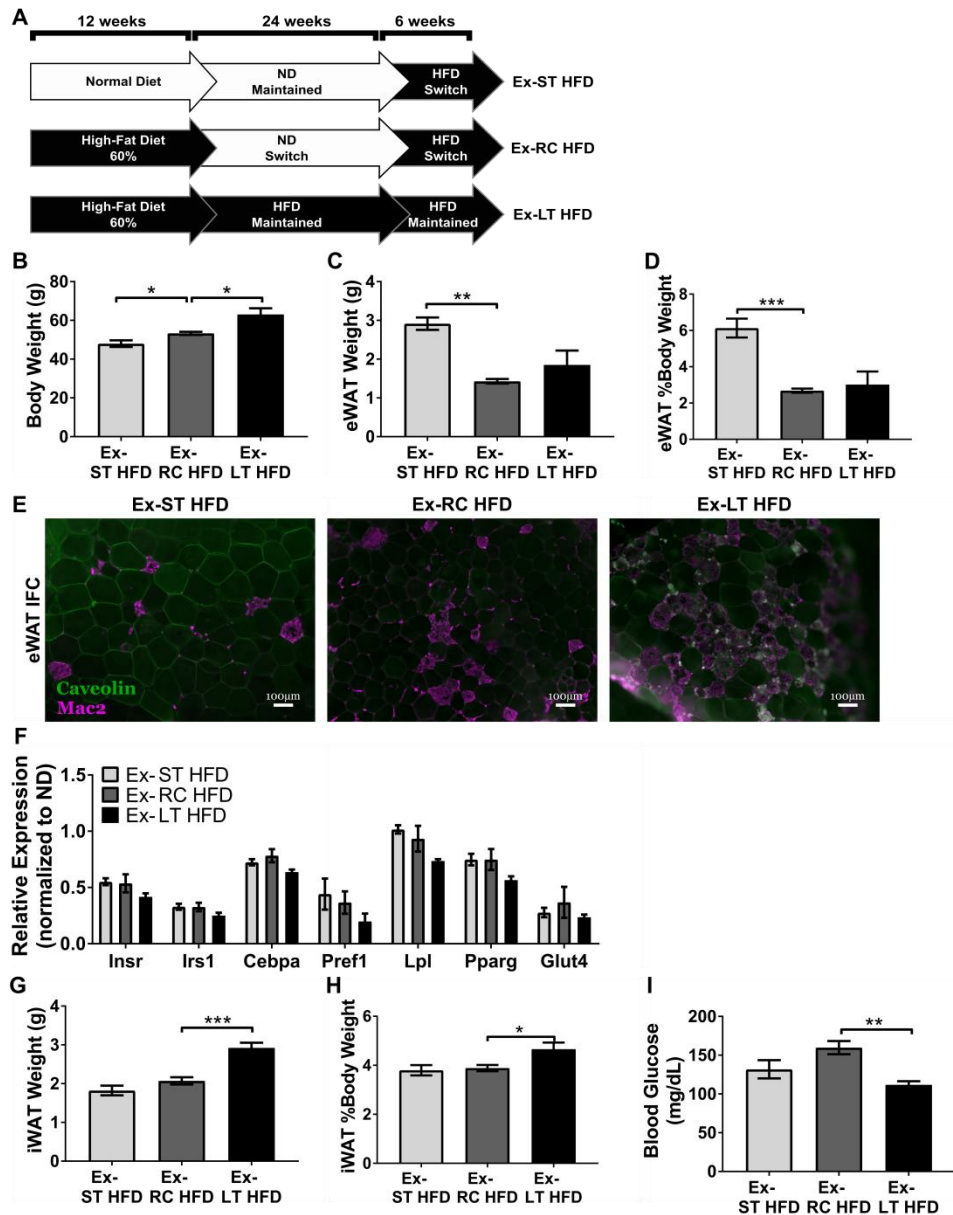
Figure 4-6 – HFD re-challenge after 24 weeks weight loss cycle reveals similar defects in eWAT expansion capacity. (A) Cartoon showing extended ND-switch period of 24 weeks followed by 6 weeks of HFD re-challenge. (B) Body weight of mice after 24wk ND-switch and then re-challenging with HFD. (C) eWAT weight and (D) eWAT as a percent of total body weight after HFD re-challenge. (E) Representative immunofluorescence images showing CLS retention. (F) Expression of select adipocyte maturation genes from whole eWAT. (G) iWAT weight and (H) iWAT as a percent of total body weight. (I) Fasting blood glucose after HFD challenge. $^*p < 0.05$, $^{**}p < 0.01$, $^{***}p < 0.001$, significance was only compared for Ex-ST HFD versus Ex-RC HFD or Ex-LT HFD versus Ex-RC HFD.
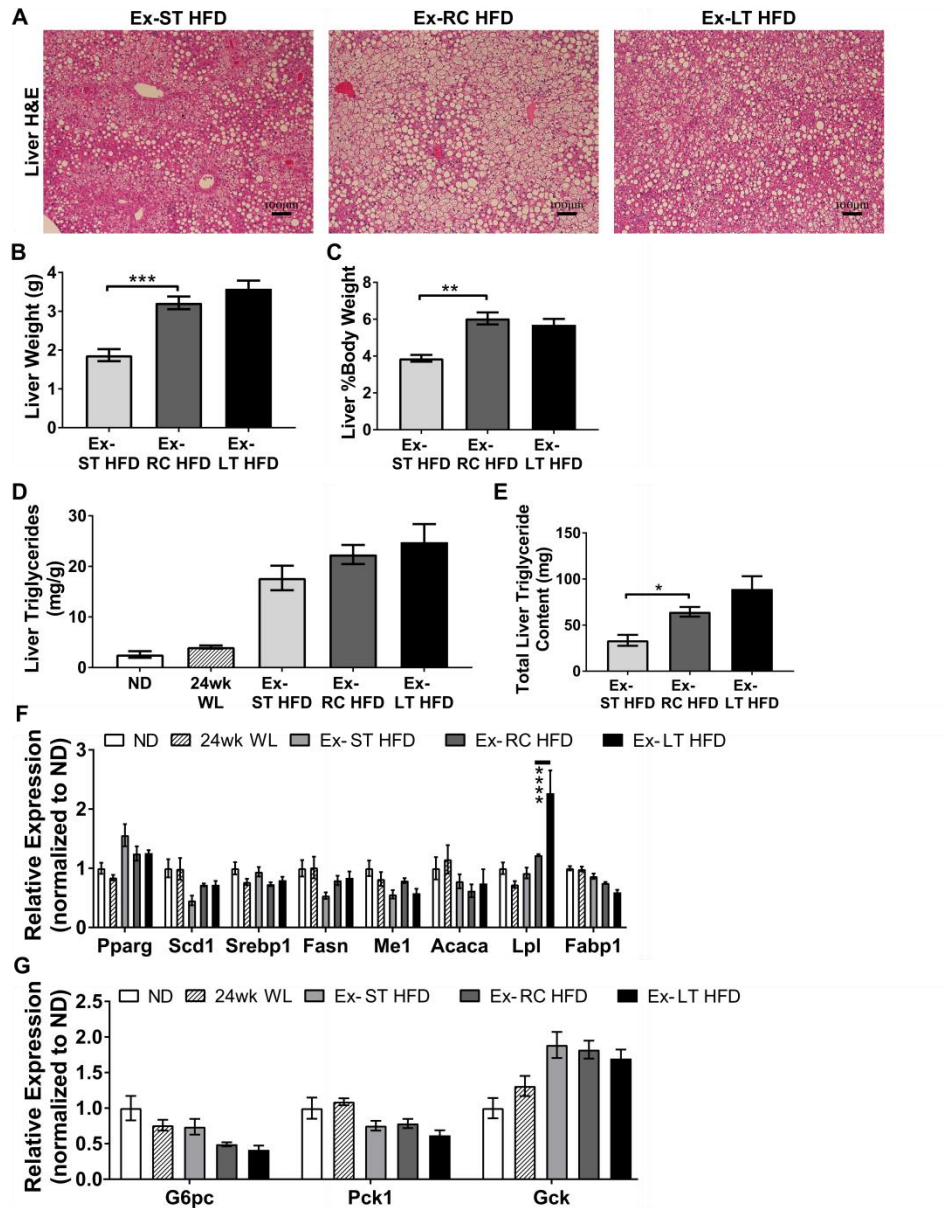
Figure 4-7 – Increased liver triglycerides and steatosis after HFD re-challenge of extended weight loss cycle mice. (A) Representative liver H&E slides showing steatosis development. (B) Liver weight and (C) liver as a percent of total body weight. (D) Liver triglyceride concentration and (E) total liver triglyceride content after HFD re-challenge. Gene expression for select liver (F) lipid metabolism and (G) glucose metabolism genes. $^{*}p < 0.05$, $^{**}p < 0.01$, $^{***}p < 0.001$, $^{****}p < 0.0001$, significance was only compared for Ex-ST HFD versus Ex-RC HFD, Ex-LT HFD versus Ex-RC HFD or ND versus WL.
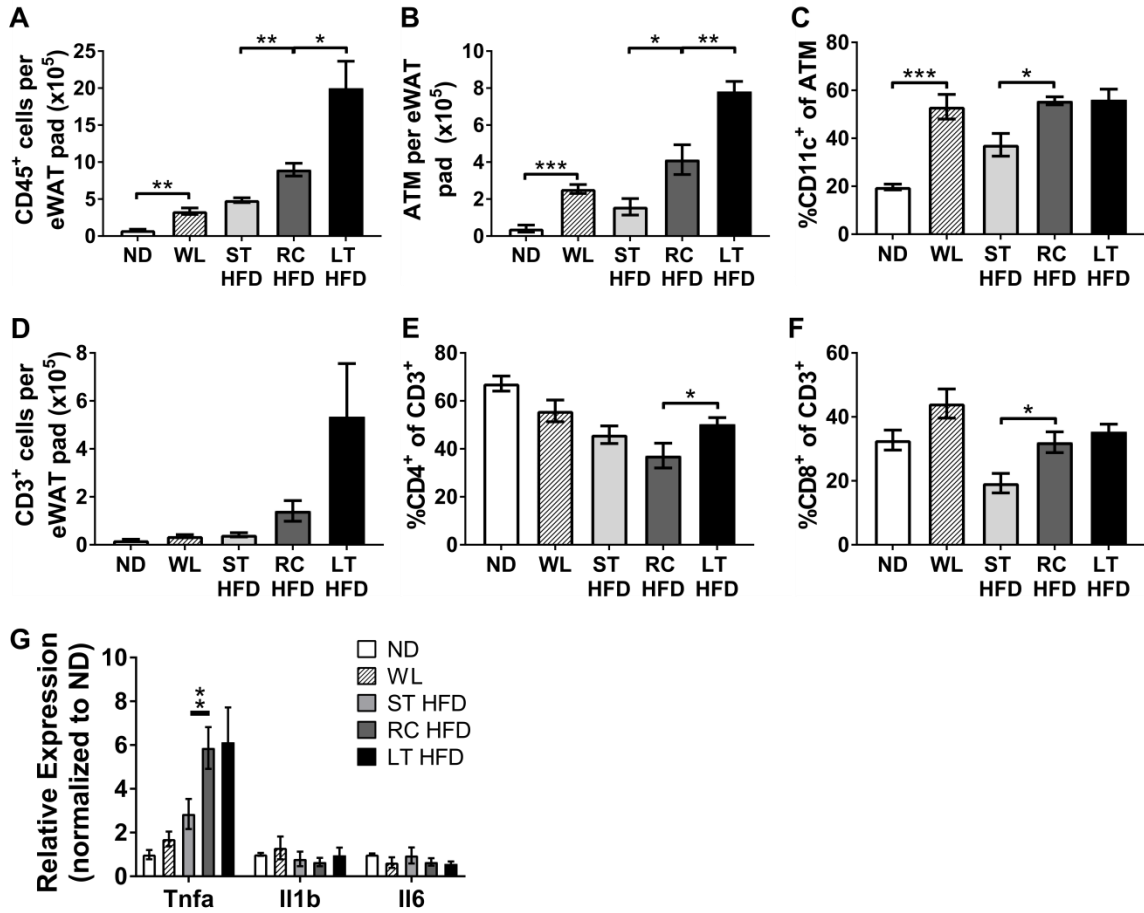
Figure 4-8 – Increased CD11c⁺ ATM accumulation and inflammation with HFD re-challenge. (A) Frequency of CD45$^+$ leukocytes of all eWAT SVF. (B) Total ATM content per eWAT pad and (C) frequency of all CD45$^+$CD64$^+$ ATM that express CD11c. (D) Total T cell content per eWAT pad. Frequency of (E) CD4$^+$ and (F) CD8$^+$ cells of all adipose tissue T cells. (G) Expression of select inflammatory cytokine genes from whole eWAT. $^*p < 0.05$, $^{**}p < 0.01$, $^{***}p < 0.001$, significance was only compared for ST HFD versus RC HFD, LT HFD versus RC HFD or ND versus WL.
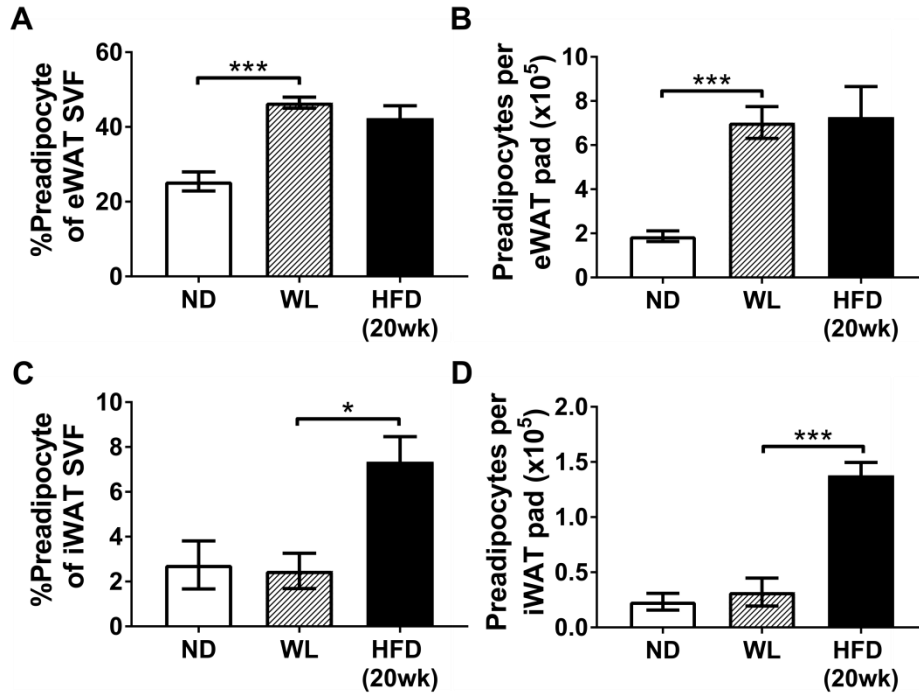
Figure 4-9 – eWAT of formerly obese mice maintains elevated numbers preadipocytes. CD45$^-$CD31$^-$Sca-1$^+$PDGFrα^+ preadipocytes as (A) a frequency of all SVF cells and (B) total preadipocytes per eWAT pad. (C) Frequency of preadipocytes in iWAT SVF and (D) total preadipocytes per iWAT pad. *p < 0.05, ***p < 0.001, significance was only compared for ND versus WL or WL versus HFD (20wk).
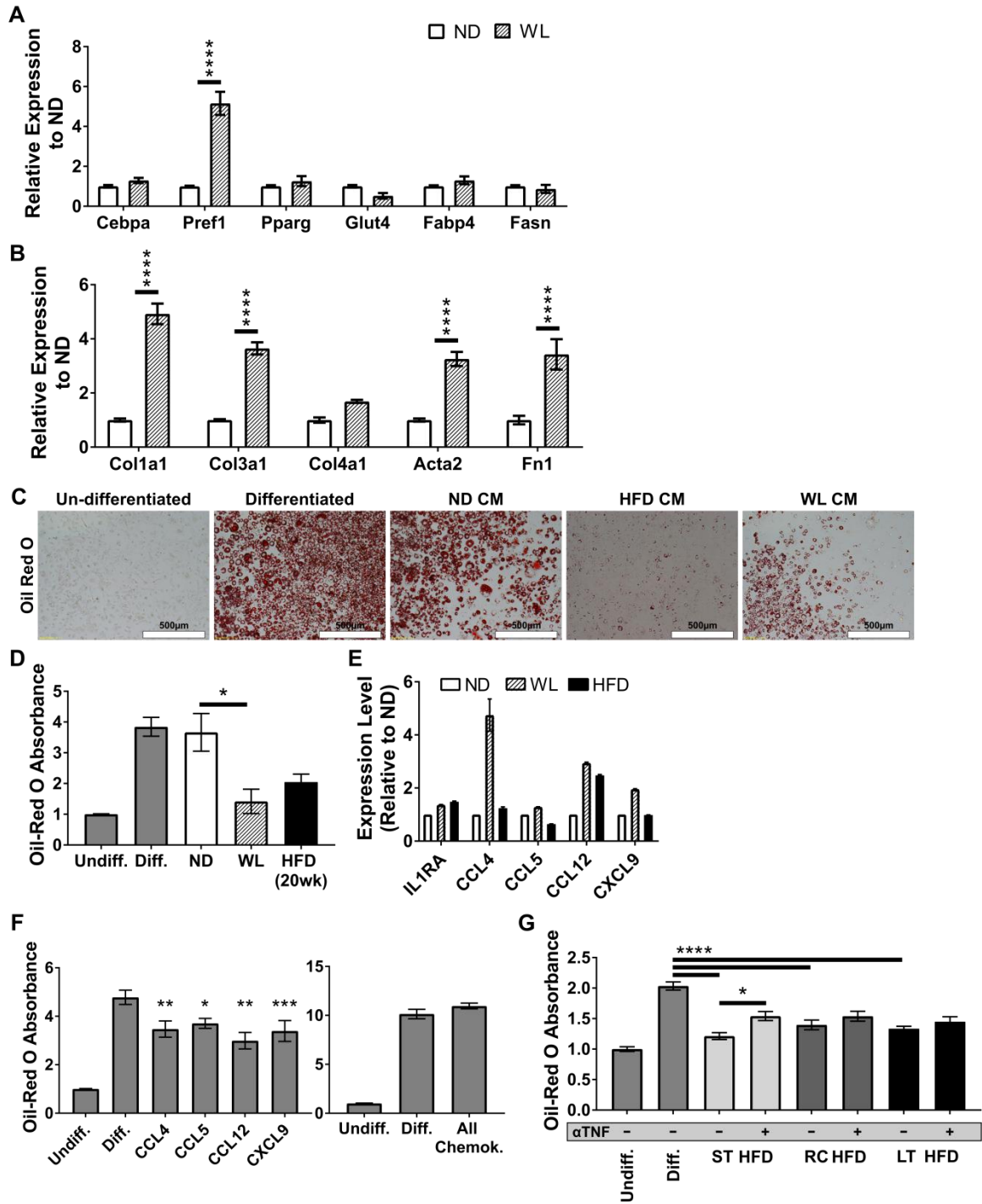
Figure 4-10 – Conditioned media from eWAT explants of formerly obese mice inhibits adipocyte differentiation and reduces lipogenesis. Gene expression for (A) adipocyte maturation genes and (B) collagen genes after differentiation induction in the presence of eWAT explant conditioned media from the respective diet conditions. Oil red O staining of lipid droplets within differentiated adipocytes shown as (C) representative micrographs and (D) relative total extracted oil red O content from wells. (E) eWAT explant multiplex cytokine array (n = 2 per diet condition). (F) Extracted relative oil red O content from differentiated 3T3-L1 cells after

treatment with (left) 10ng/mL of individual chemokines identified from multiplex cytokine array or (right) simultaneous treatment with all identified chemokines at 10ng/mL each (Significance compares to Differentiated Control). (G) Extracted relative oil red O absorbance after treatment with CM from ST HFD, RC HFD or LT HFD with or without the addition of 50ng/mL neutralizing anti-TNFα antibody (αTNF) during differentiation. Undiff. = Undifferentiated Control; Diff. = Differentiated Control; All Chemok. = All identified chemokines. *p < 0.05, **p < 0.01, ***p < 0.001, ****p <0.0001.

Obesity imposes a durable increase in eWAT preadipocyte content despite weight loss

Our observations of decreased eWAT expansion in RC HFD mice, despite similar adipocyte size as ST HFD mice, suggested that adipogenesis may be impaired in formerly obese mice. We enumerated adipose tissue preadipocytes by flow cytometry as CD45^{-}CD31^{-}Sca-1^{+}PDGFrα^{+} cells from the SVF (206; 207). The eWAT tissue of WL and 20wk HFD mice had elevated preadipocyte content, both as a frequency of SVF and in total number, when compared to ND mice (Figure 4-9A-B). 20wk HFD mice also had elevated preadipocytes in iWAT, but ND and WL iWAT had similar numbers of preadipocytes (Figure 4-9C-D). The data show that the eWAT of formerly obese mice maintains more preadipocytes and suggests obesity imposes a durable change to eWAT adipogenic potential despite weight loss.

EWAT of formerly obese mice secretes factors that directly inhibit adipogenesis

We utilized an *in vitro* model of adipogenesis using the 3T3-L1 preadipocyte cell line to examine if eWAT from formerly obese mice secreted factors that blocked adipogenesis. Conditioned media (CM) was collected from eWAT explant cultures in serum-free media for 24 hours. CM from formerly obese mice (WL CM) significantly increased genes normally associated with preadipocyte cells, rather than mature adipocytes, including *Pref1*, *Col1a1*, *Col3a1*, *Acta2* and *Fn1* expression compared to ND CM treatment (Figure 4-10A-B). Oil red O was used on differentiated 3T3-L1 cells to determine lipid storage capacity and adipogenesis. WL and HFD CM treatment significantly reduced lipid storage compared to ND CM treatment which was similar to control untreated differentiated cells (Figure 4-10C-D).

To determine what factors might be responsible for inhibiting adipogenesis, we used a cytokine array to evaluate cytokine concentrations in eWAT CM after 48 hours culture. Several cytokines were either not significantly different between diet conditions or were not detectable. However, we observed that IL1ra and chemokines CCL4, CXCL9, CCL5 and CCL12 were elevated in WL CM compared to ND CM (Figure 4-10E). Treatment of 3T3-L1 cells during differentiation with these chemokines revealed a small, but significant, reduction in differentiation efficiency (Figure 4-9F). However, treatment with any one chemokine failed to inhibit differentiation to the same degree as WL or HFD CM, and treatment with all four simultaneously abolished the inhibitory effect.

TNFα is a potent inhibitor of adipogenesis (208). Gene expression for *Tnfα* was found to be slightly elevated in WL eWAT and substantially elevated in RC HFD and LT HFD eWAT (Figure 4-8G). To determine if TNFα might be playing a significant role inhibiting adipogenesis in our culture model, we added a TNFα neutralizing antibody to the CM before treating 3T3-L1 cells. Treatment of differentiating 3T3-L1 cells with ST HFD, RC HFD or LT HFD CM resulted in equivalent inhibition of differentiation and was similar to what was observed after WL CM or HFD CM treatment (Figure 4-10G). Exposure to TNFα neutralizing antibody caused slight, but not significant, improvements in differentiation efficiency indicating TNFα plays, at best, a minor role for inhibiting adipogenesis in our CM culture system. Overall, the results show that the eWAT of obese and formerly obese mice secretes an unknown factor(s) which can impair adipogenesis *in vitro*.

Discussion

We've previously published that the eWAT of formerly obese mice maintains increased numbers of activated leukocytes along with persistent abnormalities in eWAT structure and adipogenic protein expression (204). In this study, we extend our observations to assess the metabolic and inflammatory consequences of re-challenging formerly obese mice with HFD. We hypothesized that basic functions of adipose tissue, such as lipid storage, may be permanently impaired in formerly obese mice and explored

this with a dietary manipulation model of obesity, weight loss, and weight regain in mice. This animal model was designed to mimic weight regain trends often observed in people after interventions of caloric restriction such as reduced calorie meal replacement for weight loss. Our major finding was that eWAT of formerly obese mice was not capable of properly storing excessive nutrients and, as a result, led to increased ectopic lipid storage in organs such as liver and iWAT. This functional derangement persists despite extended time off of HFD and suggests a prolonged, possibly permanent, impact of obesity on eWAT function and architecture. The permanent changes in eWAT in the RC HFD groups included increased: a) ATM accumulation; b) increased CD8+ T cell accumulation; c) increased inflammatory cytokine expression; and d) increased numbers of collagen+ preadipocytes. Furthermore, secreted factors produced from eWAT of formerly obese mice inhibited an *in vitro* model of adipogenesis and may be responsible for limiting the lipid storage capacity of eWAT *in vivo*.

Consistent with our hypothesis, HFD challenge of formerly obese mice led to reduced eWAT expansion compared to a similar duration of HFD challenge of weight-matched lean mice. Importantly, the identical adipocyte sizing curves suggest that the reduced eWAT expansion is not due to less lipid uptake per adipocyte. Our data suggest there are fewer functionally mature adipocytes present in formerly obese eWAT which limits the overall lipid storage capacity of the entire fat pad. In support of this interpretation, we found that expression of several critical mature adipocyte-specific genes and proteins was significantly decreased in formerly obese eWAT and remained lower after HFD re-challenge. Interestingly, the iWAT tissue of formerly obese mice was capable of expanding to HFD re-challenge proportional to body weight increases. The gene expression profile of iWAT showed some improvements compared to eWAT for several genes including *Lpl*, *Pparg*, and *Glut4*. However, this may not sufficiently explain the functional differences observed between these depots in our model. Future research is required to help identify why mouse iWAT tissue responds so differently from eWAT tissue during HFD re-challenge.

Examination of livers from RC HFD mice revealed disproportionally increased liver mass, relative to ST HFD mice, with substantially increased lipid involvement and

total triglyceride content. Increased hepatic steatosis was associated with increased serum concentrations of AST and ALT indicating liver damage or abnormal liver function. The ALT to AST ratio was greater than 2:1 in both RC HFD and LT HFD mice, compared to 1.3:1 in ST HFD mice. This ratio matches a classical change observed in patients with early stage non-alcoholic fatty liver disease (NAFLD) and is typically associated with obesity and increased risk of type 2 diabetes development (209-211). In our model, ST HFD and RC HFD mice had similar fasting glucose measures, glucose response curves, and insulin response curves despite the substantially increased triglyceride load found in their livers. However, fasting insulin levels were almost two-fold higher in RC HFD and LT HFD mice indicating increased insulin resistance in the RC HFD mice. Our results are in agreement with previous findings showing accrued liver steatosis and impaired liver insulin signaling responsiveness in murine weight cycling models (175; 212).

Increased liver steatosis can occur as a result of four broad possible mechanisms including reduced liver fatty acid oxidation, reduced triglyceride export, increased hepatic lipogenesis, and increased lipid uptake from the serum (213). In normal conditions, hepatic *de novo* lipogenesis is a relatively minor contributor to liver triglyceride content but in NAFLD this can increase due to an induction of genes critical for *de novo* lipogenesis (214-217). Several of these genes were evaluated and revealed no differences between ST HFD and RC HFD mice suggesting the increased steatosis was not due to amplified hepatic fatty acid synthesis. Liver fatty acid oxidation rates and triglyceride export have been found to not change, or even increase, with NAFLD and obesity (218-222). As a result, these pathways would not be expected to play significant roles in mediating the increased liver steatosis observed with our model. Based on the reduced lipid storage capacity of eWAT we believe the most likely explanation for increased liver steatosis in RC HFD mice is increased lipid shunting to, and uptake by, the liver. However, we can't rule out the possibility that one of these other mechanisms may be partly responsible. This merits more detailed investigation in future studies including the use of isotope-labeled tracers to identify the sources contributing to hepatic triglycerides during HFD re-challenge.

We extended the time mice were off HFD during the weight loss cycle to determine how permanent the effects of obesity were. After 24 weeks of HFD removal the eWAT tissue still failed to expand appropriately with HFD re-challenge. Examination of liver revealed the same disproportionate increase in liver mass and increased total hepatic triglyceride content. The results show the impact of diet-induced obesity on eWAT function does not resolve despite prolonged time off HFD.

The limited capacity for eWAT expansion was observed despite a quantitative increase in preadipocytes in formerly obese mice, suggesting that they may have impaired capacity for adipogenic differentiation. Consistent with this, we observe that WL CM and HFD CM inhibited 3T3-L1 adipogenic potential. Treatment of 3T3-L1 cells with individual chemokines suggested only moderate inhibition of adipogenesis. Treatment with all four identified chemokines, however, abolished the inhibitory effect and suggests limited potential for inhibiting adipogenesis *in vivo*. Treatment with an anti-TNFα neutralizing antibody also showed no differentiation improvement and confirmed that TNFα may play little, if any, role towards inhibiting adipogenesis in our culture system. Given the evidence available we investigated the most likely anti-adipogenic candidates. However, several other adipogenesis inhibitors exist that have yet to be examined in our system including, but not limited to, IL-6 (223), Wnt-5a (224), IL-1β (225; 226), macrophage inhibitory factor homolog d-dopachrome tautomerase (227), and even fatty acids like arachidonic acid (228). It's also important to note another possible explanation for limited eWAT expansion *in vivo* wherein preadipocytes may be intrinsically altered by obesity and are no longer as capable of maturing into lipid-storing adipocytes. As a result, the adipocyte precursors *in vivo* may not be capable of properly responding to increased lipid storage demands even if the secreted factor could be found and nullified. Future work will continue to explore the relative importance of direct exposure to adipogenesis inhibitors versus permanent defects in adipocyte maturation remaining after obesity.

ST HFD eWAT CM also inhibited *in vitro* adipogenesis indicating that even a short 6 week interval of HFD was sufficient to promote expression and/or secretion of the factor. Interestingly, the eWAT of ST HFD mice had expanded to near the maximum size

106

limits we tend to observe for eWAT tissue expansion before the depots begin to shrink (approximately 3g), which is a phenomenon observed by others as well (56). Expression of the factor(s) may correlate with the natural transition point for eWAT when the depot switches from an expansion phase to contraction. An interesting model to compare our study with is the adiponectin-overexpressing *ob/ob* mouse model which allows expansion of adipose tissue beyond normal limits observed in leptin deficient mice. These mice can grow to over 100g total body weight but are protected from many of the deleterious effects of diet-induced obesity including metabolic syndrome and liver steatosis (229). This suggests that limited expansion capacity of adipose tissue is central to ectopic lipid deposition and hepatic steatosis development. In agreement with this, lipodystrophy, having at least partial absence of adipose tissue, is associated with NAFLD and indicates a fundamental importance for adipose tissue expansion in preventing liver steatosis (230; 231).

Taken together, we were able to identify unique physiologic differences associated with weight regain in formerly obese mice. Our observations are part of a growing body of literature showing that features normally associated with obese adipose tissue, including inflammation and insulin resistance, are maintained despite weight loss in both mice and humans (125; 126; 129; 130; 173; 174). The results suggest that unresolved effects of obesity encourage the hastened emergence of severe metabolic abnormalities during weight regain including hepatic steatosis and insulin resistance. These findings indicate that weight gain may result in specific health consequences that are dependent on the subject's entire weight history. Future work will continue to investigate the physiologic consequences of obesity that remain despite weight loss as well as the mechanisms responsible for limiting appropriate adipocyte function and maturation.

Table 7 – Sequences for RT-PCR primers used in this chapter

Gene	Forward	Reverse
Insr	TTTGTCATGGATGGAGGCTA	CCTCATCTTGGGGTTGAACT
Irs1	CGATGGCTTCTCAGACGTG	CAGCCCGCTTGTTGATGTTG
Cebpa	CAAGAACAGCAACGAGTACCG	GTCACTGGTCAACTCCAGCAC
Pref1 (Dlk1)	TTCGGGCTTGCACCTCAA	GGAGCATTCGTACTGGCCTTT
Lpl	TGTGTCTTCAGGGGTCCTTAG	GGGAGTTTGGCTCCAGAGTTT
Pparg	GGAAGACCACTCGCATTCCTT	TCGCACTTTGGTATTCTTGGAG
Akt1	ATGAACGACGTAGCCATTGTG	TTGTAGCCAATAAAGGTGCCAT
Glut4	GTGACTGGAACACTGGTCCTA	CCAGCCACGTTGCATTGTAG
Tnfa	ACGGCATGGATCTCAAAGAC	AGATAGCAAATCGGCTGACG
Il1b	AAATACCTGTGGCCTTGGGC	CTTGGGATCCACACTCTCCAG
Il6	AGTGAGGAACAAGCCAGAGC	CATTTGTGGTTGGGTCAGG
Scd1	GCTGGAGTACGTCTGGAGGAA	TCCCGAAGAGGCAGGTGTAG
Srebp1	GATGTGCGAACTGGACACAG	CATAGGGGGCGTCAAACAG
Fasn	GGAGGTGGTGATAGCCGGTAT	TGGGTAATCCATAGAGCCCAG
Me1	GTCGTGCATCTCTCACAGAAG	TGAGGGCAGTTGGTTTTATCTTT
Acaca	TAATGGGCTGCTTCTGTGACTC	CTCAATATCGCCATCAGTCTTG
Fabp1	ATGAACTTCTCCGGCAAGTACC	CTGACACCCCCTTGATGTCC
G6pc	CGACTCGCTATCTCCAAGTGA	GTTGAACCAGTCTCCGACCA
Pck1	CTGCATAACGGTCTGGACTTC	CAGCAACTGCCCGTACTCC
Gck	ATGGCTGTGGATACTACAAGGA	TTCAGGCCACGGTCCATCT
Fabp4	AAGGTGAAGAGCATCATAACCCT	TCACGCCTTTCATAACACATTCC
Col1a1	GTGCTCCTGGTATTGCTGGT	GGCTCCTCGTTTTCCTTCTT
Col3a1	CTGTAACATGGAAACTGGGGAAA	CCATAGCTGAACTGAAAACCACC
Col4a1	GCCAAGTGTGCATGAGAAGA	AGCGGGGTGTGTTAGTTACG
Acta2	CCAGGCATTGCTGACAGGAT	CCACCGATCCAGACAGAGTAC
Fn1	CACCCGTGAAGAATGAAGA	GGCAGGAGATTTGTTAGGA

Chapter 5 – Conclusions and Future Directions

Summary

This dissertation investigated and addressed several unresolved issues regarding metabolic and inflammatory changes that occur during obesity, weight loss, and weight regain. We first identified a better marker for delineating ATMs from other adipose tissue myeloid populations in mice and humans which has been a major technical limitation within the field. We show that obesity imparts a lasting impact on adipose tissue health and function that persists despite weight loss. As a result, weight regain in formerly obese mice was accompanied by hastened development of metabolic abnormalities including hyperinsulinemia, adipose tissue functional derangement, hepatic steatosis, and hepatic damage. The following discussion will outline the specific contributions for each data chapter, potential future directions, and major implications for these studies.

Objectives, Major Findings, and Implications for Chapter 2

In chapter 2, our objective was to test CD64 as a macrophage-specific marker for better discrimination of ATMs from other adipose-resident myeloid populations. We provide evidence supporting CD64 as a better marker than F4/80 for specific identification of ATMs from other myeloid cell populations that can express F4/80 including ATDCs, eosinophils, and neutrophils. The inability to isolate ATMs from these other myeloid populations, without the use of several additional markers, has impaired our ability to properly attribute immune functions to the correct cell population. We identified significant contamination of other myeloid cells within the $CD45^+CD11b^+F4/80^+$ "macrophage-specific" pool which suggests that some previous studies utilizing this identification scheme may need to be revisited to clarify the respective functions of ATMs from other F4/80-expressing leukocytes.

An important result of this work is the definitive identifications of ATDCs as independent contributors to obesity-induced inflammation within adipose tissue. Historically, ATMs have been well studied and are believed to be essential direct contributors to the development of adipose tissue inflammation. Previous work from the Lumeng lab has also found that ATMs function as antigen-presenting cells *in situ* during obesity, indicating another mechanism by which ATMs may influence adipose tissue inflammation (144). However, we don't have a clear understanding of the potential role ATDCs play in inflammation development, antigen presentation, or metabolic health. This chapter identified specific gene signatures associated with ATMs (high lysosomal and lipid storage, inflammatory cytokines, and complement) versus ATDCs (low inflammatory cytokine expression and high antigen processing and presentation). Both ATMs and ATDCs highly express MHC-II and T cell co-stimulatory markers and both were effective APCs *ex vivo*. So while ATMs and ATDCs may be functional APCs *in vivo*, they could also have unique additional functions which can now be better investigated through use of CD64. Finally, we show that CD64 can be useful as a marker for identification of human ATMs as well.

Ongoing work continues to utilize this marker to better differentiate the respective functions of ATMs and ATDCs in different adipose tissue depots of both mice and humans. Use of this marker by researchers in the field will help reduce the number of markers necessary to delineate adipose-resident myeloid populations. As a result, it should help reduce the risk of flow cytometry results being confounded by contamination of other leukocyte populations when studying adipose tissue immune dynamics.

Objectives, Major Findings, and Implications for Chapter 3

In chapter 3, our objective was to perform a detailed investigation into the effects of weight loss on inflammatory leukocyte activation and composition within adipose tissue. Understanding leukocyte activation dynamics during weight loss helps inform our understanding of how adipose tissue inflammation continues to persist. We discovered that features normally associated with chronically-obese adipose tissue fail to resolve even with extended time removed from HFD. These results build onto recent findings

showing that adipose tissue inflammation can persist in rodents and humans after weight loss (125; 126; 129; 130). With this study we make three major contributions to the field. First, we identify that adipose-resident leukocytes, such as ATMs, remain elevated despite weight loss and retain their pro-inflammatory activation state. Second, we show that ATM accumulation and maintenance is not dependent on T or B cells, but these lymphocytes are required for maintenance of pro-inflammatory cytokine expression from ATMs after weight loss. Third, we show that eWAT tissue continues to develop structural abnormalities despite weight loss, including CLSs and fibrosis, without observed improvements in the expression of mature adipocyte-associated proteins like PPARγ and IRS-1. We conclude that obesity results in long-term alterations in mouse eWAT which fails to resolve despite extended time removed from HFD (Figure 5-1). Implications and future directions for these results will be discussed in greater detail below.
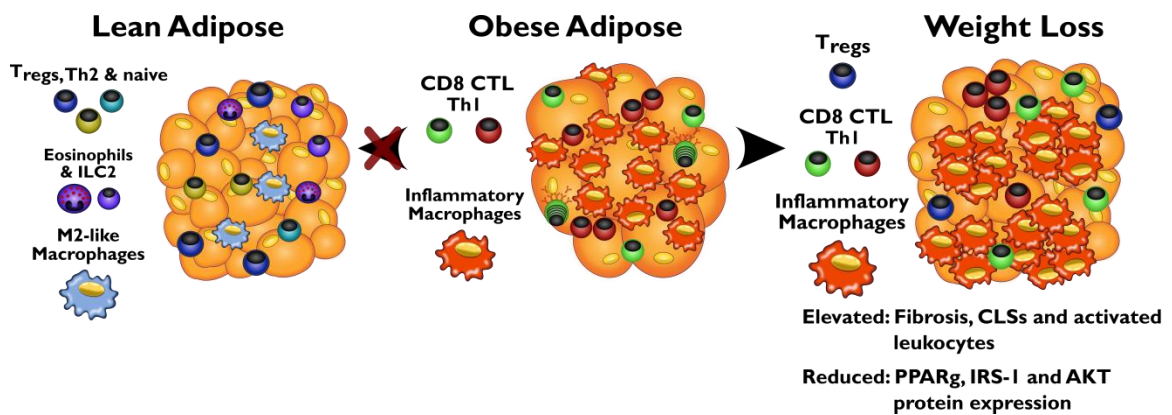
Figure 5-1 – Development of features normally associated with chronically-obese adipose tissue in the eWAT of formerly obese mice. After weight loss, adipose tissue of formerly obese mice fails to return to a lean-like state (Left) and, instead, maintains or develops several features normally only associated with obese adipose tissue (Right). These features include crown-like structures, increased leukocyte accumulation, inflammatory activation of resident leukocytes, and impaired adipogenic protein expression profile.

Maintenance of pro-inflammatory ATMs in eWAT despite weight loss

The maintenance of activated pro-inflammatory leukocytes within adipose tissue after weight loss has important implications for obesity and immunometabolism research.

111

These findings challenge previously held assumptions regarding the status of adipose-resident leukocytes in formerly obese subjects. We found that obesity can have a profound, potentially permanent, impact on the balance of leukocyte populations within adipose tissue. For example, the overall frequency of CD11c$^+$ ATMs climbs from ~20% in lean adipose to around 55%-60% during obesity. CD11c$^+$ ATMs were retained at this frequency for as long as 6 months after HFD feeding had been terminated.

The functional significance of macrophages in lean adipose tissue is still not completely understood. As research continues to shed light on the role that ATMs play in both lean and obese adipose tissue, it will be equally important to determine if ATMs are permanently changed by obesity or if they can still retain functional plasticity. If ATMs maintain polarization plasticity, then there is the possibility that adipose tissue leukocytes in formerly obese mice may be able to revert back and become "functionally equivalent" to those found in lean adipose tissue despite the differences in origin and surface marker expression. Unfortunately, we showed the ATMs in formerly obese eWAT still retained a highly pro-inflammatory expression profile suggesting they may not readily revert back. Even the CD11c$^-$ ATMs developed a pro-inflammatory activation state which failed to resolve after weight loss. Overall, this indicates that ATMs are resistant to changing their polarization state once activated during obesity; our results would suggest this is particularly true in the presence of adaptive lymphocytes which will be discussed in greater detail below. More research would be needed to determine what other functional changes are induced by obesity and whether or not they revert after weight loss.

The role of adaptive lymphocytes for maintaining inflammation after weight loss

T lymphocytes have been shown to become activated in obese adipose tissue and are believed to play important roles in establishing inflammation (184; 232). Surprisingly, we found that T and B lymphocytes are not required for ATM recruitment and activation during obesity. However, these lymphocytes do seem to be required for maintenance of ATM pro-inflammatory polarization after weight loss. These findings suggest that B or, more likely, T lymphocytes potentially play important roles in

112

establishing and maintaining inflammation during obesity and weight loss. This also indicates there may be ways of ameliorating the pro-inflammatory activation state of ATMs after weight loss without depleting them. T lymphocyte expression of CD40L and/or IFNγ are interesting potential signaling mechanisms to explore for controlling activation of ATMs during obesity and weight loss. Deficiency in IFNγ has been shown to modestly improve insulin resistance and reduce adipose tissue inflammation in murine DIO models (111; 182). While pro-inflammatory ATMs have been associated with insulin resistance and adipose dysfunction, the mechanisms remain incompletely understood. As a result, even if the pro-inflammatory activation profile of ATMs could be reduced it remains to be determined if that would result in substantial health benefits or metabolic improvements.

Continued development of eWAT structural derangements during weight loss

We've observed that several features associated with obese eWAT become progressively worse with continual exposure to HFD. After 12 weeks of HFD, the eWAT depots are around their maximal size (~1.5g each), CLSs are present but relatively infrequent and fibrosis is minimal. After 20-25 weeks of HFD, the eWAT depots have begun to shrink, CLSs become numerous, and there is extensive tissue fibrosis which can be seen both micro- and macroscopically. One of the more surprising findings from this study was that removing HFD after 12 weeks of exposure still resulted in accumulated CLSs and extensive adipose tissue fibrosis. After weight loss, the eWAT looked histologically similar to adipose from mice exposed to HFD for a full 20 weeks. This shows that 12 weeks of diet exposure is sufficient to induce adipose tissue defects that we previously believed only occurred after long-term HFD exposure. Importantly, we also show that weight loss after less time spent on HFD, for instance 6 or 9 weeks, does not result in CLS and fibrosis accumulation. Somewhere between 9 and 12 weeks of HFD exposure a threshold seems to have been met. After this point has been reached, $CD11c^+$ ATM accumulation fails to reverse, CLSs will begin to accrue, and fibrosis will develop (Figure 5-2). This threshold is likely dependent on either adiposity gained or total time exposed to HFD. To my knowledge, there is no literature available to help narrow down

113

which is most likely responsible. However, I have observed that mice with malocclusion fail to develop body weight gains beyond 30-35g even with extended HFD exposure. Interestingly, the eWAT from HFD-fed mice with malocclusion does not develop or maintain the same features after weight loss as we observe in normal mice fed HFD for the same length of time. This would suggest that weight gain and/or total adiposity is more important than time spent on HFD before weight loss.

Regardless, this concept of adiposity threshold limits has important implications for obesity and weight loss research. Definitions of obesity in mice are not nearly as clearly defined as they are in humans. While many recent manuscripts have only examined weight loss after mice have reached between 40g and 50g (51; 125; 130), some have studied obesity and weight loss in mice around 35g or less (112; 233). The findings from this dissertation would suggest that these differences in study design choice could have substantial impacts on the final results from, and conclusions reached by, different investigators. It would also be important to know if similar adiposity limits exist in human subjects which may affect the degree to which weight loss would be able to improve metabolic health and adipose tissue function.
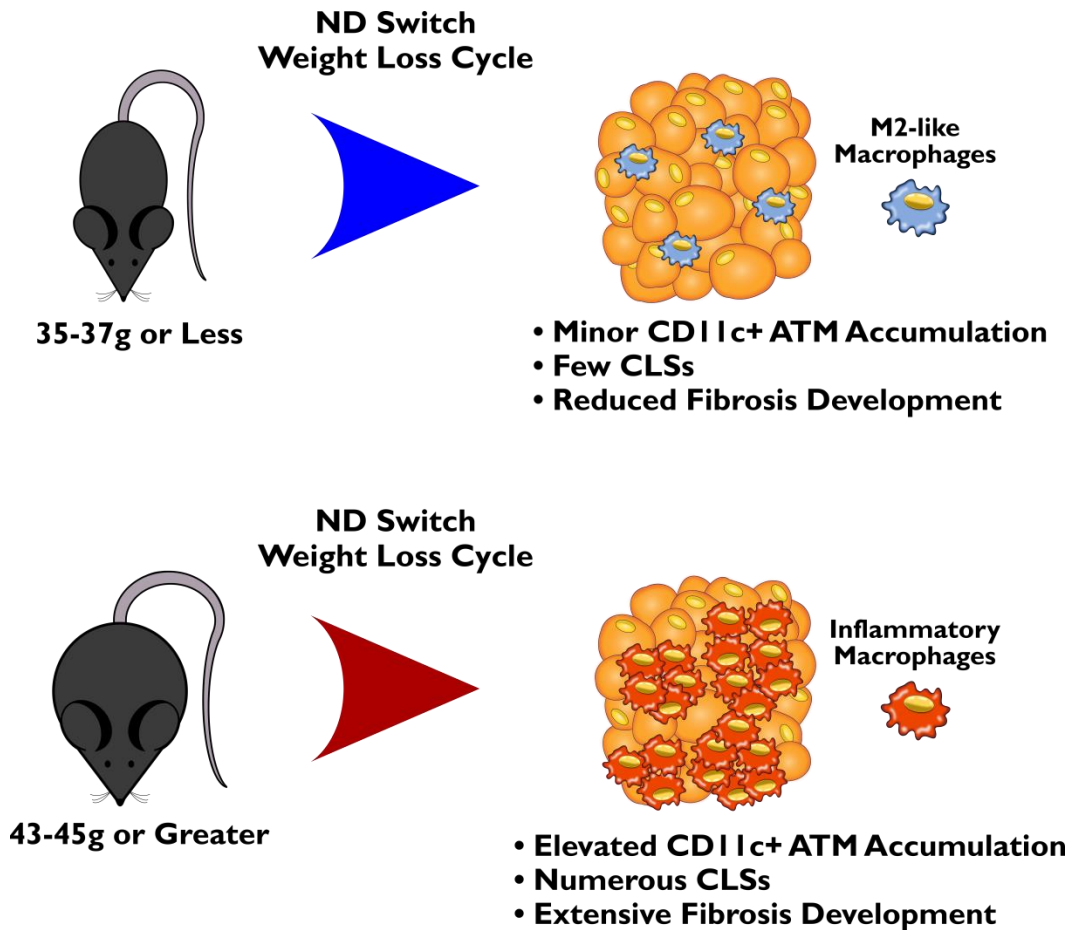
Figure 5-2 – Weight gained before weight loss influences maintenance of obesity-associated features in eWAT during weight loss. Weight loss in mice weighing around 35g allows better, though not perfect, recovery of eWAT tissue abnormalities including CLSs, CD11c$^+$ ATM accumulation, and tissue fibrosis. Weight loss in mice weighing over 43g leads to the abnormal eWAT features we report on in chapter 3.

An interesting open question is whether the pro-inflammatory ATMs remaining in formerly obese eWAT are directly responsible for encouraging continual adipose tissue derangement during weight loss. It's possible, for example, that macrophages are simply responding to recruitment signals from adipocytes that are already dying or stressed as a result of obesity. We found that CLSs and tissue fibrosis still develop during weight loss in *Rag1*$^{-/-}$ mice despite the substantially reduced inflammatory cytokine expression profile of ATMs from *Rag1*$^{-/-}$ mice. Mature adipocyte-associated protein and gene expression from whole eWAT also remained altered in *Rag1*$^{-/-}$ mice after weight loss. Overall, the results show that maintenance of inflammatory cytokine output from ATMs

is not required for the continual development of eWAT structural derangements observed during weight loss. Depletion of macrophages, through the use of clodronate-filled liposomes or diphtheria receptor expression systems, may allow us to determine if ATMs are responsible for ongoing adipose tissue derangement during weight loss. The work completed for this dissertation provides a way of evaluating whether adipose tissue can reacquire a lean-like profile during weight loss in the absence of ATMs. However, it's important to keep in mind that ATMs may have beneficial roles within adipose tissue during both obesity and weight loss which remain incompletely understood. For example, it's been suggested that ATMs may play important roles in extracellular matrix degradation and tissue remodeling in adipose tissue (234-236). In support of this, we showed that CD11c$^+$ ATMs are still elevated in eWAT of WT mice even after six months removed from HFD, but there seems to be reduced numbers of CLSs in the eWAT of these mice. The CLSs still remaining also have substantial reductions in the surrounding extracellular matrix would could be the result of the retained ATMs. Additional research is still needed to understand if ATMs can help to maintain adipose tissue function and health.

Additional general implications

Obesity can alter basic physiology in a number of tissues aside from adipose and liver. Obesity is also associated with impaired bone integrity, pancreatitis, reduced lung function, and increased skeletal muscle inflammation (237-243). Adipose isn't the only tissue that shows lasting changes after weight loss. Obesity can negatively impact bone health by increasing bone marrow adiposity, reducing trabecular bone volume, and reducing mineral content which results in deficient mechanical integrity and reduced fracture resistance. In 2016, we reported that femur trabecular bone volume and mineral content only partially recover after weight loss (244). As a result, the mechanical integrity and fracture resistance failed to recover after weight loss. We've also identified durable changes within the bone marrow hematopoietic progenitor pool, including increased myeloid progenitors, which is changed with DIO and remains altered even after serial bone marrow transplants into lean animals (154) or after weight loss (unpublished

findings). Within the pancreas, beta-cell mass increases during obesity to keep up with insulin secretion needs. Another research group found that beta-cell mass fails to be reduced after weight loss (125). It will be critical to investigate if weight loss is capable of fully resolving obesity-induced functional and inflammatory changes in other metabolically important tissues to gain a better understanding of how weight loss might impact metabolic health and whole body immune dynamics.

Major additional future directions for chapter 3

We were limited in the number of adipose tissue leukocyte populations that we could explore during weight loss due to time, expense, and the relatively low quantity of extractable leukocytes from a given mouse. T cells, macrophages, and dendritic cells were chosen based on their overwhelming presence in adipose and due to the field's strong interest in these particular immune cells. However, several other leukocyte populations have been shown to play potentially critical roles in adipose tissue inflammatory responses during obesity and almost nothing is known about these cells during weight loss. NK cells, for example, can be important contributors of cytokines like IFNγ which can modify responses of other leukocytes such as ATMs. Adipose-resident NK cells are thought to increase during obesity and this cell population may play a critical role in establishing inflammation, but little is known regarding how this population is impacted during weight loss. It will be important to fully explore the potential changes that are induced by both obesity and weight loss in all major adipose-resident leukocyte populations in both mice and humans.

It would also be interesting to examine how weight loss induction through other mechanisms, such as caloric restriction with HFD or bariatric surgery, would compare with our diet-switch model. I have no reason to suspect that caloric restriction of HFD would improve the features we see maintained through diet-switch-induced weight loss, but it remains an interesting open question nevertheless. The Lumeng lab has ongoing collaborations investigating bariatric surgery in both mice and humans. Our unpublished findings, which are currently in peer review, suggest that bariatric surgery in mice may

alter the leukocyte composition after weight loss compared to the diet-switch based model used for this dissertation. For example, CD11c⁻ ATMs, rather than CD11c+ ATMs, and T cells seem to dominate in eWAT after bariatric surgery. We were only able to explore leukocyte population changes in these mice and have no information on their inflammatory potential. Further investigation of leukocyte activation and adipose tissue functional derangements, as explored in chapter 3, are still necessary to understand if bariatric surgery is more capable of resolving obesity-induced changes in mice.

An additional major limitation within our study is the lack of data from human subjects. As discussed in the introduction chapter, murine gonadal adipose tissue is viewed as a rodent equivalent of human visceral omental tissue due to similarities in gene expression and inflammatory changes induced by obesity (23). Our results, derived from male gonadal white adipose tissue or eWAT, should help provide insight on potential expected outcomes during weight loss in human subjects regarding leukocyte changes and adipose tissue functional improvements. Schmitz *et al.* found that bariatric surgery failed to reduce omental ATM cell counts in approximately 41% of patients examined (125). Maintenance of omental ATMs in these patients was associated with increased inflammatory cytokine gene expression in adipose tissue and a failure to reduce CLSs one year after surgery. Adipocytes also maintained impaired insulin-stimulated glucose uptake in patients that did not have reduced omental ATM counts. The findings from this dissertation would suggest that ATMs in both patient subgroups may maintain their pro-inflammatory polarization state, but individual ATMs were not evaluated by Schmitz *et al*. Additional gene and protein expression analysis of adipocytes from human subjects would be useful to determine how well bariatric surgery is capable of resolving obesity-induced changes.

Objectives, Major Findings, and Implications for Chapter 4

The maintenance of features normally associated with chronic obesity in eWAT of formerly obese mice suggested the mice may also have persistent metabolic abnormalities. However, we found in chapter 3 that mice generally show improved metabolic function after weight loss including normal hepatic lipid involvement and

normal GTT/ITT responses. In chapter 4, we sought to determine if weight regain would reveal metabolic abnormalities that remain hidden while weight loss is maintained. We showed that eWAT tissue was incapable of properly expanding upon HFD re-challenge and secreted factors which inhibited *in vitro* adipogenesis of 3T3-L1 cells. We also showed that weight regain in formerly obese mice was associated with faster development of severe metabolic abnormalities, including hyperinsulinemia and hepatic steatosis, which we believe is linked to eWAT dysfunction (See model in Figure 5-3). We conclude that weight regain in formerly obese mice is associated with hastened development of metabolic abnormalities as a result of incomplete resolution of obesity-induced features. Implications and future directions for these results will be discussed in greater detail below.

Reduced expansion and lipid storage capacity of eWAT in formerly obese mice

One of the primary functions of adipose tissue is the storage of excess caloric intake as energy-dense triglycerides for future use. Obesity encourages a dramatic hypertrophic effect in adipocytes, allowing individual adipocytes to greatly expand in size to accommodate increased storage demands (245). Proliferation and differentiation of adipocytes from the preadipocyte progenitor pool, also known as adipogenesis, is the other primary mechanism which helps increase the overall storage capacity of an adipose depot (205; 230; 246). The limited expansive capacity of eWAT during HFD re-challenge suggests that obesity imparts major defects in one or both of these mechanisms. Adipocyte area was compared after weight gain in formerly obese and formerly lean mice revealing essentially identical adipocyte sizing curves. This indicates that individual adipocytes within formerly obese eWAT are as capable of storing triglyceride as adipocytes from eWAT of formerly lean mice. We believe that adipogenesis is impaired in formerly obese eWAT. As a result, there would be fewer functionally mature adipocytes within eWAT to store triglycerides which limits the overall lipid storage capacity of the entire depot. In support of this, proteins and genes critical for adipocyte differentiation and function are downregulated during obesity in whole eWAT and remain dysregulated despite weight loss. In addition, we found the preadipocyte

119

frequency in SVF from eWAT, but not iWAT, was increased by obesity and remained elevated despite weight loss which could be indicative of reduced differentiation efficiency in the preadipocyte population after weight loss.

Unknown secreted factors from eWAT can directly inhibit in vitro adipogenesis

We attempted to investigate potential mechanisms that may explain the limited expansive capacity of eWAT. We found that eWAT conditioned media from formerly obese mice, created from overnight culture of adipose tissue explants, was capable of inhibiting adipogenesis of 3T3-L1 cells. Reduced adipocyte protein expression and impaired adipogenesis has been linked to increased systemic insulin resistance in both mice and humans (247-251), and is also thought to be associated with ectopic lipid deposition during obesity (14; 247; 252). If these factors could be identified and neutralized, then eWAT lipid storage capacity could be restored in formerly obese mice potentially resulting in improved insulin sensitivity and reduced hepatic steatosis. Although we did not identify the factor(s) inhibiting adipogenesis *in vitro,* our studies effectively ruled out contribution of several putative cytokines and chemokines that might have been responsible. Several additional cytokines and signaling molecules remain to be investigated, and it's entirely possible that the synergistic effects of multiple factors may be inhibiting adipogenesis. As a result, the identification and neutralization of the factor(s) responsible may be technically quite challenging.

There may be additional derangements within eWAT that impairs expansion capacity *in vivo* during HFD re-challenge. One possibility is that the eWAT preadipocyte population is permanently impacted by obesity such that they're no longer as capable of responding to differentiation cues. Primary preadipocytes from formerly obese and formerly lean mice could be tested *in vitro* to assess their differentiation responsiveness. However, primary preadipocytes from adipose tissue may not differentiate well *in vitro* unless conditions are optimized. *In vivo* lineage tracing of preadipocyte differentiation into mature adipocytes in formerly obese mice could provide a way around this problem. Unfortunately, several of the currently available models rely upon tamoxifen induction

which has been shown to directly induce adipogenesis and can continue to induce translocation of Cre-ER^{T2} in adipocytes for more than 2 months after treatment (253). It's also unknown how weight loss and weight regain may modify tamoxifen's action in preadipocytes. Known adipogenesis inhibitors, such as TNFα, could be tested *in vitro* to see if they impart durable changes in the differentiation efficiency of 3T3-L1 cells when treated several passages before initiating adipogenesis. If differentiation remains impaired, that would provide supporting evidence and reveal potential molecular mechanisms by which preadipocytes could be permanently changed during obesity *in vivo*. Careful study design and use of multiple models, including the ones above, will be necessary to determine the primary mechanisms responsible for limited eWAT expansion during HFD re-challenge.

Despite not identifying the direct mechanism responsible, these data are still important for showing that obesity can impart changes in basic adipose tissue functionality, such as adipogenesis, which fails to recover despite a prolonged six-month removal from HFD. While weight regain has been previously linked to insulin resistance and increased adipose tissue inflammation (175; 203), to our knowledge, this is the first report showing altered adipose tissue expansion and functionality during HFD re-challenge. Future research would be necessary to determine if the maintained inflammation within eWAT is linked to reduced depot expansive capacity. Regardless, identifying the primary mechanisms responsible will help pinpoint potentially targetable pathways for modifying adipocyte development and function in obese and formerly obese patients.

HFD re-challenge of formerly obese mice leads to faster development of hepatic steatosis

Knowing that eWAT tissue expansion and lipid storage capacity is impaired begs the question of where excess lipid ends up during HFD re-challenge of formerly obese mice. We found that hepatic steatosis and triglyceride content increases faster upon HFD challenge of formerly obese mice compared to formerly lean mice. Hepatic steatosis was associated with increased concentrations of transaminases in the serum which is

121

indicative of liver stress and damage. We propose a model wherein the preadipocytes found in formerly obese eWAT fail to differentiate into functionally mature adipocytes upon HFD re-challenge which results in increased ectopic lipid storage in organs such as liver (Figure 5-3).
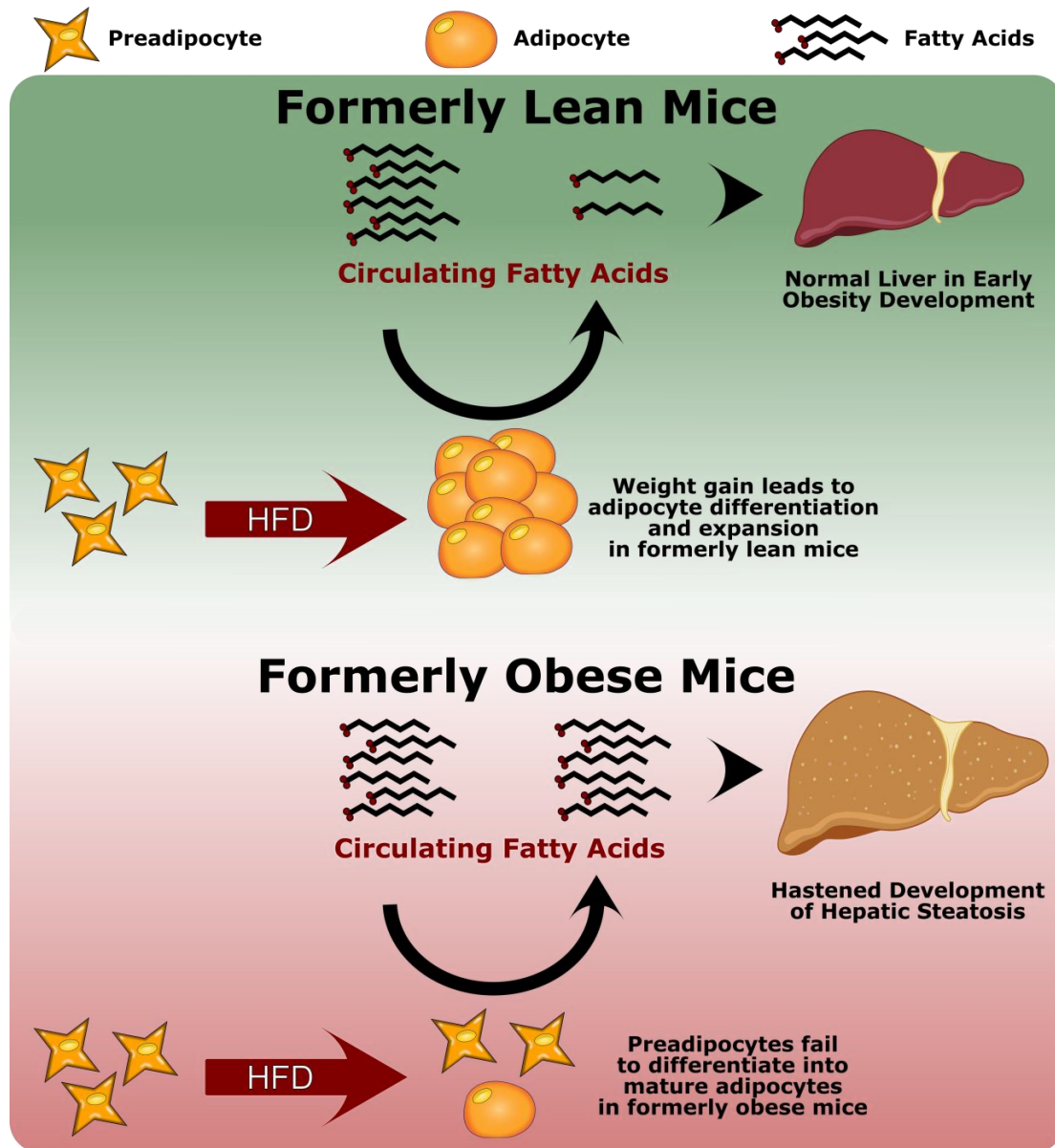
Figure 5-3 – Model showing failure of eWAT preadipocytes to properly respond to differentiation signals upon HFD re-challenge of formerly obese mice which leads to faster development of hepatic steatosis. Failed differentiation and maturation of adipocytes may be due to unknown factors directly inhibiting adipogenesis or intrinsic defects within preadipocytes imparted by previous obesity. Reduced fatty acid storage in eWAT results in increased ectopic lipid deposition in other metabolically important organs such as liver.

Major additional future directions for chapter 4

While we were able to identify failures in eWAT lipid storage capacity we were not able to test potential therapeutic solutions to correct this problem. If the lipid storage capacity or adipogenic potential of adipose tissue could be restored in formerly obese mice then the ectopic accumulation of lipid in tissues like liver may also be reduced. Identification of the primary mechanism(s) responsible for inhibiting eWAT expansion and adipogenesis would likely reveal the best potential therapeutic target, which is why we focused on this area of investigation, but the mechanism remains uncertain. Unfortunately, we also don't have a way of specifically stimulating adipogenesis effects in adipose tissue without also affecting metabolism and lipid storage in other tissues. PPAR agonists, for example, can stimulate adipogenesis in preadipocytes (254), but these drugs also have systemic effects including increasing hepatic triglyceride storage (255). In general, the literature suggests that PPAR agonists tend to reduce DIO-induced steatohepatitis (256; 257), but the widespread effects could potentially confound results in our model. The adiponectin-overexpressing *ob/ob* model allows unrestricted adipose tissue expansion and is associated with substantially ameliorated hepatic steatosis (229). It would be interesting to see if this mechanism might work in our HFD re-challenge model. The use of adiponectin, either through overexpression or administration, might allow for better eWAT adipogenesis and lipid storage in these fat depots. Our model would suggest that increased lipid storage within adipose tissue should reduce hepatic steatosis, reduce serum transaminase concentrations, and may also reduce the hyperinsulinemia effect as well.

Fatty acid uptake from the serum is believed to be the major contributor to accumulated liver triglycerides and a primary mechanism for hepatic steatosis in patients with NAFLD (258). However there are other potential sources of liver triglycerides which merit further discussion. The fatty acids taken up by liver can be derived from either dietary sources or from lipolysis of stored triglycerides within adipocytes. New fatty acids can also be created in liver through *de novo* lipogenesis from glucose stores. The evidence we've accumulated thus far suggests that fatty acid uptake, rather than

increased hepatic *de novo* lipogenesis, is responsible for the increased hepatic steatosis observed during HFD re-challenge of formerly obese mice. We found that liver genes critical for *de novo* lipogenesis are not elevated during HFD re-challenge of formerly obese versus formerly lean mice. In addition the literature suggests that *de novo* lipogenesis is a relatively small contributor towards hepatic triglyceride stores. Reduced triglyceride export from the liver and reduced fatty acid oxidation (or use) within the liver can also potentially contribute to increased hepatic steatosis. However, hepatic fatty acid oxidation rates and triglyceride export are not substantially reduced with NAFLD and obesity and in some studies may actually increase (218-222). Further intensive investigation would be necessary to definitively determine the degree to which each of these mechanisms might be involved for increasing hepatic triglyceride content. For example, isotope-labeled tracers would allow the relative sources (dietary, adipocyte lipolysis, or *de novo* lipogenesis) of hepatic triglycerides and fatty acids to be determined (214). It would also be ideal to perform hyperinsulinemic-euglycemic clamps during weight regain to better determine insulin action and glucose metabolism for the whole animal and individual tissues. These tests infuse mice with a constant physiologically-high concentration of insulin while providing variable glucose infusion which can also be labeled for tracing (259; 260). This is viewed as the gold standard for evaluating tissue sensitivity to insulin and, if using labeled glucose, allows relative glucose utilization in metabolically important tissues to be evaluated as well. The combination of isotope labeled fatty acid tracing and hyperinsulinemic clamp studies would allow for better assessment of metabolic health in HFD re-challenged mice. The number of mice and time required for these studies prevented us from exploring them further, but they would be ideal follow up experiments to pursue.

Final Thoughts

The findings from this dissertation challenge previously held assumptions regarding adipose tissue inflammatory and functional recovery after weight loss. We found that while weight loss can improve metabolic function, it's still an imperfect

resolution of the changes imparted by obesity. As a result, HFD re-challenge of formerly obese mice led to the development of metabolic abnormalities including hyperinsulinemia, adipose tissue functional derangement, hepatic steatosis, and hepatic damage.

These results still leave open the question of what role leukocyte activation and adipose tissue inflammation plays in adipose tissue dysfunction and insulin resistance during weight loss and weight regain. While our studies were not designed to answer this question, it's still central to our motivation for investigating how adipose-resident leukocytes are altered during weight cycling. Given the preponderance of literature associating adipose tissue inflammation with systemic insulin resistance, we would hypothesize that failure to fully resolve leukocyte activation state during weight loss would result in more severe insulin resistance than what was observed in chapter 3. The $Rag1^{-/-}$ experiments also showed that inflammatory cytokine production from ATMs is not necessary for maintaining insulin resistance after weight loss. If inflammatory cytokines do normally play a critical role in establishing insulin resistance during obesity, then it's possible that the overall inflammatory cytokine output of adipose tissue is reduced enough during weight loss that systemic insulin sensitivity can largely recover. This would fit with previous publications reporting reduced circulating inflammatory cytokine expression, and reduced insulin resistance, during weight loss (261; 262). HFD re-challenge of formerly obese mice, compared to formerly lean mice, led to faster accumulation of ATMs and T lymphocytes in eWAT and increased *TNFα* expression. The hyperinsulinemic effect observed in HFD re-challenged mice may be due to this increased inflammatory activity within adipose tissue, but the concomitant development of other features during re-challenge, most notably hepatic steatosis, may also influence insulin resistance in these mice. Separating recruitment and activation of adipose tissue leukocytes from hepatic steatosis during HFD challenge is difficult. If we could identify a way of restoring eWAT expansive capacity in formerly obese mice then it may be possible to reduce hepatic steatosis while preserving leukocyte accumulation in adipose tissue. Otherwise depletion studies, for instance clodronate-filled liposomes, could be used during HFD re-challenge to reduce ATMs after which systemic and local metabolism could be analyzed. Treatment with anti-inflammatory cytokines (IL-10), or

treatment with neutralizing antibodies to reduce available inflammatory cytokines, could also be useful for determining the role of inflammation in metabolic dysregulation during HFD re-challenge of formerly obese mice.

Overall, the results suggest that health complications associated with weight gain may be variable depending on prior obesity status and metabolic impairments. It's crucial to mention that this should not be construed as indicating that weight regain and/or weight cycling is worse than maintained obesity. While not tested directly, it's likely that long-term HFD challenge of formerly obese and formerly lean mice, leading to body weight and adiposity stabilization, would result in similar metabolic derangements and hepatic steatosis between these two groups. Regardless, it's important to know if even small weight regain in formerly obese subjects may result in hastened development of severe metabolic consequences. We hope these studies will promote renewed research interest in identifying ways of better resolving obesity-induced effects during and after weight loss.

REFERENCES

1. Duren DL, Sherwood RJ, Czerwinski SA, Lee M, Choh AC, Siervogel RM, Cameron Chumlea W: Body composition methods: comparisons and interpretation. J Diabetes Sci Technol 2008;2:1139-1146

2. Bosy-Westphal A, Geisler C, Onur S, Korth O, Selberg O, Schrezenmeir J, Muller MJ: Value of body fat mass vs anthropometric obesity indices in the assessment of metabolic risk factors. Int J Obes (Lond) 2006;30:475-483

3. Okorodudu DO, Jumean MF, Montori VM, Romero-Corral A, Somers VK, Erwin PJ, Lopez-Jimenez F: Diagnostic performance of body mass index to identify obesity as defined by body adiposity: a systematic review and meta-analysis. Int J Obes (Lond) 2010;34:791-799

4. Deurenberg P, Andreoli A, Borg P, Kukkonen-Harjula K, de Lorenzo A, van Marken Lichtenbelt WD, Testolin G, Vigano R, Vollaard N: The validity of predicted body fat percentage from body mass index and from impedance in samples of five European populations. Eur J Clin Nutr 2001;55:973-979

5. Obesity: preventing and managing the global epidemic. Report of a WHO consultation. World Health Organ Tech Rep Ser 2000;894:i-xii, 1-253

6. Chan RS, Woo J: Prevention of overweight and obesity: how effective is the current public health approach. Int J Environ Res Public Health 2010;7:765-783

7. Romero-Corral A, Somers VK, Sierra-Johnson J, Thomas RJ, Collazo-Clavell ML, Korinek J, Allison TG, Batsis JA, Sert-Kuniyoshi FH, Lopez-Jimenez F: Accuracy of body mass index in diagnosing obesity in the adult general population. Int J Obes (Lond) 2008;32:959-966

8. Kennedy AP, Shea JL, Sun G: Comparison of the classification of obesity by BMI vs. dual-energy X-ray absorptiometry in the Newfoundland population. Obesity (Silver Spring) 2009;17:2094-2099

9. Klein S, Allison DB, Heymsfield SB, Kelley DE, Leibel RL, Nonas C, Kahn R, Association for Weight M, Obesity P, Naaso TOS, American Society for N, American Diabetes A: Waist circumference and cardiometabolic risk: a consensus statement from Shaping America's Health: Association for Weight Management and Obesity Prevention; NAASO, The Obesity Society; the American Society for Nutrition; and the American Diabetes Association. Am J Clin Nutr 2007;85:1197-1202

10. Lean ME, Han TS, Morrison CE: Waist circumference as a measure for indicating need for weight management. BMJ 1995;311:158-161

11. Wang Y, Rimm EB, Stampfer MJ, Willett WC, Hu FB: Comparison of abdominal adiposity and overall obesity in predicting risk of type 2 diabetes among men. Am J Clin Nutr 2005;81:555-563

12. Despres JP, Lemieux I: Abdominal obesity and metabolic syndrome. Nature 2006;444:881-887

13. Bjorntorp P: Visceral obesity: a "civilization syndrome". Obes Res 1993;1:206-222

14. Despres JP: Body fat distribution and risk of cardiovascular disease: an update. Circulation 2012;126:1301-1313

15. Guebre-Egziabher F, Alix PM, Koppe L, Pelletier CC, Kalbacher E, Fouque D, Soulage CO: Ectopic lipid accumulation: A potential cause for metabolic disturbances and a contributor to the alteration of kidney function. Biochimie 2013;95:1971-1979

16. van Herpen NA, Schrauwen-Hinderling VB: Lipid accumulation in non-adipose tissue and lipotoxicity. Physiol Behav 2008;94:231-241

17. Capeau J: Insulin resistance and steatosis in humans. Diabetes Metab 2008;34:649-657

18. Bozzetto L, Prinster A, Mancini M, Giacco R, De Natale C, Salvatore M, Riccardi G, Rivellese AA, Annuzzi G: Liver fat in obesity: role of type 2 diabetes mellitus and adipose tissue distribution. Eur J Clin Invest 2011;41:39-44

19. Alexopoulos N, Katritsis D, Raggi P: Visceral adipose tissue as a source of inflammation and promoter of atherosclerosis. Atherosclerosis 2014;233:104-112

20. Wajchenberg BL, Nery M, Cunha MR, Silva ME: Adipose tissue at the crossroads in the development of the metabolic syndrome, inflammation and atherosclerosis. Arq Bras Endocrinol Metabol 2009;53:145-150

21. Mathieu P, Lemieux I, Despres JP: Obesity, inflammation, and cardiovascular risk. Clin Pharmacol Ther 2010;87:407-416

22. Nishimura S, Manabe I, Nagai R: Adipose tissue inflammation in obesity and metabolic syndrome. Discov Med 2009;8:55-60

23. Li S, Zhang HY, Hu CC, Lawrence F, Gallagher KE, Surapaneni A, Estrem ST, Calley JN, Varga G, Dow ER, Chen Y: Assessment of diet-induced obese rats as an obesity model by comparative functional genomics. Obesity (Silver Spring) 2008;16:811-818

24. Ogden CL, Carroll MD, Fryar CD, Flegal KM: Prevalence of Obesity Among Adults and Youth: United States, 2011-2014. NCHS Data Brief 2015:1-8

25. Ng M, Fleming T, Robinson M, Thomson B, Graetz N, Margono C, Mullany EC, Biryukov S, Abbafati C, Abera SF, Abraham JP, Abu-Rmeileh NM, Achoki T, AlBuhairan FS, Alemu ZA, Alfonso R, Ali MK, Ali R, Guzman NA, Ammar W, Anwari P, Banerjee A, Barquera S, Basu S, Bennett DA, Bhutta Z, Blore J, Cabral N, Nonato IC, Chang JC, Chowdhury R, Courville KJ, Criqui MH, Cundiff DK, Dabhadkar KC, Dandona L, Davis A, Dayama A, Dharmaratne SD, Ding EL, Durrani AM, Esteghamati A, Farzadfar F, Fay DF, Feigin VL, Flaxman A, Forouzanfar MH, Goto A, Green MA, Gupta R, Hafezi-Nejad N, Hankey GJ, Harewood HC, Havmoeller R, Hay S, Hernandez L, Husseini A, Idrisov BT, Ikeda N, Islami F, Jahangir E, Jassal SK, Jee SH, Jeffreys M, Jonas JB, Kabagambe EK, Khalifa SE, Kengne AP, Khader YS, Khang YH, Kim D, Kimokoti RW, Kinge JM, Kokubo Y, Kosen S, Kwan G, Lai T, Leinsalu M, Li Y, Liang X, Liu S, Logroscino G, Lotufo PA, Lu Y, Ma J, Mainoo NK, Mensah GA, Merriman TR, Mokdad AH, Moschandreas J, Naghavi M, Naheed A, Nand D, Narayan KM, Nelson EL, Neuhouser ML, Nisar MI, Ohkubo T, Oti SO, Pedroza A, Prabhakaran D, Roy N, Sampson U, Seo H, Sepanlou SG, Shibuya K, Shiri R, Shiue I, Singh GM, Singh JA, Skirbekk V, Stapelberg NJ, Sturua L, Sykes BL, Tobias M, Tran BX, Trasande L, Toyoshima H, van de Vijver S, Vasankari TJ, Veerman JL, Velasquez-Melendez G, Vlassov VV, Vollset SE, Vos T, Wang C, Wang X, Weiderpass E, Werdecker A, Wright JL, Yang YC, Yatsuya H, Yoon J, Yoon SJ, Zhao Y, Zhou M, Zhu S, Lopez AD, Murray

CJ, Gakidou E: Global, regional, and national prevalence of overweight and obesity in children and adults during 1980-2013: a systematic analysis for the Global Burden of Disease Study 2013. Lancet 2014;384:766-781

26. Tsai AG, Williamson DF, Glick HA: Direct medical cost of overweight and obesity in the USA: a quantitative systematic review. Obes Rev 2011;12:50-61

27. Field AE, Coakley EH, Must A, Spadano JL, Laird N, Dietz WH, Rimm E, Colditz GA: Impact of overweight on the risk of developing common chronic diseases during a 10-year period. Arch Intern Med 2001;161:1581-1586

28. Adams KF, Schatzkin A, Harris TB, Kipnis V, Mouw T, Ballard-Barbash R, Hollenbeck A, Leitzmann MF: Overweight, obesity, and mortality in a large prospective cohort of persons 50 to 71 years old. N Engl J Med 2006;355:763-778

29. Guh DP, Zhang W, Bansback N, Amarsi Z, Birmingham CL, Anis AH: The incidence of co-morbidities related to obesity and overweight: a systematic review and meta-analysis. BMC Public Health 2009;9:88

30. Khaodhiar L, McCowen KC, Blackburn GL: Obesity and its comorbid conditions. Clin Cornerstone 1999;2:17-31

31. Genuth S, Alberti KG, Bennett P, Buse J, Defronzo R, Kahn R, Kitzmiller J, Knowler WC, Lebovitz H, Lernmark A, Nathan D, Palmer J, Rizza R, Saudek C, Shaw J, Steffes M, Stern M, Tuomilehto J, Zimmet P, Expert Committee on the D, Classification of Diabetes M: Follow-up report on the diagnosis of diabetes mellitus. Diabetes Care 2003;26:3160-3167

32. American Diabetes A: Diagnosis and classification of diabetes mellitus. Diabetes Care 2010;33 Suppl 1:S62-69

33. Saudek CD, Brick JC: The clinical use of hemoglobin A1c. J Diabetes Sci Technol 2009;3:629-634

34. Wilcox G: Insulin and insulin resistance. Clin Biochem Rev 2005;26:19-39

35. Ganz ML, Wintfeld N, Li Q, Alas V, Langer J, Hammer M: The association of body mass index with the risk of type 2 diabetes: a case-control study nested in an electronic health records system in the United States. Diabetol Metab Syndr 2014;6:50

36. Ligthart S, van Herpt TT, Leening MJ, Kavousi M, Hofman A, Stricker BH, van Hoek M, Sijbrands EJ, Franco OH, Dehghan A: Lifetime risk of developing impaired glucose metabolism and eventual progression from prediabetes to type 2 diabetes: a prospective cohort study. Lancet Diabetes Endocrinol 2016;4:44-51

37. Clark JM: The epidemiology of nonalcoholic fatty liver disease in adults. J Clin Gastroenterol 2006;40 Suppl 1:S5-10

38. Ong JP, Younossi ZM: Epidemiology and natural history of NAFLD and NASH. Clin Liver Dis 2007;11:1-16, vii

39. Birkenfeld AL, Shulman GI: Nonalcoholic fatty liver disease, hepatic insulin resistance, and type 2 diabetes. Hepatology 2014;59:713-723

40. Gaggini M, Morelli M, Buzzigoli E, DeFronzo RA, Bugianesi E, Gastaldelli A: Non-alcoholic fatty liver disease (NAFLD) and its connection with insulin resistance, dyslipidemia, atherosclerosis and coronary heart disease. Nutrients 2013;5:1544-1560

41. Bugianesi E, Moscatiello S, Ciaravella MF, Marchesini G: Insulin resistance in nonalcoholic fatty liver disease. Curr Pharm Des 2010;16:1941-1951

42. Vanni E, Bugianesi E, Kotronen A, De Minicis S, Yki-Jarvinen H, Svegliati-Baroni G: From the metabolic syndrome to NAFLD or vice versa? Dig Liver Dis 2010;42:320-330

43. Gruben N, Shiri-Sverdlov R, Koonen DP, Hofker MH: Nonalcoholic fatty liver disease: A main driver of insulin resistance or a dangerous liaison? Biochim Biophys Acta 2014;1842:2329-2343

44. Matarese G, Moschos S, Mantzoros CS: Leptin in immunology. J Immunol 2005;174:3137-3142

45. Matarese G, Di Giacomo A, Sanna V, Lord GM, Howard JK, Di Tuoro A, Bloom SR, Lechler RI, Zappacosta S, Fontana S: Requirement for leptin in the induction and progression of autoimmune encephalomyelitis. J Immunol 2001;166:5909-5916

46. Herrera BM, Keildson S, Lindgren CM: Genetics and epigenetics of obesity. Maturitas 2011;69:41-49

47. Hinney A, Vogel CI, Hebebrand J: From monogenic to polygenic obesity: recent advances. Eur Child Adolesc Psychiatry 2010;19:297-310

48. Buettner R, Scholmerich J, Bollheimer LC: High-fat diets: modeling the metabolic disorders of human obesity in rodents. Obesity (Silver Spring) 2007;15:798-808

49. Lumeng CN, Deyoung SM, Bodzin JL, Saltiel AR: Increased inflammatory properties of adipose tissue macrophages recruited during diet-induced obesity. Diabetes 2007;56:16-23

50. Winer S, Chan Y, Paltser G, Truong D, Tsui H, Bahrami J, Dorfman R, Wang Y, Zielenski J, Mastronardi F, Maezawa Y, Drucker D, Endleman E, Winer D, Dosch HM: Normalization of Obesity-Associated Insulin Resistance through Immunotherapy: CD4+ T Cells Control Glucose Homeostasis. . Nat Med 2009;15:921-929

51. Li P, Lu M, Nguyen MT, Bae EJ, Chapman J, Feng D, Hawkins M, Pessin JE, Sears DD, Nguyen AK, Amidi A, Watkins SM, Nguyen U, Olefsky JM: Functional heterogeneity of CD11c-positive adipose tissue macrophages in diet-induced obese mice. J Biol Chem 2010;285:15333-15345

52. Hayes MR, Kanoski SE, Alhadeff AL, Grill HJ: Comparative effects of the long-acting GLP-1 receptor ligands, liraglutide and exendin-4, on food intake and body weight suppression in rats. Obesity (Silver Spring) 2011;19:1342-1349

53. Porter DW, Kerr BD, Flatt PR, Holscher C, Gault VA: Four weeks administration of Liraglutide improves memory and learning as well as glycaemic control in mice with high fat dietary-induced obesity and insulin resistance. Diabetes Obes Metab 2010;12:891-899

54. Madsen AN, Hansen G, Paulsen SJ, Lykkegaard K, Tang-Christensen M, Hansen HS, Levin BE, Larsen PJ, Knudsen LB, Fosgerau K, Vrang N: Long-term characterization of the diet-induced obese and diet-resistant rat model: a polygenetic rat model mimicking the human obesity syndrome. J Endocrinol 2010;206:287-296

55. Greenway FL, Whitehouse MJ, Guttadauria M, Anderson JW, Atkinson RL, Fujioka K, Gadde KM, Gupta AK, O'Neil P, Schumacher D, Smith D, Dunayevich E, Tollefson GD, Weber E, Cowley MA: Rational design of a combination medication for the treatment of obesity. Obesity (Silver Spring) 2009;17:30-39

56. Guo J, Jou W, Gavrilova O, Hall KD: Persistent diet-induced obesity in male C57BL/6 mice resulting from temporary obesigenic diets. PLoS One 2009;4:e5370

57. Ranasinghe C, Gamage P, Katulanda P, Andraweera N, Thilakarathne S, Tharanga P: Relationship between Body Mass Index (BMI) and body fat percentage, estimated by bioelectrical impedance, in a group of Sri Lankan adults: a cross sectional study. BMC Public Health 2013;13:797

58. Vickers SP, Jackson HC, Cheetham SC: The utility of animal models to evaluate novel anti-obesity agents. Br J Pharmacol 2011;164:1248-1262

59. Qiu J, Ogus S, Mounzih K, Ewart-Toland A, Chehab FF: Leptin-deficient mice backcrossed to the BALB/cJ genetic background have reduced adiposity, enhanced fertility, normal body temperature, and severe diabetes. Endocrinology 2001;142:3421-3425

60. Haluzik M, Colombo C, Gavrilova O, Chua S, Wolf N, Chen M, Stannard B, Dietz KR, Le Roith D, Reitman ML: Genetic background (C57BL/6J versus FVB/N) strongly influences the severity of diabetes and insulin resistance in ob/ob mice. Endocrinology 2004;145:3258-3264

61. West DB, Boozer CN, Moody DL, Atkinson RL: Dietary obesity in nine inbred mouse strains. Am J Physiol 1992;262:R1025-1032

62. Montgomery MK, Hallahan NL, Brown SH, Liu M, Mitchell TW, Cooney GJ, Turner N: Mouse strain-dependent variation in obesity and glucose homeostasis in response to high-fat feeding. Diabetologia 2013;56:1129-1139

63. Yang Y, Smith DL, Jr., Keating KD, Allison DB, Nagy TR: Variations in body weight, food intake and body composition after long-term high-fat diet feeding in C57BL/6J mice. Obesity (Silver Spring) 2014;22:2147-2155

64. Boonchaya-anant P, Apovian CM: Metabolically healthy obesity--does it exist? Curr Atheroscler Rep 2014;16:441

65. Munoz-Garach A, Cornejo-Pareja I, Tinahones FJ: Does Metabolically Healthy Obesity Exist? Nutrients 2016;8

66. Dhana K, Koolhaas CM, van Rossum EF, Ikram MA, Hofman A, Kavousi M, Franco OH: Metabolically Healthy Obesity and the Risk of Cardiovascular Disease in the Elderly Population. PLoS One 2016;11:e0154273

67. Roberson LL, Aneni EC, Maziak W, Agatston A, Feldman T, Rouseff M, Tran T, Blaha MJ, Santos RD, Sposito A, Al-Mallah MH, Blankstein R, Budoff MJ, Nasir K: Beyond BMI: The "Metabolically healthy obese" phenotype & its association with clinical/subclinical cardiovascular disease and all-cause mortality -- a systematic review. BMC Public Health 2014;14:14

68. Wildman RP, Muntner P, Reynolds K, McGinn AP, Rajpathak S, Wylie-Rosett J, Sowers MR: The obese without cardiometabolic risk factor clustering and the normal weight with cardiometabolic risk factor clustering: prevalence and correlates of 2 phenotypes among the US population (NHANES 1999-2004). Arch Intern Med 2008;168:1617-1624

69. Ebstein W: Zur therapie des Diabetes mellitus, insbesondere über die Anwendung des salicylsauren Natron bei demselben. Berliner Klinische Wochenschrift 1876;13:337-340

70. Shoelson SE, Lee J, Goldfine AB: Inflammation and insulin resistance. J Clin Invest 2006;116:1793-1801

71. Williamson RT: On the Treatment of Glycosuria and Diabetes Mellitus with Sodium Salicylate. Br Med J 1901;1:760-762

72. Hundal RS, Petersen KF, Mayerson AB, Randhawa PS, Inzucchi S, Shoelson SE, Shulman GI: Mechanism by which high-dose aspirin improves glucose metabolism in type 2 diabetes. J Clin Invest 2002;109:1321-1326

73. Yuan M, Konstantopoulos N, Lee J, Hansen L, Li ZW, Karin M, Shoelson SE: Reversal of obesity- and diet-induced insulin resistance with salicylates or targeted disruption of Ikkbeta. Science 2001;293:1673-1677

74. Hotamisligil GS, Shargill NS, Spiegelman BM: Adipose expression of tumor necrosis factor-alpha: direct role in obesity-linked insulin resistance. Science 1993;259:87-91

75. Feinstein R, Kanety H, Papa MZ, Lunenfeld B, Karasik A: Tumor necrosis factor-alpha suppresses insulin-induced tyrosine phosphorylation of insulin receptor and its substrates. J Biol Chem 1993;268:26055-26058

76. Trayhurn P, Wood IS: Adipokines: inflammation and the pleiotropic role of white adipose tissue. Br J Nutr 2004;92:347-355

77. Aronson D, Bartha P, Zinder O, Kerner A, Markiewicz W, Avizohar O, Brook GJ, Levy Y: Obesity is the major determinant of elevated C-reactive protein in subjects with the metabolic syndrome. Int J Obes Relat Metab Disord 2004;28:674-679

78. Fried SK, Bunkin DA, Greenberg AS: Omental and subcutaneous adipose tissues of obese subjects release interleukin-6: depot difference and regulation by glucocorticoid. The Journal of clinical endocrinology and metabolism 1998;83:847-850

79. Kim JE, Lee MH, Nam DH, Song HK, Kang YS, Lee JE, Kim HW, Cha JJ, Hyun YY, Han SY, Han KH, Han JY, Cha DR: Celastrol, an NF-kappaB inhibitor, improves insulin resistance and attenuates renal injury in db/db mice. PLoS One 2013;8:e62068

80. Hirosumi J, Tuncman G, Chang L, Gorgun CZ, Uysal KT, Maeda K, Karin M, Hotamisligil GS: A central role for JNK in obesity and insulin resistance. Nature 2002;420:333-336

81. Vandanmagsar B, Youm YH, Ravussin A, Galgani JE, Stadler K, Mynatt RL, Ravussin E, Stephens JM, Dixit VD: The NLRP3 inflammasome instigates obesity-induced inflammation and insulin resistance. Nat Med 2011;17:179-188

82. Chang L, Chiang SH, Saltiel AR: Insulin signaling and the regulation of glucose transport. Mol Med 2004;10:65-71

83. Aguirre V, Uchida T, Yenush L, Davis R, White MF: The c-Jun NH(2)-terminal kinase promotes insulin resistance during association with insulin receptor substrate-1 and phosphorylation of Ser(307). J Biol Chem 2000;275:9047-9054

84. Werner ED, Lee J, Hansen L, Yuan M, Shoelson SE: Insulin resistance due to phosphorylation of insulin receptor substrate-1 at serine 302. J Biol Chem 2004;279:35298-35305

85. Kwon H, Pessin JE: Adipokines mediate inflammation and insulin resistance. Front Endocrinol (Lausanne) 2013;4:71

86. Ueki K, Kondo T, Kahn CR: Suppressor of cytokine signaling 1 (SOCS-1) and SOCS-3 cause insulin resistance through inhibition of tyrosine phosphorylation of insulin receptor substrate proteins by discrete mechanisms. Mol Cell Biol 2004;24:5434-5446

87. Wernstedt Asterholm I, Tao C, Morley TS, Wang QA, Delgado-Lopez F, Wang ZV, Scherer PE: Adipocyte inflammation is essential for healthy adipose tissue expansion and remodeling. Cell Metab 2014;20:103-118

88. Tang T, Zhang J, Yin J, Staszkiewicz J, Gawronska-Kozak B, Jung DY, Ko HJ, Ong H, Kim JK, Mynatt R, Martin RJ, Keenan M, Gao Z, Ye J: Uncoupling of inflammation

and insulin resistance by NF-kappaB in transgenic mice through elevated energy expenditure. J Biol Chem 2010;285:4637-4644

89. Dominguez H, Storgaard H, Rask-Madsen C, Steffen Hermann T, Ihlemann N, Baunbjerg Nielsen D, Spohr C, Kober L, Vaag A, Torp-Pedersen C: Metabolic and vascular effects of tumor necrosis factor-alpha blockade with etanercept in obese patients with type 2 diabetes. J Vasc Res 2005;42:517-525

90. Paquot N, Castillo MJ, Lefebvre PJ, Scheen AJ: No increased insulin sensitivity after a single intravenous administration of a recombinant human tumor necrosis factor receptor: Fc fusion protein in obese insulin-resistant patients. The Journal of clinical endocrinology and metabolism 2000;85:1316-1319

91. Stanley TL, Zanni MV, Johnsen S, Rasheed S, Makimura H, Lee H, Khor VK, Ahima RS, Grinspoon SK: TNF-alpha antagonism with etanercept decreases glucose and increases the proportion of high molecular weight adiponectin in obese subjects with features of the metabolic syndrome. The Journal of clinical endocrinology and metabolism 2011;96:E146-150

92. Pollack RM, Donath MY, LeRoith D, Leibowitz G: Anti-inflammatory Agents in the Treatment of Diabetes and Its Vascular Complications. Diabetes Care 2016;39 Suppl 2:S244-252

93. Sloan-Lancaster J, Abu-Raddad E, Polzer J, Miller JW, Scherer JC, De Gaetano A, Berg JK, Landschulz WH: Double-blind, randomized study evaluating the glycemic and anti-inflammatory effects of subcutaneous LY2189102, a neutralizing IL-1beta antibody, in patients with type 2 diabetes. Diabetes Care 2013;36:2239-2246

94. Cavelti-Weder C, Babians-Brunner A, Keller C, Stahel MA, Kurz-Levin M, Zayed H, Solinger AM, Mandrup-Poulsen T, Dinarello CA, Donath MY: Effects of gevokizumab on glycemia and inflammatory markers in type 2 diabetes. Diabetes Care 2012;35:1654-1662

95. Hensen J, Howard CP, Walter V, Thuren T: Impact of interleukin-1beta antibody (canakinumab) on glycaemic indicators in patients with type 2 diabetes mellitus: results of secondary endpoints from a randomized, placebo-controlled trial. Diabetes Metab 2013;39:524-531

96. Ferrante AW, Jr.: The immune cells in adipose tissue. Diabetes Obes Metab 2013;15 Suppl 3:34-38

97. Sun S, Ji Y, Kersten S, Qi L: Mechanisms of inflammatory responses in obese adipose tissue. Annu Rev Nutr 2012;32:261-286

98. Lumeng CN, Saltiel AR: Inflammatory links between obesity and metabolic disease. J Clin Invest 2011;121:2111-2117

99. Wang X, Bao W, Liu J, Ouyang YY, Wang D, Rong S, Xiao X, Shan ZL, Zhang Y, Yao P, Liu LG: Inflammatory markers and risk of type 2 diabetes: a systematic review and meta-analysis. Diabetes Care 2013;36:166-175

100. Olefsky JM, Glass CK: Macrophages, inflammation, and insulin resistance. Annu Rev Physiol 2010;72:219-246

101. Greenberg AS, Obin MS: Obesity and the role of adipose tissue in inflammation and metabolism. Am J Clin Nutr 2006;83:461S-465S

102. Goran MI, Alderete TL: Targeting adipose tissue inflammation to treat the underlying basis of the metabolic complications of obesity. Nestle Nutr Inst Workshop Ser 2012;73:49-60; discussion p61-46

103. Mraz M, Haluzik M: The role of adipose tissue immune cells in obesity and low-grade inflammation. J Endocrinol 2014;222:R113-127

104. Lee BC, Lee J: Cellular and molecular players in adipose tissue inflammation in the development of obesity-induced insulin resistance. Biochim Biophys Acta 2014;1842:446-462

105. Molofsky AB, Nussbaum JC, Liang HE, Van Dyken SJ, Cheng LE, Mohapatra A, Chawla A, Locksley RM: Innate lymphoid type 2 cells sustain visceral adipose tissue eosinophils and alternatively activated macrophages. J Exp Med 2013;210:535-549

106. Huh JY, Park YJ, Ham M, Kim JB: Crosstalk between adipocytes and immune cells in adipose tissue inflammation and metabolic dysregulation in obesity. Mol Cells 2014;37:365-371

107. Lee BC, Kim MS, Pae M, Yamamoto Y, Eberle D, Shimada T, Kamei N, Park HS, Sasorith S, Woo JR, You J, Mosher W, Brady HJ, Shoelson SE, Lee J: Adipose Natural Killer Cells Regulate Adipose Tissue Macrophages to Promote Insulin Resistance in Obesity. Cell Metab 2016;23:685-698

108. Winer DA, Winer S, Shen L, Wadia PP, Yantha J, Paltser G, Tsui H, Wu P, Davidson MG, Alonso MN, Leong HX, Glassford A, Caimol M, Kenkel JA, Tedder TF, McLaughlin T, Miklos DB, Dosch HM, Engleman EG: B cells promote insulin resistance through modulation of T cells and production of pathogenic IgG antibodies. Nat Med 2011;17:610-617

109. Nishimura S, Manabe I, Nagasaki M, Eto K, Yamashita H, Ohsugi M, Otsu M, Hara K, Ueki K, Sugiura S, Yoshimura K, Kadowaki T, Nagai R: CD8+ effector T cells contribute to macrophage recruitment and adipose tissue inflammation in obesity. Nat Med 2009;15:914-920

110. Feuerer M, Herrero L, Cipolletta D, Naaz A, Wong J, Nayer A, Lee J, Goldfine AB, Benoist C, Shoelson S, Mathis D: Lean, but not obese, fat is enriched for a unique population of regulatory T cells that affect metabolic parameters. Nat Med 2009;15:930-939

111. Rocha VZ, Folco EJ, Sukhova G, Shimizu K, Gotsman I, Vernon AH, Libby P: Interferon-gamma, a Th1 cytokine, regulates fat inflammation: a role for adaptive immunity in obesity. Circ Res 2008;103:467-476

112. Winer S, Chan Y, Paltser G, Truong D, Tsui H, Bahrami J, Dorfman R, Wang Y, Zielenski J, Mastronardi F, Maezawa Y, Drucker DJ, Engleman E, Winer D, Dosch HM: Normalization of obesity-associated insulin resistance through immunotherapy. Nat Med 2009;15:921-929

113. Xu H, Barnes GT, Yang Q, Tan G, Yang D, Chou CJ, Sole J, Nichols A, Ross JS, Tartaglia LA, Chen H: Chronic inflammation in fat plays a crucial role in the development of obesity-related insulin resistance. J Clin Invest 2003;112:1821-1830

114. Weisberg SP, McCann D, Desai M, Rosenbaum M, Leibel RL, Ferrante AW, Jr.: Obesity is associated with macrophage accumulation in adipose tissue. J Clin Invest 2003;112:1796-1808

115. Shapiro H, Pecht T, Shaco-Levy R, Harman-Boehm I, Kirshtein B, Kuperman Y, Chen A, Bluher M, Shai I, Rudich A: Adipose tissue foam cells are present in human obesity. The Journal of clinical endocrinology and metabolism 2013;98:1173-1181

116. Cancello R, Tordjman J, Poitou C, Guilhem G, Bouillot JL, Hugol D, Coussieu C, Basdevant A, Bar Hen A, Bedossa P, Guerre-Millo M, Clement K: Increased infiltration

of macrophages in omental adipose tissue is associated with marked hepatic lesions in morbid human obesity. Diabetes 2006;55:1554-1561

117. Lumeng CN, Bodzin JL, Saltiel AR: Obesity induces a phenotypic switch in adipose tissue macrophage polarization. J Clin Invest 2007;117:175-184

118. Cinti S, Mitchell G, Barbatelli G, Murano I, Ceresi E, Faloia E, Wang S, Fortier M, Greenberg AS, Obin MS: Adipocyte death defines macrophage localization and function in adipose tissue of obese mice and humans. Journal of lipid research 2005;46:2347-2355

119. Lumeng CN, DelProposto JB, Westcott DJ, Saltiel AR: Phenotypic switching of adipose tissue macrophages with obesity is generated by spatiotemporal differences in macrophage subtypes. Diabetes 2008;57:3239-3246

120. Feng B, Jiao P, Nie Y, Kim T, Jun D, van Rooijen N, Yang Z, Xu H: Clodronate liposomes improve metabolic profile and reduce visceral adipose macrophage content in diet-induced obese mice. PLoS One 2011;6:e24358

121. Lee YS, Li P, Huh JY, Hwang IJ, Lu M, Kim JI, Ham M, Talukdar S, Chen A, Lu WJ, Bandyopadhyay GK, Schwendener R, Olefsky J, Kim JB: Inflammation is necessary for long-term but not short-term high-fat diet-induced insulin resistance. Diabetes 2011;60:2474-2483

122. Patsouris D, Li PP, Thapar D, Chapman J, Olefsky JM, Neels JG: Ablation of CD11c-positive cells normalizes insulin sensitivity in obese insulin resistant animals. Cell Metab 2008;8:301-309

123. Weisberg SP, Hunter D, Huber R, Lemieux J, Slaymaker S, Vaddi K, Charo I, Leibel RL, Ferrante AW, Jr.: CCR2 modulates inflammatory and metabolic effects of high-fat feeding. J Clin Invest 2006;116:115-124

124. Kanda H, Tateya S, Tamori Y, Kotani K, Hiasa K, Kitazawa R, Kitazawa S, Miyachi H, Maeda S, Egashira K, Kasuga M: MCP-1 contributes to macrophage infiltration into adipose tissue, insulin resistance, and hepatic steatosis in obesity. J Clin Invest 2006;116:1494-1505

125. Schmitz J, Evers N, Awazawa M, Nicholls HT, Brönneke HS, Dietrich A, Mauer J, Blüher M, Brüning JC: Obesogenic memory can confer long-term increases in adipose tissue but not liver inflammation and insulin resistance after weight loss. Molecular Metabolism 2016;

126. Cancello R, Zulian A, Gentilini D, Mencarelli M, Della Barba A, Maffei M, Vitti P, Invitti C, Liuzzi A, Di Blasio AM: Permanence of molecular features of obesity in subcutaneous adipose tissue of ex-obese subjects. Int J Obes (Lond) 2013;37:867-873

127. Misharin AV, Morales-Nebreda L, Mutlu GM, Budinger GR, Perlman H: Flow cytometric analysis of macrophages and dendritic cell subsets in the mouse lung. Am J Respir Cell Mol Biol 2013;49:503-510

128. Dutton GR, Lewis CE: The Look AHEAD Trial: Implications for Lifestyle Intervention in Type 2 Diabetes Mellitus. Prog Cardiovasc Dis 2015;58:69-75

129. Magkos F, Fraterrigo G, Yoshino J, Luecking C, Kirbach K, Kelly SC, de Las Fuentes L, He S, Okunade AL, Patterson BW, Klein S: Effects of Moderate and Subsequent Progressive Weight Loss on Metabolic Function and Adipose Tissue Biology in Humans with Obesity. Cell Metab 2016;

130. Jung DY, Ko HJ, Lichtman EI, Lee E, Lawton E, Ong H, Yu K, Azuma Y, Friedline RH, Lee KW, Kim JK: Short-term weight loss attenuates local tissue inflammation and

improves insulin sensitivity without affecting adipose inflammation in obese mice. Am J Physiol Endocrinol Metab 2013;304:E964-976

131. Mathis D: Immunological goings-on in visceral adipose tissue. Cell Metab 2013;17:851-859

132. Lumeng CN: Innate immune activation in obesity. Molecular aspects of medicine 2013;34:12-29

133. Skinner AC, Steiner MJ, Henderson FW, Perrin EM: Multiple markers of inflammation and weight status: cross-sectional analyses throughout childhood. Pediatrics 2010;125:e801-809

134. Poitou C, Dalmas E, Renovato M, Benhamo V, Hajduch F, Abdennour M, Kahn JF, Veyrie N, Rizkalla S, Fridman WH, Sautes-Fridman C, Clement K, Cremer I: CD14dimCD16+ and CD14+CD16+ monocytes in obesity and during weight loss: relationships with fat mass and subclinical atherosclerosis. Arterioscler Thromb Vasc Biol 2011;31:2322-2330

135. Wentworth JM, Naselli G, Brown WA, Doyle L, Phipson B, Smyth GK, Wabitsch M, O'Brien PE, Harrison LC: Pro-inflammatory CD11c+CD206+ adipose tissue macrophages are associated with insulin resistance in human obesity. Diabetes 2010;59:1648-1656

136. Talukdar S, Oh da Y, Bandyopadhyay G, Li D, Xu J, McNelis J, Lu M, Li P, Yan Q, Zhu Y, Ofrecio J, Lin M, Brenner MB, Olefsky JM: Neutrophils mediate insulin resistance in mice fed a high-fat diet through secreted elastase. Nat Med 2012;18:1407-1412

137. Xu X, Grijalva A, Skowronski A, van Eijk M, Serlie MJ, Ferrante AW, Jr.: Obesity activates a program of lysosomal-dependent lipid metabolism in adipose tissue macrophages independently of classic activation. Cell Metab 2013;18:816-830

138. Kratz M, Coats BR, Hisert KB, Hagman D, Mutskov V, Peris E, Schoenfelt KQ, Kuzma JN, Larson I, Billing PS, Landerholm RW, Crouthamel M, Gozal D, Hwang S, Singh PK, Becker L: Metabolic dysfunction drives a mechanistically distinct proinflammatory phenotype in adipose tissue macrophages. Cell Metab 2014;20:614-625

139. Wu H, Perrard XD, Wang Q, Perrard JL, Polsani VR, Jones PH, Smith CW, Ballantyne CM: CD11c expression in adipose tissue and blood and its role in diet-induced obesity. Arteriosclerosis, Thrombosis, and Vascular Biology 2010;30:186-192

140. Tao T, Li S, Zhao A, Zhang Y, Liu W: Expression of the CD11c gene in subcutaneous adipose tissue is associated with cytokine level and insulin resistance in women with polycystic ovary syndrome. European journal of endocrinology / European Federation of Endocrine Societies 2012;167:705-713

141. Wu H, Gower RM, Wang H, Perrard XY, Ma R, Bullard DC, Burns AR, Paul A, Smith CW, Simon SI, Ballantyne CM: Functional role of CD11c+ monocytes in atherogenesis associated with hypercholesterolemia. Circulation 2009;119:2708-2717

142. Cho KW, Morris DL, DelProposto JL, Geletka L, Zamarron B, Martinez-Santibanez G, Meyer KA, Singer K, O'Rourke RW, Lumeng CN: An MHC II-dependent activation loop between adipose tissue macrophages and CD4+ T cells controls obesity-induced inflammation. Cell Reports 2014;9:605-617

143. Kolodin D, van Panhuys N, Li C, Magnuson AM, Cipolletta D, Miller CM, Wagers A, Germain RN, Benoist C, Mathis D: Antigen- and cytokine-driven accumulation of regulatory T cells in visceral adipose tissue of lean mice. Cell Metab 2015;21:543-557

144. Morris DL, Cho KW, Delproposto JL, Oatmen KE, Geletka LM, Martinez-Santibanez G, Singer K, Lumeng CN: Adipose tissue macrophages function as antigen-presenting cells and regulate adipose tissue CD4+ T cells in mice. Diabetes 2013;62:2762-2772

145. Bertola A, Ciucci T, Rousseau D, Bourlier V, Duffaut C, Bonnafous S, Blin-Wakkach C, Anty R, Iannelli A, Gugenheim J, Tran A, Bouloumie A, Gual P, Wakkach A: Identification of adipose tissue dendritic cells correlated with obesity-associated insulin-resistance and inducing Th17 responses in mice and patients. Diabetes 2012;61:2238-2247

146. Zlotnikov-Klionsky Y, Nathansohn-Levi B, Shezen E, Rosen C, Kagan S, Bar-On L, Jung S, Shifrut E, Reich-Zeliger S, Friedman N, Aharoni R, Arnon R, Yifa O, Aronovich A, Reisner Y: Perforin-Positive Dendritic Cells Exhibit an Immuno-regulatory Role in Metabolic Syndrome and Autoimmunity. Immunity 2015;43:776-787

147. Pamir N, Liu NC, Irwin A, Becker L, Peng Y, Ronsein GE, Bornfeldt KE, Duffield JS, Heinecke JW: Granulocyte/Macrophage Colony-stimulating Factor-dependent Dendritic Cells Restrain Lean Adipose Tissue Expansion. J Biol Chem 2015;290:14656-14667

148. Stefanovic-Racic M, Yang X, Turner MS, Mantell BS, Stolz DB, Sumpter TL, Sipula IJ, Dedousis N, Scott DK, Morel PA, Thomson AW, O'Doherty RM: Dendritic cells promote macrophage infiltration and comprise a substantial proportion of obesity-associated increases in CD11c+ cells in adipose tissue and liver. Diabetes 2012;61:2330-2339

149. Chen Y, Tian J, Tian X, Tang X, Rui K, Tong J, Lu L, Xu H, Wang S: Adipose tissue dendritic cells enhances inflammation by prompting the generation of Th17 cells. PLoS One 2014;9:e92450

150. Kuan EL, Ivanov S, Bridenbaugh EA, Victora G, Wang W, Childs EW, Platt AM, Jakubzick CV, Mason RJ, Gashev AA, Nussenzweig M, Swartz MA, Dustin ML, Zawieja DC, Randolph GJ: Collecting lymphatic vessel permeability facilitates adipose tissue inflammation and distribution of antigen to lymph node-homing adipose tissue dendritic cells. J Immunol 2015;194:5200-5210

151. Gautier EL, Shay T, Miller J, Greter M, Jakubzick C, Ivanov S, Helft J, Chow A, Elpek KG, Gordonov S, Mazloom AR, Ma'ayan A, Chua WJ, Hansen TH, Turley SJ, Merad M, Randolph GJ: Gene-expression profiles and transcriptional regulatory pathways that underlie the identity and diversity of mouse tissue macrophages. Nature Immunology 2012;13:1118-1128

152. Tamoutounour S, Henri S, Lelouard H, de Bovis B, de Haar C, van der Woude CJ, Woltman AM, Reyal Y, Bonnet D, Sichien D, Bain CC, Mowat AM, Reis e Sousa C, Poulin LF, Malissen B, Guilliams M: CD64 distinguishes macrophages from dendritic cells in the gut and reveals the Th1-inducing role of mesenteric lymph node macrophages during colitis. Eur J Immunol 2012;42:3150-3166

153. De Calisto J, Villablanca EJ, Mora JR: FcgammaRI (CD64): an identity card for intestinal macrophages. Eur J Immunol 2012;42:3136-3140

154. Singer K, DelProposto J, Morris DL, Zamarron B, Mergian T, Maley N, Cho KW, Geletka L, Subbaiah P, Muir L, Martinez-Santibanez G, Lumeng CN: Diet-induced obesity promotes myelopoiesis in hematopoietic stem cells. Mol Metab 2014;3:664-675

155. Martinez-Santibanez G, Cho KW, Lumeng CN: Imaging white adipose tissue with confocal microscopy. Methods in enzymology 2014;537:17-30

156. Cho KW, Morris DL, Lumeng CN: Flow cytometry analyses of adipose tissue macrophages. Methods in enzymology 2014;537:297-314

157. Westcott DJ, Delproposto JB, Geletka LM, Wang T, Singer K, Saltiel AR, Lumeng CN: MGL1 promotes adipose tissue inflammation and insulin resistance by regulating 7/4hi monocytes in obesity. J Exp Med 2009;206:3143-3156

158. Kosteli A, Sugaru E, Haemmerle G, Martin JF, Lei J, Zechner R, Ferrante AW, Jr.: Weight loss and lipolysis promote a dynamic immune response in murine adipose tissue. J Clin Invest 2010;120:3466-3479

159. Weisberg SP, Hunter D, Huber R, Lemieux J, Slaymaker S, Vaddi K, Charo I, Leibel RL, Ferrante AW: CCR2 modulates inflammatory and metabolic effects of high-fat feeding. Journal of Clinical Investigation 2005;116:115-124

160. Collin M, McGovern N, Haniffa M: Human dendritic cell subsets. Immunology 2013;140:22-30

161. Orr JS, Puglisi MJ, Ellacott KL, Lumeng CN, Wasserman DH, Hasty AH: Toll-like receptor 4 deficiency promotes the alternative activation of adipose tissue macrophages. Diabetes 2012;61:2718-2727

162. Sano T, Iwashita M, Nagayasu S, Yamashita A, Shinjo T, Hashikata A, Asano T, Kushiyama A, Ishimaru N, Takahama Y, Nishimura F: Protection from diet-induced obesity and insulin resistance in mice lacking CCL19-CCR7 signaling. Obesity (Silver Spring) 2015;23:1460-1471

163. Poitou C, Perret C, Mathieu F, Truong V, Blum Y, Durand H, Alili R, Chelghoum N, Pelloux V, Aron-Wisnewsky J, Torcivia A, Bouillot JL, Parks BW, Ninio E, Clement K, Tiret L: Bariatric Surgery Induces Disruption in Inflammatory Signaling Pathways Mediated by Immune Cells in Adipose Tissue: A RNA-Seq Study. PLoS One 2015;10:e0125718

164. Kang YS, Cha JJ, Hyun YY, Cha DR: Novel C-C chemokine receptor 2 antagonists in metabolic disease: a review of recent developments. Expert Opin Investig Drugs 2011;20:745-756

165. Obstfeld AE, Sugaru E, Thearle M, Francisco AM, Gayet C, Ginsberg HN, Ables EV, Ferrante AW, Jr.: C-C chemokine receptor 2 (CCR2) regulates the hepatic recruitment of myeloid cells that promote obesity-induced hepatic steatosis. Diabetes 2010;59:916-925

166. Tacke F, Alvarez D, Kaplan TJ, Jakubzick C, Spanbroek R, Llodra J, Garin A, Liu J, Mack M, van Rooijen N, Lira SA, Habenicht AJ, Randolph GJ: Monocyte subsets differentially employ CCR2, CCR5, and CX3CR1 to accumulate within atherosclerotic plaques. J Clin Invest 2007;117:185-194

167. Thaler JP, Yi CX, Schur EA, Guyenet SJ, Hwang BH, Dietrich MO, Zhao X, Sarruf DA, Izgur V, Maravilla KR, Nguyen HT, Fischer JD, Matsen ME, Wisse BE, Morton GJ, Horvath TL, Baskin DG, Tschop MH, Schwartz MW: Obesity is associated with hypothalamic injury in rodents and humans. J Clin Invest 2012;122:153-162

168. Gregor MF, Hotamisligil GS: Inflammatory mechanisms in obesity. Annu Rev Immunol 2011;29:415-445

169. Amano SU, Cohen JL, Vangala P, Tencerova M, Nicoloro SM, Yawe JC, Shen Y, Czech MP, Aouadi M: Local proliferation of macrophages contributes to obesity-associated adipose tissue inflammation. Cell Metab 2014;19:162-171

170. Clement K, Viguerie N, Poitou C, Carette C, Pelloux V, Curat CA, Sicard A, Rome S, Benis A, Zucker JD, Vidal H, Laville M, Barsh GS, Basdevant A, Stich V, Cancello R, Langin D: Weight loss regulates inflammation-related genes in white adipose tissue of obese subjects. FASEB J 2004;18:1657-1669

171. Steckhan N, Hohmann CD, Kessler C, Dobos G, Michalsen A, Cramer H: Effects of different dietary approaches on inflammatory markers in patients with metabolic syndrome: A systematic review and meta-analysis. Nutrition 2016;32:338-348

172. Franz MJ, Boucher JL, Rutten-Ramos S, VanWormer JJ: Lifestyle weight-loss intervention outcomes in overweight and obese adults with type 2 diabetes: a systematic review and meta-analysis of randomized clinical trials. J Acad Nutr Diet 2015;115:1447-1463

173. Miller RS, Becker KG, Prabhu V, Cooke DW: Adipocyte gene expression is altered in formerly obese mice and as a function of diet composition. J Nutr 2008;138:1033-1038

174. Kalupahana NS, Voy BH, Saxton AM, Moustaid-Moussa N: Energy-restricted high-fat diets only partially improve markers of systemic and adipose tissue inflammation. Obesity (Silver Spring) 2011;19:245-254

175. Anderson EK, Gutierrez DA, Kennedy A, Hasty AH: Weight cycling increases T-cell accumulation in adipose tissue and impairs systemic glucose tolerance. Diabetes 2013;62:3180-3188

176. Kosteli A, Sugaru E, Haemmerle G, Martin JF, Lei J, Zechner R, Ferrante AW, Jr.: Weight loss and lipolysis promote a dynamic immune response in murine adipose tissue. J Clin Invest 2010;120:3466-3479

177. Smyth GK: Linear models and empirical bayes methods for assessing differential expression in microarray experiments. Stat Appl Genet Mol Biol 2004;3:Article3

178. Irizarry RA, Hobbs B, Collin F, Beazer-Barclay YD, Antonellis KJ, Scherf U, Speed TP: Exploration, normalization, and summaries of high density oligonucleotide array probe level data. Biostatistics 2003;4:249-264

179. Gautier EL, Shay T, Miller J, Greter M, Jakubzick C, Ivanov S, Helft J, Chow A, Elpek KG, Gordonov S, Mazloom AR, Ma'ayan A, Chua WJ, Hansen TH, Turley SJ, Merad M, Randolph GJ, Immunological Genome C: Gene-expression profiles and transcriptional regulatory pathways that underlie the identity and diversity of mouse tissue macrophages. Nat Immunol 2012;13:1118-1128

180. Huang da W, Sherman BT, Lempicki RA: Systematic and integrative analysis of large gene lists using DAVID bioinformatics resources. Nat Protoc 2009;4:44-57

181. Morris DL, Oatmen KE, Mergian TA, Cho KW, DelProposto JL, Singer K, Evans-Molina C, O'Rourke RW, Lumeng CN: CD40 promotes MHC class II expression on adipose tissue macrophages and regulates adipose tissue CD4+ T cells with obesity. J Leukoc Biol 2015;

182. O'Rourke RW, White AE, Metcalf MD, Winters BR, Diggs BS, Zhu X, Marks DL: Systemic inflammation and insulin sensitivity in obese IFN-gamma knockout mice. Metabolism 2012;61:1152-1161

183. Mito N, Hosoda T, Kato C, Sato K: Change of cytokine balance in diet-induced obese mice. Metabolism 2000;49:1295-1300

184. Strissel KJ, DeFuria J, Shaul ME, Bennett G, Greenberg AS, Obin MS: T-cell recruitment and Th1 polarization in adipose tissue during diet-induced obesity in C57BL/6 mice. Obesity (Silver Spring) 2010;18:1918-1925

185. Jenkins SJ, Ruckerl D, Thomas GD, Hewitson JP, Duncan S, Brombacher F, Maizels RM, Hume DA, Allen JE: IL-4 directly signals tissue-resident macrophages to proliferate beyond homeostatic levels controlled by CSF-1. J Exp Med 2013;210:2477-2491

186. Divoux A, Tordjman J, Lacasa D, Veyrie N, Hugol D, Aissat A, Basdevant A, Guerre-Millo M, Poitou C, Zucker JD, Bedossa P, Clement K: Fibrosis in human adipose tissue: composition, distribution, and link with lipid metabolism and fat mass loss. Diabetes 2010;59:2817-2825

187. Chavey C, Mari B, Monthouel MN, Bonnafous S, Anglard P, Van Obberghen E, Tartare-Deckert S: Matrix metalloproteinases are differentially expressed in adipose tissue during obesity and modulate adipocyte differentiation. J Biol Chem 2003;278:11888-11896

188. Bourlier V, Zakaroff-Girard A, Miranville A, De Barros S, Maumus M, Sengenes C, Galitzky J, Lafontan M, Karpe F, Frayn KN, Bouloumie A: Remodeling phenotype of human subcutaneous adipose tissue macrophages. Circulation 2008;117:806-815

189. Tian XY, Ganeshan K, Hong C, Nguyen KD, Qiu Y, Kim J, Tangirala RK, Tonotonoz P, Chawla A: Thermoneutral Housing Accelerates Metabolic Inflammation to Potentiate Atherosclerosis but Not Insulin Resistance. Cell Metab 2016;23:165-178

190. Frikke-Schmidt H, O'Rourke RW, Lumeng CN, Sandoval DA, Seeley RJ: Does bariatric surgery improve adipose tissue function? Obes Rev 2016;

191. Wing RR, Hill JO: Successful weight loss maintenance. Annu Rev Nutr 2001;21:323-341

192. Soleymani T, Daniel S, Garvey WT: Weight maintenance: challenges, tools and strategies for primary care physicians. Obes Rev 2016;17:81-93

193. Puzziferri N, Roshek TB, 3rd, Mayo HG, Gallagher R, Belle SH, Livingston EH: Long-term follow-up after bariatric surgery: a systematic review. JAMA 2014;312:934-942

194. Karmali S, Brar B, Shi X, Sharma AM, de Gara C, Birch DW: Weight recidivism post-bariatric surgery: a systematic review. Obes Surg 2013;23:1922-1933

195. te Riele WW, Boerma D, Wiezer MJ, Borel Rinkes IH, van Ramshorst B: Long-term results of laparoscopic adjustable gastric banding in patients lost to follow-up. Br J Surg 2010;97:1535-1540

196. Mackie GM, Samocha-Bonet D, Tam CS: Does weight cycling promote obesity and metabolic risk factors? Obes Res Clin Pract 2016;

197. Mehta T, Smith DL, Jr., Muhammad J, Casazza K: Impact of weight cycling on risk of morbidity and mortality. Obes Rev 2014;15:870-881

198. Stevens VL, Jacobs EJ, Sun J, Patel AV, McCullough ML, Teras LR, Gapstur SM: Weight cycling and mortality in a large prospective US study. Am J Epidemiol 2012;175:785-792

199. Action for Health in Diabetes Study G: Association of Weight Loss Maintenance and Weight Regain on 4-Year Changes in CVD Risk Factors: the Action for Health in Diabetes (Look AHEAD) Clinical Trial. Diabetes Care 2016;39:1345-1355

200. Sea MM, Fong WP, Huang Y, Chen ZY: Weight cycling-induced alteration in fatty acid metabolism. Am J Physiol Regul Integr Comp Physiol 2000;279:R1145-1155

201. Kochan Z, Karbowska J, Swierczynski J: The effects of weight cycling on serum leptin levels and lipogenic enzyme activities in adipose tissue. J Physiol Pharmacol 2006;57 Suppl 6:115-127

202. Fried SK, Hill JO, Nickel M, DiGirolamo M: Prolonged effects of fasting-refeeding on rat adipose tissue lipoprotein lipase activity: influence of caloric restriction during refeeding. J Nutr 1983;113:1861-1869

203. Barbosa-da-Silva S, Fraulob-Aquino JC, Lopes JR, Mandarim-de-Lacerda CA, Aguila MB: Weight cycling enhances adipose tissue inflammatory responses in male mice. PLoS One 2012;7:e39837

204. Zamarron BF, Mergian TA, Cho KW, Martinez-Santibanez G, Luan D, Singer K, delProposto JL, Geletka LM, Muir LA, Lumeng CN: Macrophage Proliferation Sustains Adipose Tissue Inflammation in Formerly Obese Mice. Diabetes 2017;66:392-406

205. Ntambi JM, Young-Cheul K: Adipocyte differentiation and gene expression. J Nutr 2000;130:3122S-3126S

206. Lee YH, Petkova AP, Granneman JG: Identification of an adipogenic niche for adipose tissue remodeling and restoration. Cell Metab 2013;18:355-367

207. Lee YH, Petkova AP, Mottillo EP, Granneman JG: In vivo identification of bipotential adipocyte progenitors recruited by beta3-adrenoceptor activation and high-fat feeding. Cell Metab 2012;15:480-491

208. Torti FM, Torti SV, Larrick JW, Ringold GM: Modulation of adipocyte differentiation by tumor necrosis factor and transforming growth factor beta. J Cell Biol 1989;108:1105-1113

209. Sattar N, Forrest E, Preiss D: Non-alcoholic fatty liver disease. BMJ 2014;349:g4596

210. Wannamethee SG, Shaper AG, Lennon L, Whincup PH: Hepatic enzymes, the metabolic syndrome, and the risk of type 2 diabetes in older men. Diabetes Care 2005;28:2913-2918

211. Vozarova B, Stefan N, Lindsay RS, Saremi A, Pratley RE, Bogardus C, Tataranni PA: High alanine aminotransferase is associated with decreased hepatic insulin sensitivity and predicts the development of type 2 diabetes. Diabetes 2002;51:1889-1895

212. Barbosa-da-Silva S, da Silva NC, Aguila MB, Mandarim-de-Lacerda CA: Liver damage is not reversed during the lean period in diet-induced weight cycling in mice. Hepatol Res 2014;44:450-459

213. Fabbrini E, Sullivan S, Klein S: Obesity and nonalcoholic fatty liver disease: biochemical, metabolic, and clinical implications. Hepatology 2010;51:679-689

214. Donnelly KL, Smith CI, Schwarzenberg SJ, Jessurun J, Boldt MD, Parks EJ: Sources of fatty acids stored in liver and secreted via lipoproteins in patients with nonalcoholic fatty liver disease. J Clin Invest 2005;115:1343-1351

215. Diraison F, Moulin P, Beylot M: Contribution of hepatic de novo lipogenesis and reesterification of plasma non esterified fatty acids to plasma triglyceride synthesis during non-alcoholic fatty liver disease. Diabetes Metab 2003;29:478-485

216. Mitsuyoshi H, Yasui K, Harano Y, Endo M, Tsuji K, Minami M, Itoh Y, Okanoue T, Yoshikawa T: Analysis of hepatic genes involved in the metabolism of fatty acids and iron in nonalcoholic fatty liver disease. Hepatol Res 2009;39:366-373

217. Kohjima M, Enjoji M, Higuchi N, Kato M, Kotoh K, Yoshimoto T, Fujino T, Yada M, Yada R, Harada N, Takayanagi R, Nakamuta M: Re-evaluation of fatty acid metabolism-related gene expression in nonalcoholic fatty liver disease. Int J Mol Med 2007;20:351-358

218. Kotronen A, Seppala-Lindroos A, Vehkavaara S, Bergholm R, Frayn KN, Fielding BA, Yki-Jarvinen H: Liver fat and lipid oxidation in humans. Liver Int 2009;29:1439-1446

219. Sanyal AJ, Campbell-Sargent C, Mirshahi F, Rizzo WB, Contos MJ, Sterling RK, Luketic VA, Shiffman ML, Clore JN: Nonalcoholic steatohepatitis: association of insulin resistance and mitochondrial abnormalities. Gastroenterology 2001;120:1183-1192

220. Bugianesi E, Gastaldelli A, Vanni E, Gambino R, Cassader M, Baldi S, Ponti V, Pagano G, Ferrannini E, Rizzetto M: Insulin resistance in non-diabetic patients with non-alcoholic fatty liver disease: sites and mechanisms. Diabetologia 2005;48:634-642

221. Adiels M, Taskinen MR, Packard C, Caslake MJ, Soro-Paavonen A, Westerbacka J, Vehkavaara S, Hakkinen A, Olofsson SO, Yki-Jarvinen H, Boren J: Overproduction of large VLDL particles is driven by increased liver fat content in man. Diabetologia 2006;49:755-765

222. Fabbrini E, Mohammed BS, Magkos F, Korenblat KM, Patterson BW, Klein S: Alterations in adipose tissue and hepatic lipid kinetics in obese men and women with nonalcoholic fatty liver disease. Gastroenterology 2008;134:424-431

223. Gustafson B, Smith U: Cytokines promote Wnt signaling and inflammation and impair the normal differentiation and lipid accumulation in 3T3-L1 preadipocytes. J Biol Chem 2006;281:9507-9516

224. Bilkovski R, Schulte DM, Oberhauser F, Mauer J, Hampel B, Gutschow C, Krone W, Laudes M: Adipose tissue macrophages inhibit adipogenesis of mesenchymal precursor cells via wnt-5a in humans. Int J Obes (Lond) 2011;35:1450-1454

225. Bing C: Is interleukin-1beta a culprit in macrophage-adipocyte crosstalk in obesity? Adipocyte 2015;4:149-152

226. Gagnon A, Foster C, Landry A, Sorisky A: The role of interleukin 1beta in the anti-adipogenic action of macrophages on human preadipocytes. J Endocrinol 2013;217:197-206

227. Kim BS, Pallua N, Bernhagen J, Bucala R: The macrophage migration inhibitory factor protein superfamily in obesity and wound repair. Exp Mol Med 2015;47:e161

228. Petersen RK, Jorgensen C, Rustan AC, Froyland L, Muller-Decker K, Furstenberger G, Berge RK, Kristiansen K, Madsen L: Arachidonic acid-dependent inhibition of adipocyte differentiation requires PKA activity and is associated with sustained expression of cyclooxygenases. Journal of lipid research 2003;44:2320-2330

229. Kim JY, van de Wall E, Laplante M, Azzara A, Trujillo ME, Hofmann SM, Schraw T, Durand JL, Li H, Li G, Jelicks LA, Mehler MF, Hui DY, Deshaies Y, Shulman GI, Schwartz GJ, Scherer PE: Obesity-associated improvements in metabolic profile through expansion of adipose tissue. J Clin Invest 2007;117:2621-2637

230. Heilbronn L, Smith SR, Ravussin E: Failure of fat cell proliferation, mitochondrial function and fat oxidation results in ectopic fat storage, insulin resistance and type II diabetes mellitus. Int J Obes Relat Metab Disord 2004;28 Suppl 4:S12-21

231. Safar Zadeh E, Lungu AO, Cochran EK, Brown RJ, Ghany MG, Heller T, Kleiner DE, Gorden P: The liver diseases of lipodystrophy: the long-term effect of leptin treatment. J Hepatol 2013;59:131-137

232. Sell H, Habich C, Eckel J: Adaptive immunity in obesity and insulin resistance. Nat Rev Endocrinol 2012;8:709-716

233. Hoevenaars FP, Keijer J, Herreman L, Palm I, Hegeman MA, Swarts HJ, van Schothorst EM: Adipose tissue metabolism and inflammation are differently affected by weight loss in obese mice due to either a high-fat diet restriction or change to a low-fat diet. Genes Nutr 2014;9:391

234. Suganami T, Ogawa Y: Adipose tissue macrophages: their role in adipose tissue remodeling. J Leukoc Biol 2010;88:33-39

235. Martinez-Santibanez G, Lumeng CN: Macrophages and the regulation of adipose tissue remodeling. Annu Rev Nutr 2014;34:57-76

236. Sun K, Kusminski CM, Scherer PE: Adipose tissue remodeling and obesity. J Clin Invest 2011;121:2094-2101

237. Shapses SA, Sukumar D: Bone metabolism in obesity and weight loss. Annu Rev Nutr 2012;32:287-309

238. Rebours V, Gaujoux S, d'Assignies G, Sauvanet A, Ruszniewski P, Levy P, Paradis V, Bedossa P, Couvelard A: Obesity and Fatty Pancreatic Infiltration Are Risk Factors for Pancreatic Precancerous Lesions (PanIN). Clin Cancer Res 2015;21:3522-3528

239. Tomita T, Doull V, Pollock HG, Krizsan D: Pancreatic islets of obese hyperglycemic mice (ob/ob). Pancreas 1992;7:367-375

240. Melo LC, Silva MA, Calles AC: Obesity and lung function: a systematic review. Einstein (Sao Paulo) 2014;12:120-125

241. Pedersen BK, Febbraio MA: Muscles, exercise and obesity: skeletal muscle as a secretory organ. Nat Rev Endocrinol 2012;8:457-465

242. Saghizadeh M, Ong JM, Garvey WT, Henry RR, Kern PA: The expression of TNF alpha by human muscle. Relationship to insulin resistance. J Clin Invest 1996;97:1111-1116

243. Wu H, Ballantyne CM: Skeletal muscle inflammation and insulin resistance in obesity. J Clin Invest 2017;127:43-54

244. Scheller EL, Khoury B, Moller KL, Wee NK, Khandaker S, Kozloff KM, Abrishami SH, Zamarron BF, Singer K: Changes in Skeletal Integrity and Marrow Adiposity during High-Fat Diet and after Weight Loss. Front Endocrinol (Lausanne) 2016;7:102

245. Jo J, Gavrilova O, Pack S, Jou W, Mullen S, Sumner AE, Cushman SW, Periwal V: Hypertrophy and/or Hyperplasia: Dynamics of Adipose Tissue Growth. PLoS Comput Biol 2009;5:e1000324

246. Sarjeant K, Stephens JM: Adipogenesis. Cold Spring Harb Perspect Biol 2012;4:a008417

247. Gustafson B, Hedjazifar S, Gogg S, Hammarstedt A, Smith U: Insulin resistance and impaired adipogenesis. Trends Endocrinol Metab 2015;26:193-200

248. Carvalho E, Jansson PA, Axelsen M, Eriksson JW, Huang X, Groop L, Rondinone C, Sjostrom L, Smith U: Low cellular IRS 1 gene and protein expression predict insulin resistance and NIDDM. FASEB J 1999;13:2173-2178

249. Yang X, Jansson PA, Nagaev I, Jack MM, Carvalho E, Sunnerhagen KS, Cam MC, Cushman SW, Smith U: Evidence of impaired adipogenesis in insulin resistance. Biochem Biophys Res Commun 2004;317:1045-1051

250. Jansson PA, Pellme F, Hammarstedt A, Sandqvist M, Brekke H, Caidahl K, Forsberg M, Volkmann R, Carvalho E, Funahashi T, Matsuzawa Y, Wiklund O, Yang X, Taskinen MR, Smith U: A novel cellular marker of insulin resistance and early atherosclerosis in humans is related to impaired fat cell differentiation and low adiponectin. FASEB J 2003;17:1434-1440

251. Hammarstedt A, Graham TE, Kahn BB: Adipose tissue dysregulation and reduced insulin sensitivity in non-obese individuals with enlarged abdominal adipose cells. Diabetol Metab Syndr 2012;4:42

252. Virtue S, Vidal-Puig A: Adipose tissue expandability, lipotoxicity and the Metabolic Syndrome--an allostatic perspective. Biochim Biophys Acta 2010;1801:338-349

253. Ye R, Wang QA, Tao C, Vishvanath L, Shao M, McDonald JG, Gupta RK, Scherer PE: Impact of tamoxifen on adipocyte lineage tracing: Inducer of adipogenesis and prolonged nuclear translocation of Cre recombinase. Mol Metab 2015;4:771-778

254. Tontonoz P, Hu E, Spiegelman BM: Stimulation of adipogenesis in fibroblasts by PPAR gamma 2, a lipid-activated transcription factor. Cell 1994;79:1147-1156

255. Ables GP: Update on ppargamma and nonalcoholic Fatty liver disease. PPAR Res 2012;2012:912351

256. Yang SJ, Choi JM, Chae SW, Kim WJ, Park SE, Rhee EJ, Lee WY, Oh KW, Park SW, Kim SW, Park CY: Activation of peroxisome proliferator-activated receptor gamma by rosiglitazone increases sirt6 expression and ameliorates hepatic steatosis in rats. PLoS One 2011;6:e17057

257. Nan YM, Fu N, Wu WJ, Liang BL, Wang RQ, Zhao SX, Zhao JM, Yu J: Rosiglitazone prevents nutritional fibrosis and steatohepatitis in mice. Scand J Gastroenterol 2009;44:358-365

258. Parks EJ, Krauss RM, Christiansen MP, Neese RA, Hellerstein MK: Effects of a low-fat, high-carbohydrate diet on VLDL-triglyceride assembly, production, and clearance. J Clin Invest 1999;104:1087-1096

259. DeFronzo RA, Tobin JD, Andres R: Glucose clamp technique: a method for quantifying insulin secretion and resistance. Am J Physiol 1979;237:E214-223

260. Ayala JE, Bracy DP, Malabanan C, James FD, Ansari T, Fueger PT, McGuinness OP, Wasserman DH: Hyperinsulinemic-euglycemic clamps in conscious, unrestrained mice. J Vis Exp 2011;

261. Ryan AS, Nicklas BJ: Reductions in plasma cytokine levels with weight loss improve insulin sensitivity in overweight and obese postmenopausal women. Diabetes Care 2004;27:1699-1705

262. Tajik N, Keshavarz SA, Masoudkabir F, Djalali M, Sadrzadeh-Yeganeh HH, Eshraghian MR, Chamary M, Ahmadivand Z, Yazdani T, Javanbakht MH: Effect of diet-induced weight loss on inflammatory cytokines in obese women. J Endocrinol Invest 2013;36:211-215